A Risk Based Approach to Module Tolerance Specification

by

Yasaman Shahtaheri

A thesis
Presented to the University of Waterloo
in fulfillment of the
thesis requirement for the degree of
Master of Applied Science
in
Civil Engineering

Waterloo, Ontario, Canada, 2014

AUTHOR'S DECLARATION

I hereby declare that I am the sole author of this thesis. This is a true copy of the thesis, including any required final revisions, as accepted by my examiners.

I understand that my thesis may be made electronically available to the public.

Abstract

This research investigates tolerance strategies for modular systems on a project specific basis. The objective of the proposed research is to form a guideline for optimizing the construction costs/risks with the aim of developing an optimal design of resilient modular systems. The procedures for achieving the research objective included: (a) development of 3D structural analysis models of the modules, (b) strength/stability investigation of the structure, (c) developing the fabrication cost function, (e) checking elastic and inelastic distortion, and (f) constructing the site-fit risk functions. The total site-fit risk function minimizes the cost/risk associated with fabrication, transportation; alignment, rework, and safety, while maximizing stiffness in terms of story drift values for site re-alignment and fitting alternatives. The fabrication cost function was developed by collecting 61 data points for the investigated module chassis using the SAP2000 software while reducing the initial section sizes, in addition to the fabrication costs at each step (61 steps). With the reduction of the structural reinforcement, story drift values increase, therefore there will be a larger distortion in the module. This generic module design procedure models a trade-off between the amount of reinforcement and expected need for significant field alterations. Structural design software packages such as SAP2000, AutoCAD, and Autodesk were used in order to model and test the module chassis. This research hypothesizes that the influential factors in the site-fit risk functions are respectively: fabrication, transportation, alignment, safety, and rework costs/risks. In addition, the site-fit risk function provides a theoretical range of possible solutions for the construction industry. The maximum allowable modular out-of-tolerance value, which requires the minimum amount of cost with respect to the defined function, can be configured using this methodology. This research concludes that over-reinforced or lightly-reinforced designs are not the best solution for mitigating risks, and reducing costs. For this reason the site-fit risk function will provide a range of pareto-optimal building solutions with respect to the fabrication, transportation, safety, alignment, and rework costs/risks.

Acknowledgements

First and foremost I would like to express my gratitude to god, whose many blessings have made me who I am today, encouraged me to pursue my dreams, and reminded me that all things are possible as long as we have faith in ourselves and in him.

I take immense pleasure to express my sincere and deep sense of gratitude to my supervisors, Professor Carl T. Haas, and Professor Jeffery S. West for their continued guidance throughout my entire research. Your support, motivation, collaboration, devotion, inspiration and constant belief in me assisted me in realizing my potential. I have appreciated, and enjoyed every minute of this journey.

I gratefully acknowledge the guidance and assistance of PCL Construction Company, for the completion of this work. I would specially like to thank Mr. Robert LaCosta, Operations Manager; and Mr. Mark Taylor, P.Eng, CCA, Vice President of the permanent modular construction, for their advices, technical support, and guidance through the research. I would also like to acknowledge Aecon Industrial, especially Mr. Dennis Samolczyk**,** Mechanical Engineer, for his skillful advice, valuable ideas, and extra support throughout the research **.**Without their contribution and the support and guidance of Professor Jeffery S. West and Professor Carl T. Haas it would not have been possible to join the crew at PCL Construction Company and Aecon Industrial and have their insight on this research.

I would like to submit my appreciation to my Undergraduate Research Assistant colleague, Riley McMillan, for all his support, investigations, and hard work throughout my research program. His effort, contributions, and reputation made the difficulties manageable.

I would like to extend my sincere thanks to my colleagues, Mr. Mohammad Nahangi, Mr. Yu Hong, and Mr. Jamie Yeung for giving me helpful advice, invaluable support, and for sharing experience.

I wish to extend my gratitude all my dear friends and colleges, who provided unconditional support and guidance in many ways throughout my studies.

My sincerest appreciation goes to my parents Soussan and Shahram, for their unconditional love, support, guidance, encouragement, and for giving me the wings to fly. I offer my profound gratitude to my sister Maryam, for always being there for me as my best friend and mentor in the journey of life.

To my caring sister, Maryam;
my compassionate mother, Soussan; and
my encouraging father, Shahram

Table of Contents

List of Figures

List of Tables

Chapter 1
Introduction

1.1 Background

Challenging but demanding, construction is one of the world's largest industries. To address one of the needs of this challenging industry, prefabrication and modular work have been developed and used since the 14th century in Italy at the age of renaissance. Modular construction improves the quality of manufacturing and the speed of on-site installation (Lawson et al., 2012). Prefabrication sites are weather independent, convenient for remote areas, and reduce the wastage of material. These sites also decrease the risks associated with on-site fabrication including: mold, rust, and sun damage that can often lead to human respiratory problems.

Modularization is experiencing a renaissance in North America, because of skilled craft labour shortages, technological advances, and increased capacity to manage complex and geographically dispersed staged fabrication supply chains. With advances in 3D design, metrology and BIM (Building Information Modelling), as well as precision fabrication, it has become possible to largely avoid the historically significant impediment of field-fit problems for modules. The underlying premise to reduce field-fit problems is the definition and control of strict tolerances from shop fabrication to erection at the construction site. While modern technologies and processes for precision fabrication have facilitated very tight tolerance control for the modules themselves, several challenges exist to further optimize modular construction systems.

One such challenge is the definition and optimization of the relationship between the various levels of tolerances, including shop (fabrication) tolerance, hardware or embedment tolerance, and site tolerance. Each tolerance level presents different design and construction challenges with associated financial implications and risks. Another challenge presented in the design of the modules, is the need to resist deformation (for tolerance control) during transportation and handling, which also comes with the cost of extra material to achieve levels of structural stiffness far exceeding required strength limited design. For industrial modules, this equates to 10-20% more structural steel, embedded in costs associated with materials, labour, shipping weight, and cascading requirements. This leads to even more steel on larger assemblies. This thesis explores strategies to address these challenges through a risk based approach to module tolerance specification.

It should be noted that the term module is defined as a standardized unit of a larger structure or system. Modularization is the decomposition of the structure or system into modules with specified interfaces that should be assembled to another module or assembly. An assembly is different from a module. A module can be a sub-assembly; however a sub-assembly is not necessarily a module (Ericsson & Erixon, 1999). This implies that modularized buildings are comprised of several smaller modules that should be built within a certain tolerance limit in order to minimize miss-fitting.

The adoption of prefabrication compared to traditional construction has significant advantages. In one study, advantages were described as: improved quality control and reduction of construction time up to 20%, 56% reduction of construction waste, 9.5% reduction in labour requirements, as well as less dust and noise on the construction site (Jaillon & Poon, 2008). On the other hand, although prefabrication may lead to better performance results, rework has an adverse effect on project performance that requires attention. Rework is defined as ‘‘the unnecessary effort of redoing a process or activity that was incorrectly implemented the first time.’’ This adverse effect may lead to a 52% increase in the total project cost according to one study and it is not explicitly correlated with project characteristics (Love P. D., 2002). For this reason in order to benefit from the significant advantages of modular construction, the prefabricated subsections/sections must be monitored at an early stage during the fabrication process. This can be done by having a strategic approach for improving business approach (Pan et al., 2007), in addition to achieving tolerance specifications (Bureau of Indian Standards, 1990). This will assist with the reduction of rework costs and risks.

Recent studies show that modular construction reduces the wastage of material up to about 52% (Jaillon et al., 2008); thus, it is an environmental friendly process. Large modular production has favourable pricing for suppliers and may save commissioning and repair costs up to about 2% over traditional construction. However, even in highly modular buildings there still maybe a significant amount of the work is done on the construction site. In many modular projects up to about 55% of the work needs to be done on the construction site (e.g., seventeen story modular building with a concert core). Three case studies on modular construction in England show that modular construction reduces the construction waste from 10% to 15% in a traditional building site to less than 5% in a factory. The number of site visits by delivery vehicles is reduced to about 70% and most of the transportation activities are moved to the factory. Noise and disruption are also reduced by 30% to 50%. In summary, factory production is more efficient than on-site production; nevertheless, it requires more investment and repeated output to become economically viable (Lawson et al., 2012).

During the site-fitting process, tolerance control is a major source of problems in construction projects. Designers should consider that tolerance control should be done for every detail (Accelerated Bridge Construction Manual, 2011). To eliminate rework and additional site-fitting costs a method of tolerance control during fabrication can assist in reduction of risk and of material wastage associated with miss-fittings. Tolerance charts (Section 2.5) for dimensional control have been used for minimizing production costs since 1959 in manufacturing. They provide the engineer with a precise method for identifying the allowable tolerances and working (allowable operating) dimensions for increasing efficiency (Gadzala, 1959).With the aim to reduce risks and extra costs associated with modules during fabrication, transportation and field-fitting, this thesis introduces a procedure for deriving tolerances for fabrication in construction with a project specific basis.

1.2 Statement of Research

Previous researchers have developed a computerized tool that supports the decision making process on the use of prefabrication, preassembly, modularization and offsite fabrication in the construction process (Song et al., 2005). Similar research has been done for improving decision making during fabrication and for choosing modularization as a key to reducing construction costs. In order to reduce the adverse effect of miss-fittings in modularization, a framework needs to be defined for setting tolerance limits for modular structures. Industry experts have clearly stated that most of the problems associated with complex modules are process management problems between organization units and fitting adjustments that need to be done at each stage during fabrication. This implies that a methodology for setting a tolerance strategy can reduce the risk associated with miss-fittings and rework.

This first aspect of this research investigates tolerance strategies for modular systems. This involves studying the relationships between fabrication and site tolerances to optimize the trade-offs between the costs related to engineering, materials, fabrication and transportation and the risks or costs associated with field-fit during erection. The concepts and relationships developed will be demonstrated and evaluated using a case study for modular systems, and could be extended eventually to room clusters and utility modules for buildings.

The second component of the research will pursue the concept of resilient module design. In this context, “resilience” is defined as the ability of a modular system to experience minimum life cycle risk while promptly and efficiently responding to negative events during transportation, handling and erection. For example, while materials, fabrication process, dimensions, and factory environment may be controllable

within limits, it is costlier and sometimes impossible to control shipping risks and site dimensions. The development of a resilient modular systems design approach would allow optimization of the structural and process configuration to address the multi-objective problem of minimizing materials, shop and site labour hours, transportation costs, and complexity, while maximizing flexibility for site re-alignment or fitting options. The goal of the conducted research is to formalize the solution of this optimization problem into a process for ensuring the optimal design of resilient modular systems.

In summary, the research conducted herein is intended to enable the optimization of modular construction systems by developing a process whereby tolerances can be defined for the fabrication and construction of modular systems on a project-specific basis. As well, the research will explore the concept of module resiliency as a parallel approach for reducing the costs and risk associated with the fabrication and assembly of modular systems.

1.3 Scope and Objectives

The overall objective of this research was to develop a systems design approach to define tolerances for the fabrication and construction of modular systems on a project-specific basis. The process included the concept of module resiliency as an approach for establishing tolerances to reduce costs and risks associated with fabrication and assembly of modular systems.

The initial hypothesis of the proposed research was that a process can be developed whereby the required tolerances are determined for a particular modular construction application within an overall cost and risk framework. The definition of tolerances would consider a number of inter-related factors, wherein the relationships between the costs of the module structure (material, labour, transportation) as a function of tolerance requirements are compared to the costs and risks associated with site fit or module assembly.

The module structure cost function was based largely on the structural design process for a given module, considering the unique loading and demands placed on the module during fabrication, handling, transportation and erection/assembly, and relating the resulting cost of the structure to the ability of the design to meet tolerances in terms of displacements and distortions. The site fit risk function considered the factors that affect fit problems (module to site, module to module, etc.) and the resulting rework, planned site adjustments (e.g., adjustable studs, pipe cut lengths, or use of more advanced concepts), delays and costs. Structure cost includes materials, labour, and equipment located at the fabrication facility. The concept of module resilience will be considered as a scenario in establishing both functions.

Through systematic development of these functions, an optimal tolerance regime can be selected for a given project, expediting construction and reducing overall project cost.

An understanding of risk analysis is required to make informed, logical decisions in development of the tolerance strategy. In the conducted research, risks will be considered as the product of their probability and their cost or schedule impact. One research challenge is to develop a thorough risk identification approach and a means by which such risk can be quantified.

In summary the specific objectives of this research are as follows:

1. Identify the typical tolerances and tolerance interactions in modular construction, and develop methodologies to define application-appropriate tolerance escalation ladders considering the characteristics of the tolerances involved.
2. Develop a process to establish the relationship between the module structural design and fabrication cost and the resulting risk of distortions or damage occurring during transportation, handling and erection.
3. Develop a process to establish the relationship between site fit costs and the degree of module damage and distortion, and misalignments between module and site conditions.
4. Use risk analysis techniques, and assess the trade-off between the fabrication cost of a module and the site fit cost of correcting a damaged module or misalignment problem.
5. Develop a systematic process to determine the optimal tolerance and resiliency strategy for module design to minimize the risk of construction site-fit problems.

1.4 Research Methodology

The methodology employed to attain the research objectives was as follows:

1. Literature review: Completed a detailed literature review that focuses on modular construction techniques, various tolerance classifications, lean construction, risk management, safety and occupational health.

2. Identify prototype modular construction scenarios to use as the basis of the research study: The module design requirements were identified based on the permanent or final conditions during transportation, handling and erection. Additional modular construction scenarios were selected for future testing and refinement of the tolerance and resilience strategy. A basic case study of a pipe module chassis was analyzed.

3. Develop 3D structural analysis models of a case study module: A commercial structural analysis program was used to develop structural models of the case study module. These models reflect the module geometry and usage requirements, and incorporate the design loading conditions identified for the permanent application as well as those actions anticipated during transportation, handing and erection. These structural models along with the modelled loading conditions were used to design the module for the critical design loading combinations.

4. Conduct module parametric design and performance analyses: Using the structural analysis models developed in Step 3, a parametric analysis was performed to establish the relationship between structural configuration, member sizes and connection properties and the resulting likelihood of permanent distortions, misalignment or damage resulting from transportation, handling and erection. The structural analysis models incorporate non-linear member and connection responses in key structural elements to capture behavior that may lead to permanent deformations under the design loading. The module structural design was incrementally revised by changing member sizes, bracing arrangements and connection details to establish the relationship between module material and fabrication cost and the resulting permanent distortions. These results were used to establish module structure cost functions.

5. Identify tolerance types and interactions: Working with constructors, the types of tolerances and tolerance problems in various modular construction applications were identified. The tolerances were categorized as manufacturing, interfacing and erection tolerances, and practical tolerance levels were determined based on actual project applications. The characteristics of

expected variations (e.g., dimensional, positional, orientation, etc.) associated with each tolerance type was established, and used in the development of tolerance accumulation or escalation relationships. These tolerance escalation relationships were used in the development of the site risk function and for the risk analysis (Steps 6 and 7).

6. Develop the site-fit risk function: The factors affecting costs associated with fitting the modules to each other and to the site constructed components (e. g., building foundation) were explored. This aspect of the research drew upon data and experience from partners PCL Constructors, and Aecon Industrial Inc., to estimate material and labour costs of rework, and associated schedule delays for a broad range of misalignment and out-of-tolerance conditions. The data were used to establish the site-fit costs as a function of potential module distortions or misalignments.

7. Perform a risk analysis of the trade-off between the risk of site-fit costs due to realignment and the cost of over-reinforcement in module design: The decision regarding the strength of a module is not a straightforward one. A module can be heavily-reinforced and over-designed, from a structural point of view, and it will require little or no adjustment when it arrives on site. The downside of this alternative is that the material and labour costs to construct the module will be much greater. Alternatively, a module can be designed for the loading associated with its permanent end-use condition, largely ignoring the higher loads that it will experience during transport. This approach would reduce module fabrication costs, but will likely require significant alterations in order to correct the damage sustained during transport. A risk analysis made it possible to determine the optimal trade-off between over-design and significant alterations, as well as assessing the potential impact of techniques for module resiliency. The risk analysis used the module structure cost function developed in Steps 4 and the site-fit cost function developed in Step 6 and 7.

8. Adapt the standard module design procedure to optimize the trade-off between the risk of realignment and the cost of over-reinforcement: Using the results of the risk analysis, a generic module design procedure was proposed to properly account for the trade-off between over-design and significant alterations. This design procedure defines an optimal tolerance strategy that a designer can follow when designing the structural configuration of the module.

9. Provide conclusions and recommendations regarding future research

1.5 Structure of the Thesis

This thesis consists of four chapters, which cover the research objectives, methodology, and background information regarding modular construction techniques; various tolerance classifications; lean construction; risk management; safety; occupational health and finally conclusions and recommendations.

Chapter 1 provides a brief description of the previous research achievements in modular construction, which are related to tolerance classifications, modularization techniques, structure occupational health and safety, risk management systems and lean construction. The scope, objectives and research methodology has also been briefly discussed in this chapter.

Chapter 2 reviews background information including (1) an introduction to the modularization industry and its contributions to the modern construction industry; (2) tolerance classification systems and their relationships; (3) resiliency as a design option for modularized construction; (4) 3D imaging techniques for enhancement of the tolerance measurement systems, and (5) risk management systems with a focus on transportation, re-alignment and rework risks. The connection among the stated research categories builds the initial platform of this research.

Chapter 3 presents the data collection and analysis based on the case study modules and commercial structural analysis programs. The validation of a methodology for module resilience is also included in this chapter, in addition to the evaluation of the proposed methodology and the presentation of the model, which improves module resiliency by optimizing structural costs, transportation, rework, re-alignment and safety risks (costs) on a project specific basis.

Chapter 4 summarizes the conclusions, recommendations and suggestions for future work in this field.

Chapter 2
Literature Review

This section builds the basis of the research by introducing modularization as a solution to the construction industry, modularization techniques, tolerances for construction, resiliency for modular construction, 3D imaging as an enhancement to tolerance measurements, and risk management systems. Knowledge gaps and the need for the research are thus identified.

2.1 An Introduction to Modularization

The construction industry has traditionally been craft trade based with skilled groups working together to complete a project on a site. This is often referred to colloquially as the "stick-build" paradigm. While modularization has been a part of the construction industry for many years, North America is now at a stage where much of the construction industry is shifting away from the stick-build paradigm and towards prefabrication and the use of pre-constructed modules in an effort to reduce construction time, expense and risk while providing improved quality (Burke and Miller 1998, Gibb 1999, Nadim and Goulding 2009, Sacks et al. 2010, Friedman et al. 2013, Yu et al. 2013). Modularization in construction has two main approaches: prefabrication of components and application of manufacturing principles. Haas et al. (2000) and Burke and Miller (1998) found that prefabrication and preassembly reduce jobsite congestion, lower environmental impact, result in higher craft productivity, and increase worker safety. However, added costs include extra materials for transportation reinforcement, transportation difficulties, and lower flexibility. Yu et al. (2013) contend that further savings can be realized through the application of lean production principles from the manufacturing industry to modular construction. The lean production principles of reduced variability, reduced duration, increased flexibility, increased standardization and continual improvement are readily applicable to modular construction (Sacks et al. 2010). Moghadam et al. (2012) investigated the integration of building information modeling with lean production, and demonstrated a reduction in waste, time and materials.

While research on lean production applied to modular construction has demonstrated clear advancements, opportunities to further optimize modular construction exist by addressing the technical challenges associated with the prefabrication, transportation and assembly of large, complex modules and resulting site-fit problems. The factory production of modules can also be made extremely accurate through the use of high dimensional tolerance control techniques and automated fabrication (e.g., cutting, welding, etc.)

under controlled environmental conditions. Maintaining the dimensional tolerance control during transportation and handling may present challenges, as the dynamic loads caused by acceleration and lifting, along with static loads caused by securing the module to the truck can produce a critical design load case that can distort and alter the alignment of the module. These errors in module geometry, along with non-conformity in site control dimensions and alignments, can lead to delays, rework and wasted materials, thus increasing project costs. This is the historically fatal flaw of modularization that shop fabrication precision and reinforced structures have not yet overcome. While innovative solutions such as adjustable length metal studs exist, modules often may not fit easily with each other on the site. The typical practice to minimize the risks associated with geometry and alignment problems is to specify very strict fabrication tolerances, and to design the modules to structurally resist the forces and imposed deformations during transportation, handling and erection in order to meet the strict tolerance requirements. This approach to tolerance control typically requires over-design from a permanent or final condition perspective, as over-sized structural members and bracing are required to achieve the stiffness required to minimize distortions during construction. Nevertheless, the additional costs associated with the over-design requirements for the temporary condition of construction are typically justified by the reduced costs associated with assembly or site fit enabled by tighter tolerance control. In addition to understanding such trade-off for modular systems, practices, barriers and benefits, it is important to clarify the tolerance definition for modular systems.

Modules act as structural building blocks. Load bearing and corner supported modules are the two different types of modules in high-rise buildings. Modules in such buildings are typically designed to resist vertical forces only. For horizontal loadings, additional measures such as a concrete core for taller buildings (>10 floors) are required (Lawson et al., 2012). High-rise modular buildings should be reinforced for sway stability. The notional horizontal forces in modular construction are an additional way of evaluating the sway stability of a group of modules and it represents the minimum horizontal force that is used to measure the sway stability of a frame. Normally, it corresponds to 0.5% of the factored vertical load acting per floor. The combination of wind and horizontal load should be such that the wind load should not be less than 1% of the factored dead load which is acting horizontally. This combination can be used in the absence of wind loading. Modules are settled around a core and transfer loads to the core (Lawson et al., 2012). In taller buildings additional forces and moments are produced in the walls of the modules. These forces are caused by the influence of installation eccentricities and manufacturing and are shown in Figure 1. This figure illustrates the elevation drawing of these actions. The key factors for

designing a high-rise modular system are (a) the additional forces and moments that are affecting the walls of the module due to the eccentricities and construction tolerances; (b) using the notional horizontal load approach and the design standard for steelwork and steel frames; (c) considering the second-order effects caused by the sway stability of a group of modules, especially for the corner columns; (d) concrete cores which transfer the horizontal loads to the establishing system, and (e) structural integrity for modular systems which control the robustness to accidental actions (Lawson & Richards, 2010).

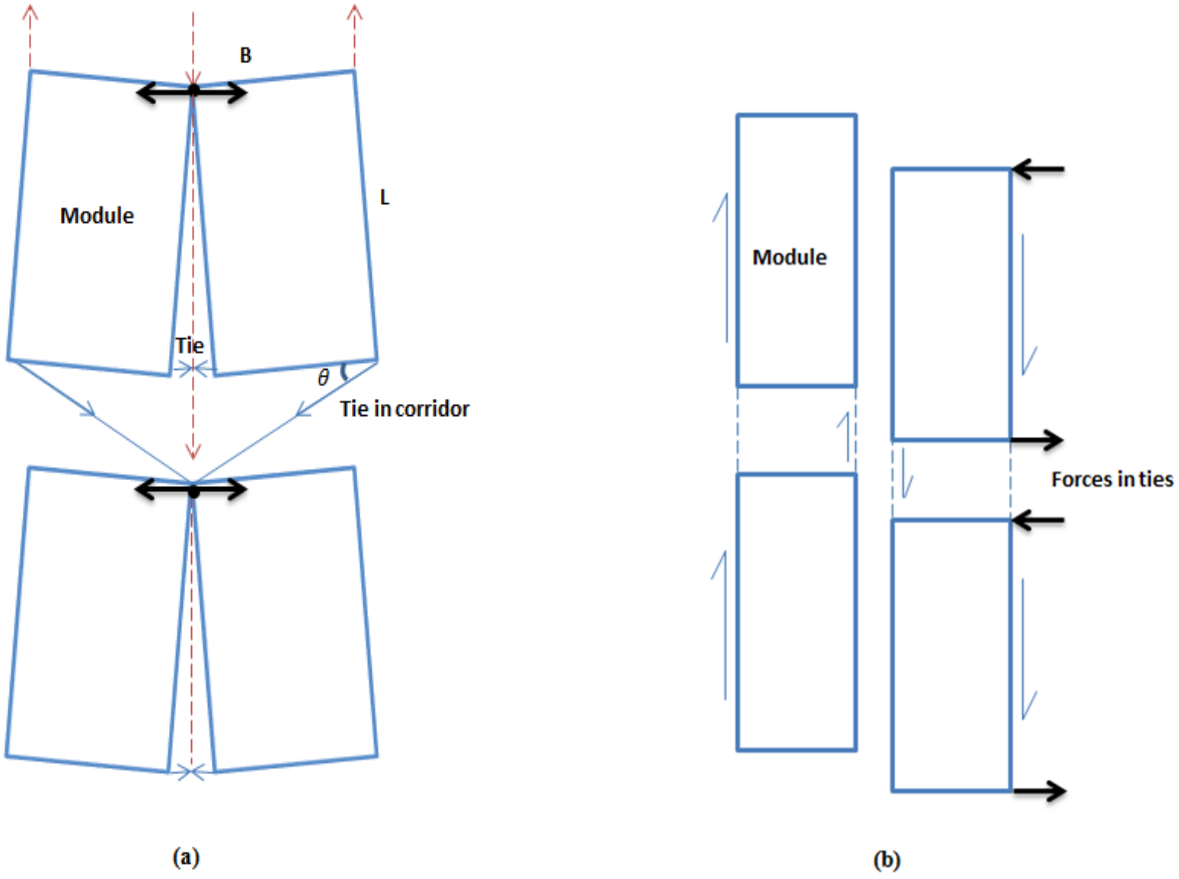

Figure 1: Elevation view of force transmissions between modules: (a) force transmission at corridor and bending action; (b) force transmission at corridor and pure shear (Lawson &Richards, 2010)

The stability and capacity of the modules are also extremely important for fire resistance and acoustic insulation. There are a few important factors which influence the fire resistance of a modular system. These factors depend on the fire protection on the interior faces of the module; eliminating the heat and fire spread by the fire barriers between the modules prevents the spread of smoke or fire in the void between the modules; the limited heat transfer through double-leaf wall and floor-ceiling construction of the modules (Lawson et al., 2012) .

While the current module design approach is a practical response to tolerance control and minimization of risk due to misalignment, an opportunity exists to develop a design process to define tolerances and practices for tolerance control (and/or relaxation via adjustable elements) to optimize module fabrication costs while minimizing the risk of rework and delays during assembly. For this reason the recent modularization practices will be reviewed in the next background section.

2.2 Recent Modularization Techniques, Benefits, and Barriers

With a brief overview of modularization, this section will summarize some of the modularization techniques in addition to the benefits and obstacles of off-site fabrication and modularization. High capital costs, challenging to achieve the economic scale, complex system interfacing, absence of ability to check the design at an early stage, and the routine of planning systems are some of the barriers that discourage the use of off-site fabrication and modularization. Manufacturing capacity, the risk-averse culture, disjointed industrial structures and concerns of loan lenders with non-traditional buildings are also some of the additional barriers that modularization industries may face. However, modularization reduces time, structural defects, safety risks, environment impacts, and life cost of the structure and increases productivity, liability and profitability. This encourages the use of modern modularization practices. In summary the benefits of off-site technology are overlooked due to the perceived barriers of "different" technology (Pan & Goodier, 2012).

An example of a preassembled, modularized construction project in Canada is a 2.8 billion lb/year ethylene plant. This plant consists of 154 modules, each weighing about 400 tons. These modules were built in Edmonton and transported to the site for installations. Approximately 15% of the installation work of this large ethane cracker was done off-site (Jergeas & Put, 2001). Assessing the key factors which impact the performance and productivity of oil and project in Alberta justify that modularization practices may lead to a better productivity in construction projects. Projects with severe weather conditions and labour deficiency are approximately 11% more productive with modularization practices

(Chanmeka, et al., 2012). A survey of 95 U.S qualified experts including clients (15), engineers (19), contractors (39), and precast concrete manufactures (22) was collected. The results of this survey stated that about 48% of the qualified construction experts have collaborated in more than 55 concrete prefabricated projects (Chen et al., 2012).

Off-site MMC (Modern Methods of Construction in house building) has been long used in the UK construction industry. Statistical analyses on the trend of off-site MMC applications justify that 58% of the house builders in the UK intent to increase their use of off-site MMC, by volume (Pan et al., 2008). The remaining 42% planned to continue their level of construction. The rationale behind the construction groups which like to continue the traditional building methods could be the risk-adverse attitude. The 58% that are willing to practice off-site MMC would like to increase the performance of their trial projects. In addition kitchen and bathrooms, external walls, timber frame structures, and roofs are the best solution for the growth in modularized construction and their growth rates are as followed respectively, 44%, 41%, 37%, and 33%. This encourages the use of prefabrication practices (Pan et al., 2008). However, high capital costs, achieving the economical scale and complex interfacing between the systems are some of the barriers for prefabrication in the UK. This exposes the fact that prefabrication is a beneficial method, however similar to all the other construction methods has some barriers and risks. It should also be noted that 71% of the off-site MMC is taken into consideration during the basic house design stage. Detailed planning application, outlining the planning application, other responses and pre-construction respectively consider, 23%, 13%, 10%, and 6% prefabrication in their design stage. Some of the derivers for using off-site MMC due to a survey of 100 house builders also included achieving high quality, minimizing on-site duration, ensuring certainty time, addressing skills shortages, reducing health and safety risks, etc. (Pan et al., 2008). Yet, there have still been doubts in practicing the recent modularization techniques.

Statistical studies in the UK justify that that 97% of the construction companies were willing to use off-site production (OSP) for time reduction, 86% for the quality improvements and 54% for decreasing the on-site accidents. The two least reasons for using OSP were to fulfill client request to employ OSP methods (43%), and to reduce cost (31%). In summary, offsite Production is recognized for having the potential to significantly change the production industry in the future however the major boundary is getting the entire industry “off the ground” so it can sustain itself (Nadim & Goudling, 2010).

Prefabrication assists with eliminating the extra cut-length and saves material and labour costs. Extra cut-lengths are associated with the conventional building methods for adjustments and fittings. With the application of prefabrication techniques, the extra cut-length will be eliminated. On-site alignment costs that are associated with labour hours are 3 times higher compared to the fabrication shop alignments (Innovations in Mechanical Construction Productivity-RT252). Material wastage costs, and additional meetings use up to 1.5-2 hours weekly between structural engineers and construction managers. All of the mentioned factors can be reduced significantly with the practice of prefabrication and modularization techniques. An analysis of this innovation was done on an assembly of pipe modules.

Figure 2 illustrates the conventional method of the pipe modules in comparison to the elimination of the cut-length (prefabrication) method. Analysis based on handling a 28"-7/8" wall P91 pipe assisted with the illustration of the eliminating cut-length benefits. 10 labour days was saved at a cost of $1,536,000, which is up to 50% savings in the labor cost. 98% of the pipe material needed for the cut-length was saved versus the 110% pipe material needed for the cut-length and 10% savings in the material. Merging all the saved costs on labor, material, and total cost improvements were found to be up to about 60% (Innovations in Mechanical Construction Productivity-RT252).

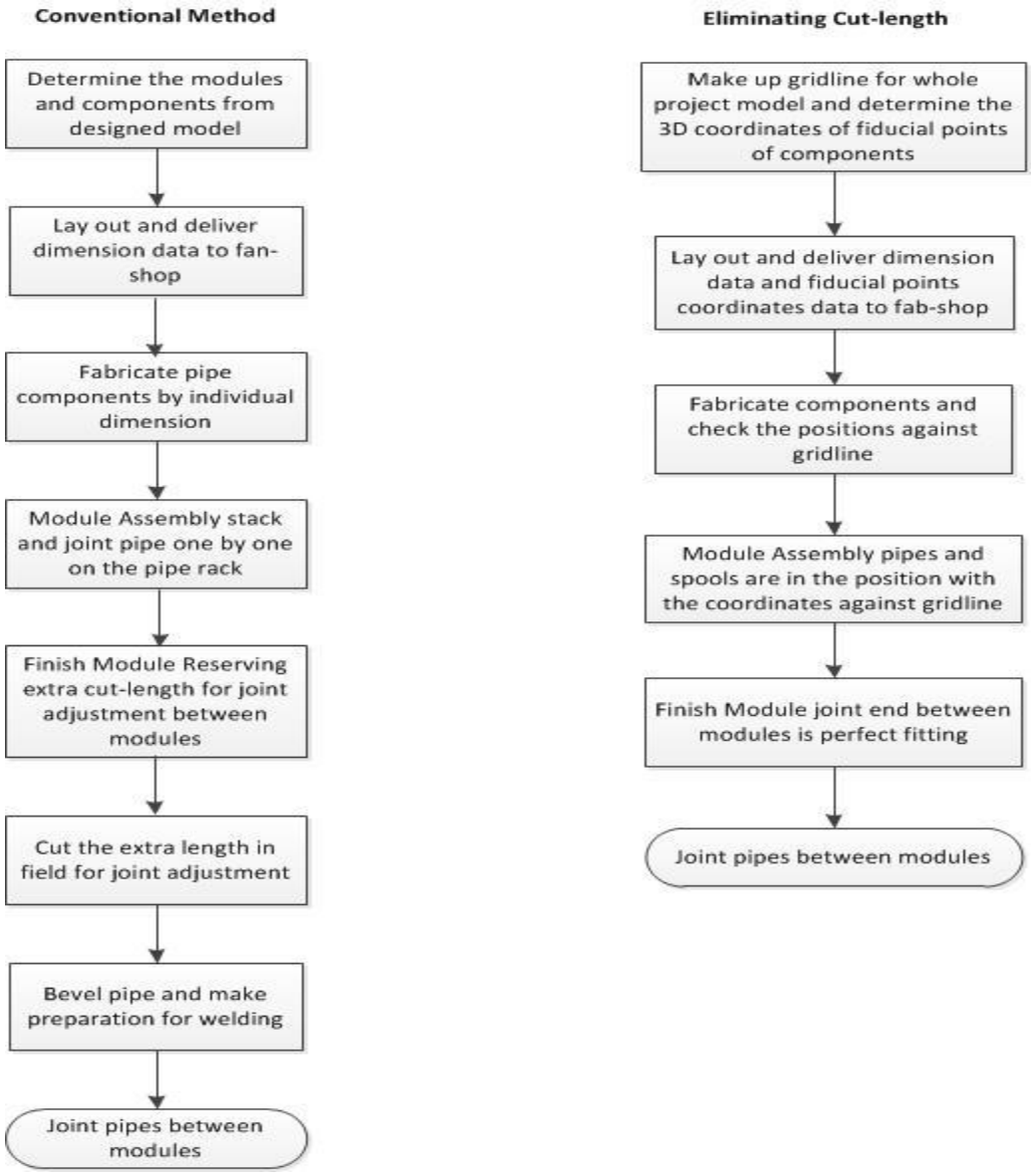

Figure 2: Conventional and modularized construction comparison (Innovations in Mechanical Construction Productivity-RT252)

Once the benefits and barriers of off-site fabrication are identified, builders will be encouraged to substitute the traditional building systems with the recent modularization techniques. However, the modularization process, techniques, and practices are complex and need verification and a deep understanding of modular systems at an early stage. For these reasons modularizations techniques and practices will be discussed briefly. The decision making process of modular construction is a method which needs verification. Investigations at the corporate, subsidiary firm and project levels have revealed

good practices and learning techniques from integrating the use of off-site production. Four of these practices regarding off-site fabrication are described below:

1. The importance of a strategic approach for improving business efficiency at an early stage, in comparison to the alternative construction techniques.
2. Organizational learning and information sharing will embrace the acceptance of off-site fabrication. In addition, the communication mechanism in companies will lead to the integration of prefabrication and promotion of innovations. This will help with the improvement of efficiency, commitment, and management efforts.
3. The off-site suppliers and contractors should be consulted at an early design stage. The expertise of the contractors assists with the early decision making process. However early arrangements in the supply chain maybe difficult and can lead to uncertainties of planning, housing market, and lack of supply chain knowledge for modern off-site fabrication technologies.
4. Companies which are committed to improving their design methods will benefit from standardization of efficiency and good practices. It should be noted that the modern fabrication systems increase repeatability and are favored for off-site fabrications. These systems demand the company to use specific off-site supply chains (Pan et al., 2007).

In summary off-site technology needs to be considered as a design option from day one, otherwise the design will not suit the off-site fabrication methods.

Maintenance costs over the life of a building are also an important factor that need to be considered in the prefabrication process. Bathrooms are one type of structural system which is widely designed offsite with the use of prefabrication techniques. For this reason researchers have done analysis on the maintenance cost implications of utilizing offsite bathroom modules. Maintenance costs for both labour and material were tracked over 3 years for student washrooms. The washrooms were divided into 3 categories: in-situ (built onsite); concrete modules, and glass reinforced polyester modules. The maintenance costs associated with the off-site modules were significantly lower than maintenance costs for in-situ bathrooms if poor decisions had not been made. The maintenance cost reduction was attributed to higher quality construction in the factory setting. In conclusion, the higher quality construction coupled with maintenance oriented design decisions, which would fully realize the benefits of modular bathrooms and lead to significantly cheaper lifecycle alternatives in comparison to in-situ construction (Pan et al., 2008).

Off-site and modular construction processes moreover assists with a reduction in injuries and increase of productivity in construction. A few of these off-site fabrication practices for safety are mentioned below:

1. **Delivery Method:** In order to reduce injuries associated with congestion, on-site material handling can be reduced by delaying the delivery of ready-to-go modules until all components are ready to be delivered to the exact location.
2. **Labour Costs**: Modular components replace construction work with assembly work on the construction site. Components that can be easily and rapidly fitted together will allow relatively simple assembly work. Assembly work requires fewer workers and workers with fewer skills, which reduces labour costs and will lead to improvements in productivity and quality of delivery.
3. **Risk Mitigation**: Delivering components as they are needed creates risk if the supply chain is disrupted. As a result, component requirements need to be predictable. A safety stock of components should be present at most levels of the supply chain to mitigate the effects of disruptions or delays in the supply process (Court et al., 2009).

Once the modularization benefits, barriers, and techniques have been identified, a detailed clarification of tolerance classifications and definitions will assist with building an enhanced basis of this research. Builders, who are encouraged to practice modularizations techniques, require knowledge on how to initiate this procedure. The initial step for designing modular systems, similar to other building systems is defining tolerance limits. The next section of this thesis will describe tolerances for construction.

2.3 Types of Tolerances in Construction

A tolerance is a permissible variation from a specified requirement and in the context of construction can be applied to many parameters including variation in dimension, quantity, alignment, position or form. Therefore, tolerance identification is highly important stage in the construction process. Industry experts clearly stated that, specified tolerances are generally much stricter than the value that can be achieved with the building process. The result of unobtainable tolerances is time consuming design and modification work on all of the components. The design of the components needs to account for achievable tolerances. Using a less ideal connection may actually simplify the process of joining components, if it has a relaxed or loose tolerance. Additionally the cost of components that can accommodate larger variations may be less than the cost of rework on components that are out of tolerance (Milberg & Tommelein, 2003). The desirable dimensional tolerance referred to as the “nominal dimension”, and the ± number around the nominal dimension is the tolerance. As an example for a 1 inch

diameter hole, the engineer knows that the exact number cannot be achieved. For this reason a tolerance value of ±0.01 inch, or ± 0.05, or ±0.01 inch will be considered (Berk, 1951).

The need for tolerances arises from the fact that deviations from specified requirements are unavoidable and may result from human error, limitations in fabrication processes, and imprecision in measurements, volumetric material changes (e.g., thermal, shrinkage, or creep strains), or deformations from handling and loading. Tolerances may be broadly categorized as:

- **Manufacturing**: is the permissible variation in the production of a component or module, and includes dimensional form and orientation tolerances.
- **Interfacing (site tolerance)**: defines the permissible variation in layout points or lines on the construction site or existing site or structure condition, and includes positional and orientation tolerances.
- **Erection**: is the permissible variation of the position and orientation of a point, line or surface of a component or module in its final position on site.

The accumulation of these tolerance categories defines the overall construction tolerance (Bureau of Indian Standards, 1990). The effects of these variations, and thus the different tolerance limits, are cumulative (e.g., manufacturing tolerance and interfacing tolerance affect erection tolerance). The tolerance escalation may involve an algebraic or statistical combination of tolerances depending on the types and scale of tolerances involved. Once types of construction tolerances have been categorized, the strategies for achieving, setting, and avoiding the need for tolerance specifications need to be discussed. This will assist with the definition of tolerance limits in the design phase and will be briefly overviewed in the next section.

2.4 Strategies for Achieving Tolerance Specifications

These strategies are categorized as:

- **Fabrication control:** As discussed earlier, fabrication control and early project planning will assist with achieving the correct specified tolerance values at the design phase which is prior to the project execution.
- **Stiffness:** Modular reinforcement will reduce the amount of distortion and displacement in the structural system. This allows for reduction in specified tolerance limits. This topic will be further discussed in the thesis methodology.
- **Flexible connection and mating systems**: Assuming the connection consists of a mate and a hole, the tolerance of the hole should in all scenarios be compatible with the tolerance of the mate. This compatibility allows for sufficient confidence level during assembly of different fitting sections (Berk, 1951).

With an input from manufacturing, quality assurance, and suppliers design engineers should identify where tight tolerances increase fabrications costs, and where tolerances can me more relaxed. (Berk, 1951). A variety of tolerance types are specified in conventional or stick-built construction, including bolt-hole dimensions, steel member dimensions and straightness, concrete reinforcement placement and clear cover. However, the specification of tolerances, and more importantly the interaction and accumulation of tolerances, is sometimes not considered in the design or construction processes. Such inattention to tolerances or the specification of unattainable tolerances may result in construction and site-fit problems, leading to delays and requiring additional resources (engineering, labour, materials) to resolve the problem.

Modular construction typically takes a proactive approach to tolerance specification and control. The general philosophy is to employ tight manufacturing tolerance control thereby minimizing dimensional variation of the modules. The additional time and expense of module fabrication to relatively tight or strict tolerances is justified through the reduction of site-fit problems during assembly (module to module, and module to site connections). While modular construction offers many advantages in comparison to traditional construction (Jaillon and Poon 2008, Lawson et al. 2012) the need for rework due to site fit problems still remains a significant risk to project performance and cost regardless of project type (Love, 2002).

Optimization of modular construction within a project, in order to reduce the variability and uncertainty resulting from site-fit problems and rework requires the development of a strategy or process for defining tolerance limits. A tolerance strategy would include an explicit definition of tolerance types and limits, as well as an understanding of the relationships between tolerances that define the accumulation or escalation of tolerances for the project. Definition of the tolerance strategy requires an analysis of the correlation between cumulative tolerance and risks and/or cost associated with site-fit problems and rework at each level. The relationship between tolerance definition and the resulting module fabrication, transportation and site costs associated with achieving a specified tolerance must be established. Optimization of a tolerance strategy for a particular project requires simultaneous consideration of both of these tolerance relationships.

For a single module, the maximum allowable tolerance in geometry could be taken as shown in Figure 3. The units for these limits are in mm. These limits are similar to Canadian Institute of Steel Construction (CISC) and American Institute of Steel Construction (AISC) limits for steel structures construction which will be described in Section 3.5.1.

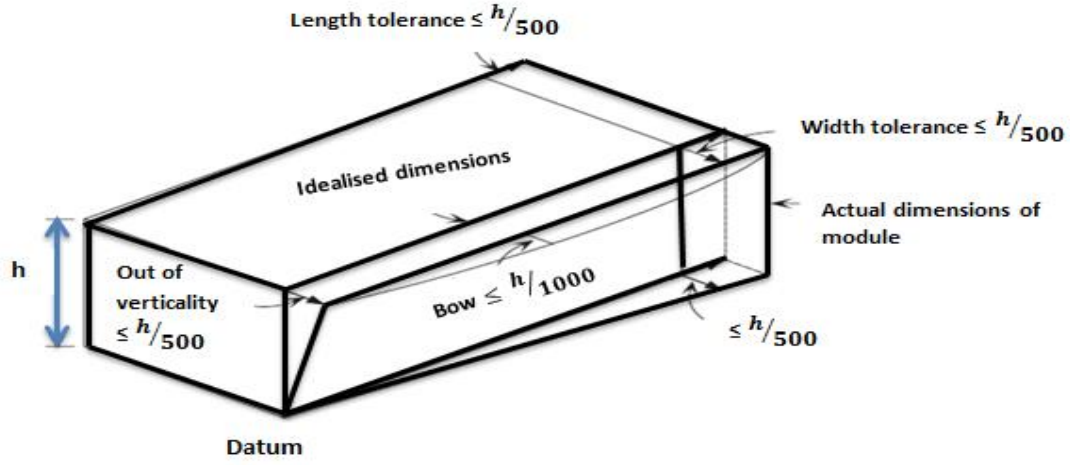

Figure 3: Maximum allowable geometric errors in fabrication of modules (Lawson & Richards, 2010)

Combined eccentricity is an additional factor that affects the constructional tolerance. This eccentricity on a vertical assembly of modules considers the effect of eccentricities of modules placed on one another and lessens the compression forces on the walls acting at the increased eccentricity with respect to the structural height and is shown in Figure 4. Light steel walls in compression are unable to resist build-up moments caused by axial loads transferred by direct wall-wall bearing. Eccentricities and module installations cause build-up moment and emphasize the local bearing stresses at the base of the wall; therefore, the corresponding horizontal forces requisite for equilibrium are transmitted as shear forces into ceiling, walls and floors of the module. In this case the effective eccentricity Δ_{eff} multiplied by the compression force in the modular base is the total additional moment acting on the base of the module as shown in Equation 1 and Equation 2 (Lawson& Richards, 2010). The units for these equations are in mm.

Equation 1: $$\boldsymbol{M_{add}= P_{wall}\Delta_{eff=}P_{wall}[\frac{(n-1)}{n}+2\frac{(n-2)}{n}+3\frac{(n-3)}{n}\ldots+\frac{1}{n}]\times(e+\frac{h}{1000})}$$

Where P_{wall}= nW_u and is the compression force at the base of the ground floor module, n is the number of modules in a vertical assembly, e is the average positional eccentricity per module, h is the height of the module and W_u is the factored load acting on each module. The equation shown below is a good approximation for the effective eccentricity formula and holds for the effective eccentricity of the vertical stack of modules as a function of n:

Equation 2: $$\Delta_{eff}= [\frac{n-1}{6}] \times 8n$$

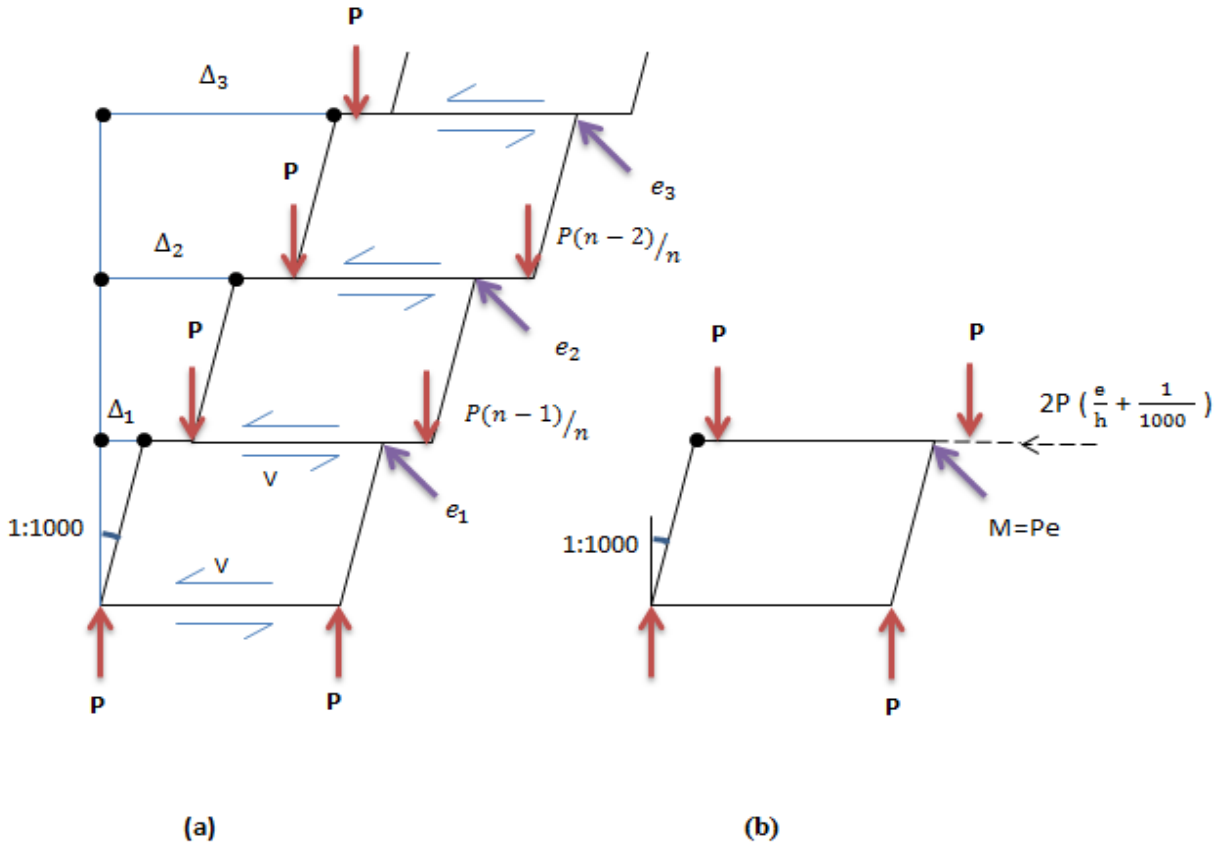

Figure 4: Elevation view of combined eccentricities acting on the ground-floor modules: (a) end wall shears due to eccentric loading for a four-sided module; (b) transmission of eccentric loading to the initial system for corner-supported module (Lawson&Richards, 2010)

A brief overview of strategies for achieving and controlling construction tolerance specifications has been discussed; however structural sections need to be manufactured prior to the modularization step. For this reason a tolerance control method for the manufacturing phase will be described in the next section.

2.5 Tolerances Control in Manufacturing

Tolerance charts for dimensional control are a well-established technique used for dimensional control in precision manufacturing. This assists with cost reduction, practicality, precision, and establishing maximum allowable tolerances. Elements of historical tolerance charts include:

1. Continuous justification of dimensional planning.
2. Assuring that specified tolerances meet the allowable tolerance limits.
3. Reduce calculation errors and proofs that discrete steps, once followed by each other, will lead to a satisfactory result.
4. Display a record of figures which are easy to follow through.
5. Provide sufficient stock for each cut, even in rare conditions.
6. Can be referenced for describing the process and for checking the feasibility of an anticipated alteration.
7. Time savings for necessary result interpretations, once changes are made (Gadzala, 1959) .

There are a few points which need to be considered for constructing a manufacturing process tolerance chart:

1. Reference faces in the product design are not the best procedure from a manufacturing point of view, for this reason the location surfaces should be precisely chosen and discretion should be used in choosing other surfaces.
2. “Stack-up” problems are caused once location surfaces are changed; therefore as few surface location changes as possible should be made in the design.
3. Dimensions should be designed so that they could be checked in the holding device and after the design phase.
4. The chosen dimensions should permit the use of standard tools and techniques without lowering the fabrication quality.
5. Tolerances must be economical and rational and stocks must allow cutting and clean up in an unusual situation without exceeding the permissible tolerance allowance.

6. During indirect machining positions, similar to surface machined, the tolerances on the working dimension should be large enough to allow for the actual tolerance on the cut to be achieved.
7. Any conditions that may be conflicting with the acceptable practices (mentioned above) and affecting tolerance limits must not be used.

Figure 5 illustrates a dimensional chart for tolerance control in manufacturing from 1959. It should be noted that balanced dimensions are to be shown after heat-treating, machining a diameter, and plating. Heat-training is necessary once the piece shrunk or grown in the design process. Machining a diameter only should be done once the length of the diameter has changed and plating, when the plating thickness affects the final dimensions (Gadzala, 1959). Such concepts may be applicable eventually to prefabrication processes in construction as well. The dimensional chart shown in Figure 5 can be constructed using the steps below:

1. Draw the entire cross section of the part and the vertical lines such that the lines do not coincide. On lengthy charts, number these lines and repeat the numberings at approximately every 2 ft of the chart length so that the accumulation of tolerances can be tracked.
2. Below each of the numbers/letters draw a horizontal line and create columns to the left and right side of the columns that have already been formed using the cross section of the part. The added columns on the right show the stock removal and balanced dimensions. The added columns on the left represent the operations number, working dimensions, and machine specifications.
3. The operations number and machine specifications of all operations that affect dimensioning must be added for tolerance calculations. Heat-treating, stabilizing, carburizing, and hardening are some of the operations which effect the dimensioning.
4. The lower right side of the chart represents the resultant dimensions and the ultimate blueprint dimensions for assessment. In this part the final blueprint and resultant dimensions should be added together.
5. Each machining operations should have a designated locating surface shown by X. Each prospective dimension for individual operations should have a horizontal line. The surface measured from is shown by a dotted lined and the machined surface is designated by an arrowhead pointing to it. The working dimensions are shown from a dot to an overhead and resultant dimension are the extending lines from a dot to a dot.

6. Tolerances (not the mean dimensions) should only be allocated to linear working dimensions, eliminating the chamfers for now. Once the resultant tolerances are computed at the bottom of the chart, the mean resultant dimensions can be added to the chart using the mean blueprint dimensions.

7. Compute tolerances for all stock removals and add the basic-stock-removal (no tolerances) to all of the working dimensions. Check the chart and make any necessary adjustments at this step. Estimate and insert the mean values for working and heat-treatment balance dimensions from the bottom of the chart moving upward. Add, or subtract the basic stock removals to or from the resultant mean whenever the surface is cut in machining or changed length in heat-treating.

8. Insert the working dimensions and operation numbers for all diameters and compute all the necessary diametric chamfers. Check all the parts of the tolerance chart and if the procedure is followed accurately, it may not be obligatory to record the balancing dimensions. Balance dimensions as mentioned earlier are after heat-treating, machining a diameter only, and plating.

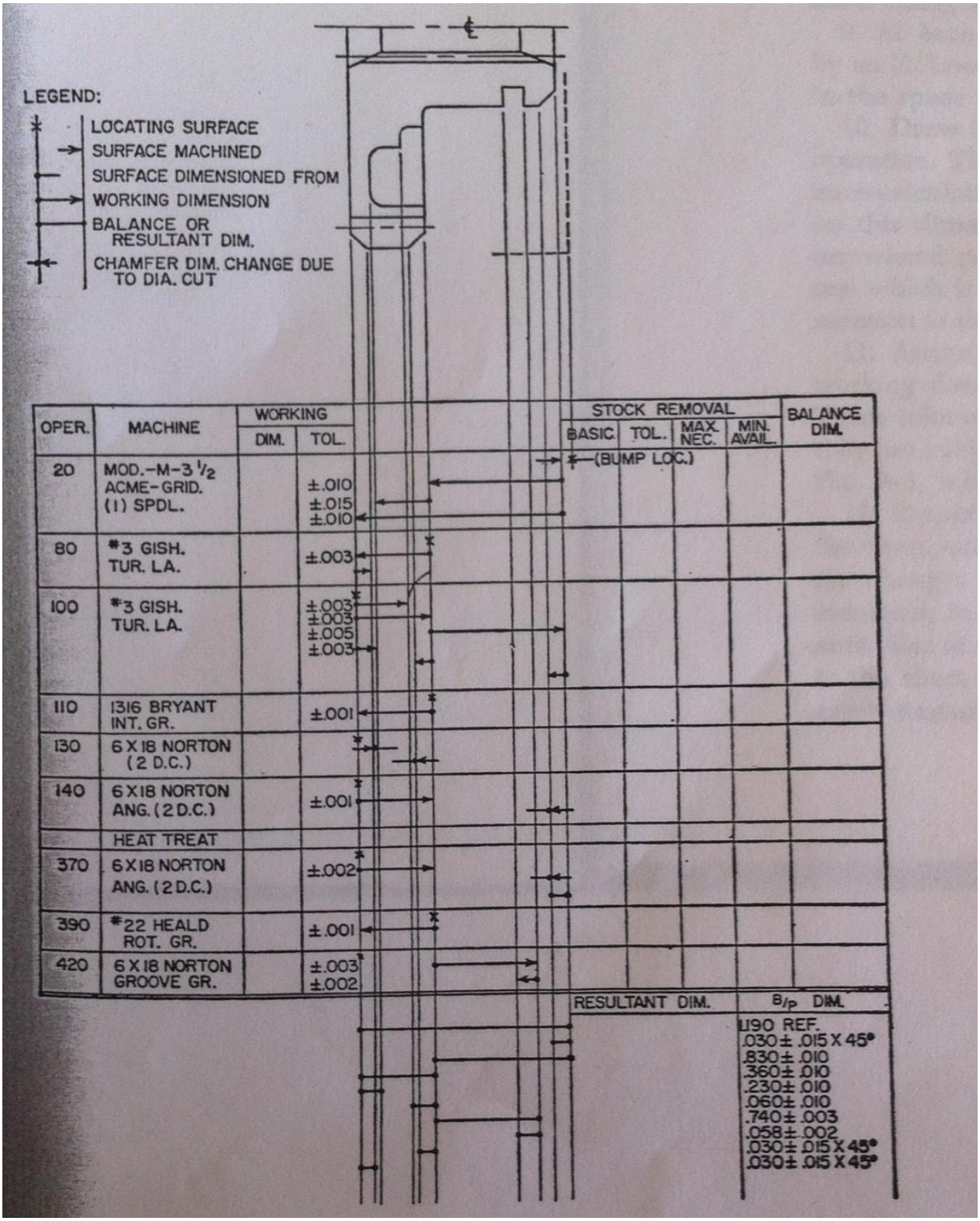

Figure 5: Tolerance chart (Gadzala, 1959)

2.6 Resilience as a Design Objective for Modular Construction

The concept of structural resiliency is prominent in modern seismic design and failure analysis. Simply stated, seismic resilience implies that the structure has been designed to reduce the probability of failure during a seismic event, to limit the consequence of failures that do occur, and to reduce the time to recover from a failure. Seismic resilience may be applied to individual structures, or to entire communities, and researchers have attempted to quantify the resilience of systems for the purposes of comparing different strategies and demonstrating readiness. The features of a resilient seismic system may be described as robustness, redundancy, resourcefulness, and rapidity (Bruneau et al. 2003). The concepts of seismic resilience can be applied to other situations, including modular construction. The four features of a resilient seismic system can be reworked to be applied to modular construction with regard to tolerance control and minimizing assembly and construction risks and costs, which is as follows:

Robustness: strength and stiffness of modules to withstand loading associated with fabrication, handling, transportation and assembly/erection without experiencing unacceptable degradation of geometric control (i.e. out of tolerance) or loss of function;

Redundancy: extent to which modules, or elements of modules, are substitutable or adaptable in the event that degradation of geometric control or loss of functionality occurs due to handling, transportation and assembly/erection;

Resourcefulness: capacity to identify errors in geometry, out of tolerance or loss of functionality in modules or elements of modules, and to establish priorities and develop solutions to correct or compensate for the problems; and,

Rapidity: rate of resourcefulness and the capacity to meet construction timelines and assure quality while minimizing costs, risks and future problems.

While current approaches to modular design and construction have primarily focused on achieving cost efficiency and "rapidity" through "robustness," several concepts and methodologies exist that could be applied to further improve cost efficiency by more explicitly addressing what is described above as "redundancy" and "resourcefulness." These include: (1) 3D imaging and object fitting, (2) dimensional flexibility using adjustable metal studs for instance, and (3) structural system identification and principals applied to re-alignment planning and work. These tools would facilitate a deeper understanding of typical module distortions that may occur during handling, transportation and assembly/erection so that they are considered in design. As well, tools may include the use of onsite 3D imaging of modules and real-time

analysis to determine the optimal pattern of adjustments to facilitate field-fit, whether resorting to adjustable elements, structural realignment or a combination. Moreover, the potential use of advanced realignment concepts (e.g., system of controllable tension elements within or attached to the module) could be explored as a means to rapidly correct misaligned modules. Encompassing these technical approaches must be a lean construction philosophy and set of processes, in order to realize the full benefits of the solutions developed. Each of these concepts is described briefly below.

2.7 3D Imaging and Visualization as Tools to Enhance Module Tolerance Measurement

Measuring the deviations in geometry and alignment on construction sites is a challenging task that needs to be performed in order to monitor and control construction processes including tolerance control. Traditional methods for tolerance measurement are prone to error and lack sufficient level of automation. With tremendous advances in computing and processing technology, 3D imaging has been introduced as a key tool for quality monitoring and tolerance measurement which is particularly applicable to modular construction (Bosche and Haas, 2007). A comprehensive study on existing approaches for reconstruction and infrastructure object recognition using 3D imaging that are commonly used in the construction industry has recently been done by Brilakis et al. (2012). These techniques assist with restoring and urban improvements of infrastructures. For measurement purposes, 3D image (point cloud) registration is a solution to enhance the comparison between the as-built status and the original 3D CAD drawings. This comparison results in the identification of any incurred defects and the corresponding required corrective realignments in a timely manner. The fabrication errors or other tolerance problems resulting from transportation and handling are then caught early and before causing significant construction delays and rework costs.

3D imaging is a specific type of data visualization and should not be confused with simulation. Simulation is used to model the project procedures with the goal of understanding and improving construction projects; however, it may be misinterpreted without the usage of visualization. The combination of visualization and simulations assists with a detailed-level model to lower the chances of misinterpretation of information and production procedures. The main differences between simulation and visualization are as follows:

1. Construction participants which have no or little knowledge regarding simulations techniques, cannot fully understand the process, however 3D visualization assists with a quick and easy way of understanding structural systems.
2. Workspace requirements and limitations are not provided in a simulations model, 3D visualization, on the other hand contains information such as coordination of the components which are required to identifying the work space.
3. Simulation models focus on movements of a target object; however 3D imaging and data visualization provides detailed information of the construction activities.
4. In the simulation models the identification of the schedule errors cannot be done easily, on the other hand 3D visualization provides animations of the construction activities. Therefore, schedule errors can be identified easily.

However, researchers argue that the combination of 3D visualization and simulations can assist with a better understanding of the new manufacturing systems. This will decrease rework costs and save time. Animation also assists with predicting spatial crew interferences and identifying space limitation. In summary, visualization allows simulations results to be checked from a practical point of view (Han et al., 2012). Once the 3D imaging techniques for the measurement enhancements have been verified, the risks of the various 3D imaging and modularization techniques need to be discussed in order to enhance the modularization process. The next section of the thesis will describe the methods for reducing risks associated with construction projects and modularization techniques.

2.8 Risk Management

An understanding of risk analysis is required to make informed, logical decisions. As outlined by Kahneman and Tversky (1979), people have a tendency to consistently make illogical decisions when risk is involved. Risk analysis procedures are one way to avoid making this type of mistake. Similar decision systems have been used in modular construction in the past. Song et al. (2005), presents a decision making tool for the applicability of modularization for a given construction project. Through their work with industry partners, Song et al. found that their tool was useful for initiating discussion, providing transparency, and creating team alignment. It was also easily maintained and could be used to identify key factors and risks in the use of modularization. Additional rework reductions models (Rework Reduction Program) were presented by Zhang, et al., (2012); by the aim of reducing the field fit rework. The RRP

reduces rework with four procedures: (1) rework tracking and source organization, (2) evaluating the rework and its origins, (3) action planning, and (4) implementing the changes into the system.

Risks in a construction projects are typically measured based on three main steps: (1) identifying risks and including them in a "risk register" (2) qualitatively and then quantitatively analyzing risks, and (3) treating risks through strategies such as avoidance, transfer, acceptance, and mitigation. Risks in modular construction include: (1) module deformation during transportation handling or lifting, (2) module misfit due to deformation, fabrication error, site construction misalignment, erroneous as-built information, interface design errors, and, (3) unpredicted tolerance escalation due to sequential module joining and increasing dead load defection and second-order effects in tall structures.

Most of the risks researchers that emphasize are safety risks with high severity risks for large construction activities; however, low severity safety, high frequency risks need to be targeted as well. The construction of a concrete formwork was chosen for the analysis of low severity risk (Hallowell & Gambatese, 2009). Modularized and prefabricated systems are similar to formwork systems due to their complexity and similarity in risks. For this reason, the analysis of this formwork can assist us with analyzing the future model. To initiate this methodology, first various types of risk classifications were identified. With respect to the construction safety book, there are 10 safety risk classifications: Struck by, Struck against object, caught in or compressed, fall to lower level, fall on same level, overextension, repetitive motion, exposure to harmful substances, transportation accidents, and other (Hinze, 1997).

For measuring the low severity, high frequency risks, two basic equations were used; Equation 3 and Equation 4 show the unit risk, and cumulative activity risk equations (Jannadi & Almishari, 2003).

Equation 3: $\boldsymbol{Unit\ Risk = Frequency \times Severity}$

Equation 4: $\boldsymbol{Activity\ Risk = Severity \times Exposure \times Probability}$

$$Severity = potential\ severity\ of\ hazard\ associated\ with\ the\ activity$$
$$Exposure = degree\ of\ exposure\ of\ hazard\ associ\ ated\ with\ the\ activity$$
$$Probability = likelihood\ that\ damage\ will\ occur\ if\ a\ hazardous\ event\ takes\ place$$

The understanding the formulas mentioned above provide a better understanding of the "risk", "exposure" and "severity" definitions. It should be mentioned that with respect to the above mentioned formula:

Equation 5: $\boldsymbol{Cumulative\ Risk = Frequency \times Severity \times Exposure}$ (Hallowell & Gambatese, 2009)

Exposure and severity in the above formula have the same definition; however frequency is a score which identifies the incidents per working hour. At this stage construction activities need to be identified in order to define low severity, high frequency risk of a concrete formwork. Some of these activities include, ascend/descend ladder, static lift, nail/screw/drill, motorized transport, etc. Each of the formwork construction activities has an exposure, frequency and severity score. Work inspection and planning for subsequent activities have the highest exposure value. Having the risk value defined as $^{\text{Severity}}/_{\text{Working hour}}$ among the safety risk classifications by Hinze, exposure to harmful substances had the highest and repetitive motion the lowest risk value.

In order to determine the highest risk activities in formwork construction, the total safety risk score was added to the risk value for each activity in the risk classifications by Hinze, which was explained earlier. The risk classification methods used for this methodology are the Hinze classification method, and low severity, high risk formwork construction activities (e.g. lubrication and preparation). The added risk value for both risk classifications justify that, lubrication and preparation (18.67 S/w-h), ascending and descending ladders (1.86 S/w-h), accepting and loading materials from a crane (0.51 S/w-h), and motorized transport (0.48 S/w-h) are the activities with highest risks. The lowest risk activities are: inspection and planning (0.01 S/w-h), static lifts (0.03 S/w-h), and nailing, screwing, or drilling form components (0.03 S/w-h). The total risk value for constructing a concrete formwork, including all activities, is 22.63 S/w-h. In addition the two mentioned risk classification methods, the risk associated with formwork activities can also be categorized to traditional formwork construction, panelized formwork and slipping forming. This classification method indicates that working hours and risk values decrease respectively once the construction of concrete formwork changes from traditional to panelized and slip forming. However, once the risk values for different formwork activities (e.g. lubrication/preparation, crane material, etc.) are added together, traditional and slip forming respectively have the lowest (S=1366) and highest (S=2004) risk values (Hallowell & Gambatese, 2009).

Construction Hazards Prevention through Design (CHPtD) is an additional safety/risk factor which should be considered for the safety of construction workers. Toole and Gambatese (2008) have reviewed the underlying processes of CHPtD which change over time. CHPtD follows four specific routes: increased prefabrication, use of less hazardous material and systems, increased application of construction

engineering, and spatial investigation and consideration. Prefabrication is an environmental friendly process and allows the location of the work to be shifted to a less hazardous location. Tasks which are moved to a factory location are safer; moreover the use of automated equipment assists with improving the environment. Construction activities such as bending, heating, screwing, etc., are generally safer with the permanent equipment in comparison to the portable field equipment. Increasing the use of less hazardous materials and systems also assists with CHPtD. Materials are generally specified by performance and cost, however safety in a rarely considered factor. Designers should be aware that materials with the same cost and performance level have the ability to be less hazardous and safe during installation. In summary, this method proposed that CHPtD will change among increased prefabrications, increased use of less harmful substances, increased construction engineering techniques, and increased 3D investigations; however the risk reduction associated with this method has not been quantified.

In addition to the Construction Hazards Prevention through Design methods and procedures, tipping points are an effective factor in complex construction projects. Tipping points are conditions that cause change in the behavior of the system. Researchers have done analysis on identifying tipping point dynamics which explains the failure of nuclear power plant projects. Tipping points are used to describe the project progress and manage the project failure. Analysis verifies that projects are less robust to rework, schedule pressure, and are more robust to project deadlines. This methodology can assist project managers with understanding relative sensitivity of project specific factors with asking simple questions like “what systems in this project are likely to require the most iteration (rework)?”, and “How can this iteration be minimized?” “Could this iteration lead to work that has not been anticipated (Ripple effects)?” (Taylor & Ford, 2008).

Rework is also an additional risk factor that affects poorly planned construction projects. Reduction of rework in projects requires an understanding of constructability knowledge and plan of contract. A case study has identified the factors that need to be considered in order to reduce rework in construction projects. This methodology proposes that production and management of contract documentation, client initiated modifications, and unproductive use of information technology are the key factors causing rework in construction projects. Planning and management of the site and subcontractors is also an area which need attention for rework reduction purposes. This analysis indicates that design management and procurement strategies have not been executed successfully. This procurement modeling for reducing client initiated changes, encouraging the adoption of value management (VM) techniques, and improving production and management of contract documentation is shown in Figure 6 (Love, et al., 2004). This

method ranks the procurement methods in a 1(ineffective) to 5(highly effective) point scale, and identifies that team building, constructability analysis, and pre-qualifications have the highest rankings in the procurement strategies. These strategies relatively had a mean value of 3.35, 3.12, and 3.10. This implies that this methodology can quantify the risk reduction and impacts within the procurement techniques. A questionnaire survey on 161 construction projects for benchmarking rework at the project life cycle interfaces reveals that inadequate managerial and supervisory skills, ineffective use of quality management practices, damage to other trades due to carelessness, low labor skill level, and the use of poor quality materials respectively have high to low impact on rework for the contractor. For the project manager and design consultants, the rankings are the same; except for ineffective use of quality management practices which ranks first and inadequate managerial and supervisory skills that ranks second for rework (Love & Smith, 2003).

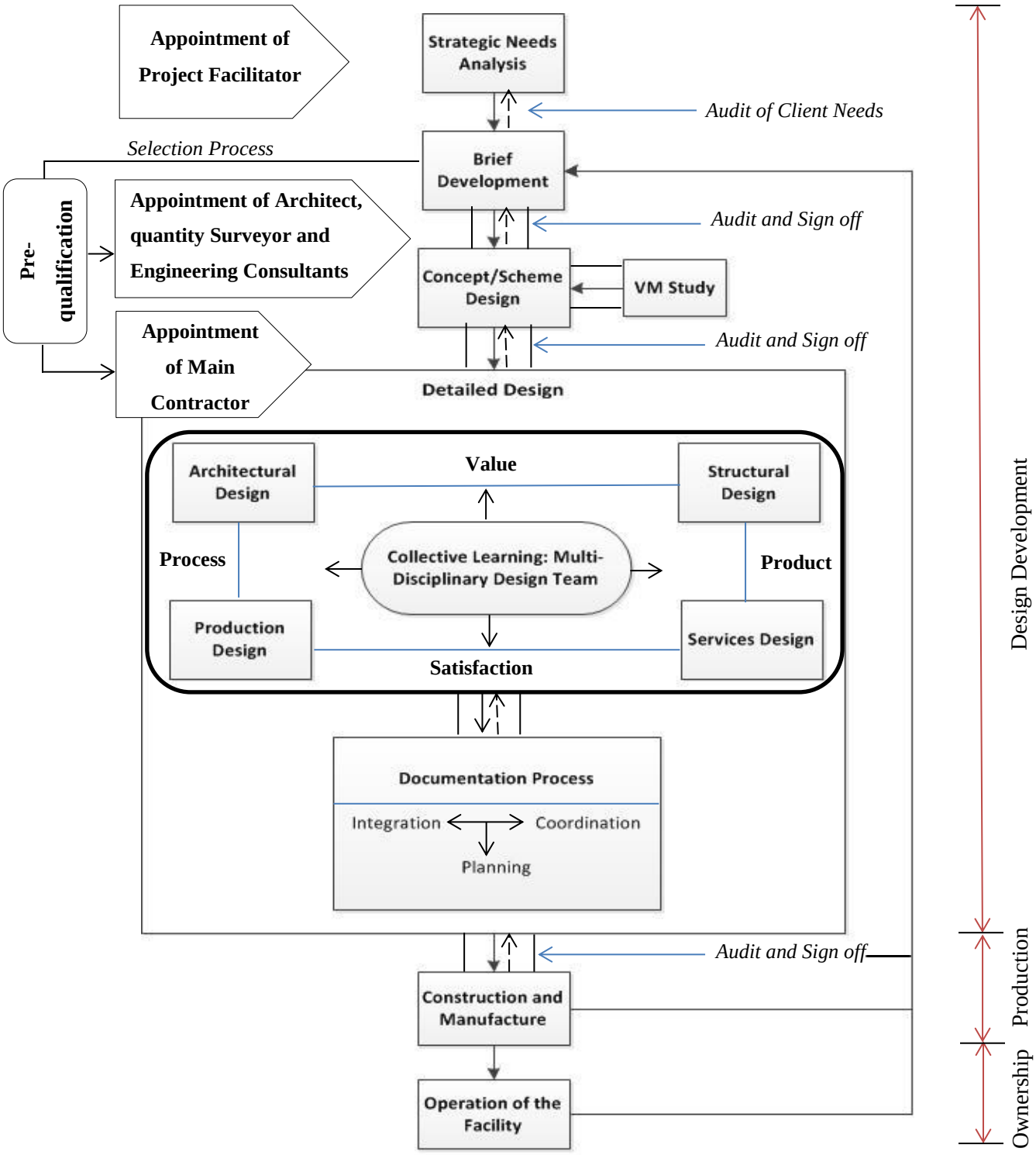

Figure 6: Rework reduction model (Love et al., 2004)

Further investigation has been done by researchers for the reduction of rework and its associated risks. With categorizing industry groups, work types, project nature, project sizes, project locations, and types of rework, project cost performance can be improved with the rework reduction. Industry groups can be categorized to buildings, heavy/light industrial and infrastructure; project natures as add-on, grass rods, and modernization; project sizes as <$15MM, $15MM-$50MM, $50MM-$10MM, and >$100MM; project locations as domestic and international; work type for contactors as construct only and design and construct. Rework sources can be caused due to owner change, design errors/change, design change, vendor error/change, constructor errors/change and transportation errors. Measuring the impact of rework on construction projects verifies that rework mostly affects light engineering owner reported projects and heavy industrialized contractor reported projects. Modernized and domestic projects chosen from the project classification above, with a cost range of $50 to $100 million have the highest liability (in terms of rework) for both owners and contractor. In owner and contactor reported projects, the owner change and design errors had the highest impact on rework. Design errors in owner reported projects have greater impact in comparison to design change in the contractor reported projects. As a recommendation, project managers should be aware of rework cost impacts during the pre-project drafting and quality management phase. Project owners should implement a tracking and controlling systems for constructor errors/design errors (Hwang et al., 2009).

4D CAD models were also found to be an effective tool for displaying and communicating the risks of a construction project. Kang et al. (2013) developed a systematic, quantitative method for assessing and communicating the risk associated with a construction projects. Once the background information on modularization, defining construction tolerances, modular resiliency, enhancing tolerance measurement techniques, and risk management has been covered, a risk based approach to module tolerance specification could be described in detail with a better understanding of the basis of the research.

Chapter 3
Development of A Risk Based Approach to Module Specification

While the effectiveness of a strategy designed for a theory of tolerance for modular design has been reviewed in the previous chapters, the methodology and validation of this strategy has not yet been described. This validation is obligatory for gaining insight into the proper application of this method and to distinguish the key factors, which influence the boundaries and outputs of this method. The purpose of this chapter is to provide a rationale for the research methodology and attained results based on a tolerance configuration on an industrial module chassis.

3.1 Background

As discussed in the literature review, previous researchers have developed a computerized tool that affects the decision making process on the use of prefabrication, preassembly, modularization and offsite fabrication in the construction process (Song et al., 2005). Similar research has been done for improving decision making during fabrication and choosing modularization as a key to reduce construction costs. In order to reduce the adverse effect of miss-fittings in modularization, a framework needs to be defined for setting tolerance limits for modular structures. Industry experts clearly stated that most of the problems associated with complex modules are process management problems between organization units and fitting adjustments that need to be done at each stage during fabrication. This implies that a methodology for tolerance strategy can reduce the risk associated with miss-fittings and rework. The first section of the research methodology will cover the modular prototype options.

3.2 Identification of Modular Construction Applications and Module Types for Case Study

The identification of the various types of modular prototype scenarios in the construction industry assists with the basis of this study. As mentioned in the first chapter on this thesis, the design requirements will be identified based on the anticipated conditions during transportation, handling and erection. The design requirements will also be identified based on the permanent/final conditions. For this reason a case study should be identified and tested under the stated construction phases. Pipe module chassis, room cluster (e.g., hotel), stacked structural chassis and interior building module (e.g., Hospital and bathroom) are the four types of modular construction scenarios that can be selected for testing and refinement of the tolerance and resilience strategy which will be described in the following steps. It should be noted that

bathroom modules can also be categorized under the utility module class. An example of the stacked structural chassis and interior building module is shown in Figure 7. This figure illustrates the under-plan of a modular 32-story apartment tower. In this module, living units were pre-assembled in the factory from the modules shown in the left side of Figure 7. Each unit is based on a steel-tube chassis. Finishes and mechanical systems would be added to the module before the modules are shipped to the site. They are stacked and mated after shipping and most of the mating is done from the module roofs in order to avoid disturbing the living units shown in the right side of Figure 7 (Post, 2013).

The modular construction scenario selected for this study is an industrial pipe module chassis (pipe-rack), shown in Figure 8. This pipe-rack module is from an industrial energy-sector project, and design information including detailed geometric and structural properties was made available by the industrial partner for the purposes of this research. The structural system in this case study is clearly defined and relatively simple and the applied loading from the supported piping could be estimated with good confidence. The module is part of a much larger assembly in an industrial facility. Unfortunately, the final configuration of the assembled modules, including details of the overall structural system and associated system-level loading, was not made available for this research. A structural analysis model was created for this module using the design information supplied by the industry partner. Details are provided in the following section. The structural analysis model was used extensively in the development of the tolerance strategy for modular construction. Although the case study used in this research was an industrial piping module, the concepts and methodology developed is general and can be applied to any modular construction scenario.

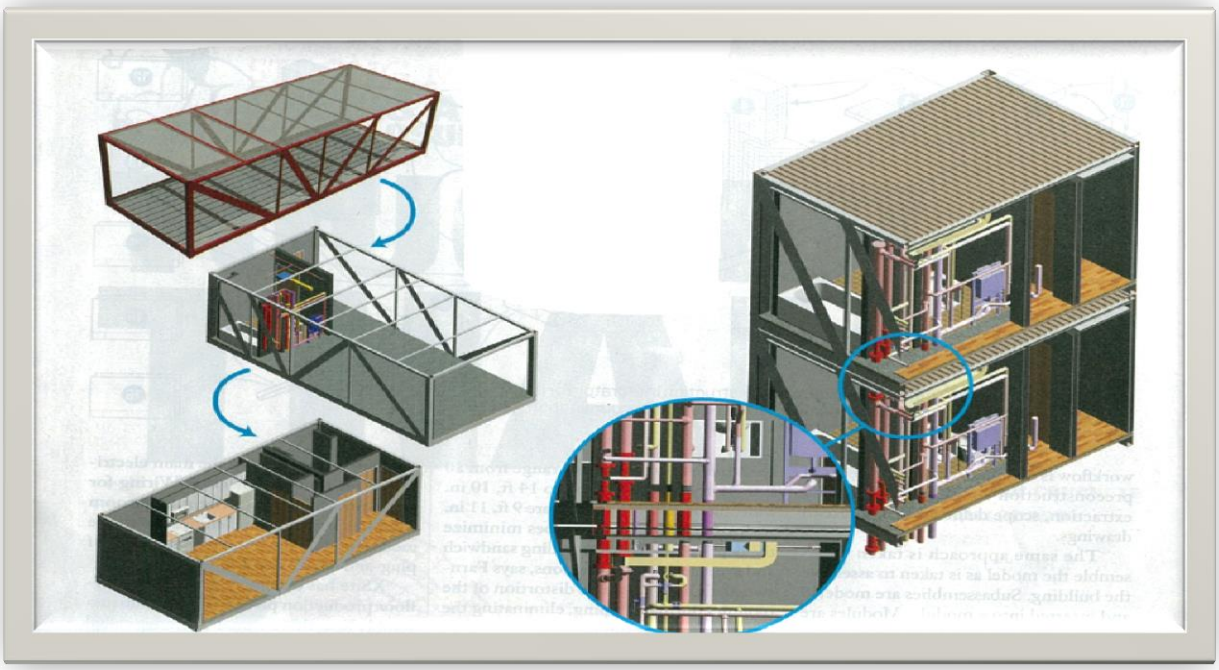

Figure 7: Stacked structural chassis and interior building module (Post, 2013)

Figure 8: Industrial piping modular chassis

3.3 Structural Analysis Model of the Case Study Module

A three-dimensional (3D) structural analysis model of the industrial piping module (Figure 8) was created using the as-built 3D laser scans, as-planned AutoCAD, Autodesk drawings and the structural drawings provided by the industry partner. The structural design drawing of this module was used to determine the section sizes and dimensions for each member in the module. All members consisted of standard structural steel sections. A commercial structural analysis program, SAP2000, was used to develop the model and perform structural analyses and design checks. The overall geometry of the SAP2000 model is shown in Figure 9. The model was assumed to be supported at each of the four corner columns, as well as at the two interior columns. Pinned supports were assumed at all six locations. The model geometry in SAP2000 takes the Z-axis in the vertical direction. The X-axis is aligned in the longitudinal direction of the module, as indicated by the axis arrows shown in Figure 9. All member connections were assumed to be rigid (i.e., transmit force and moment in all degrees of freedom), except as discussed in later sections.

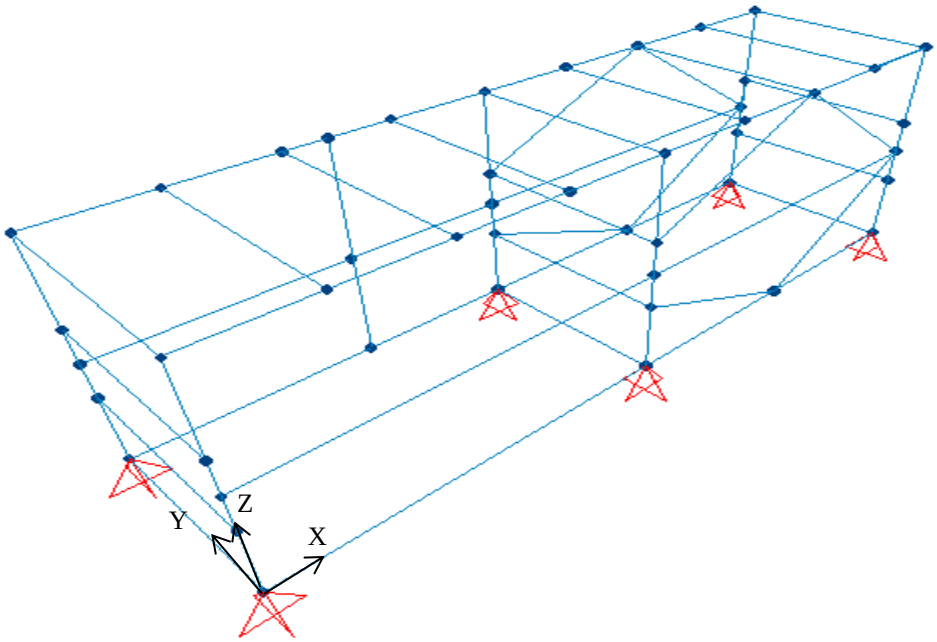

Figure 9: SAP2000 model of the industrial piping modular chassis

3.4 Design Loading Conditions

As mentioned previously, detailed information was not available for the overall structural system of which the case study module was a part. As such, the design loading for the permanent or final installation of the module was not known. As well, the transportation and handling conditions assumed in the original module design were not known. For the purposes of the current research, the design loading conditions were limited to module self-weight, assumed piping loads, and assumed transportation/handling conditions.

The self-weight of the module structure (D_s) was determined automatically by SAP2000 using the properties of the standard structural shapes selected. The gravity loads due to the piping supported by the module (D_p) were estimated using the pipe placements on each floor as indicated in the AUTODESK and AUTOCAD drawings of this module, and the module photographs (Figures 10 and 11). The approximate size and diameter of the pipes were found using the ASTM A53-86 standard which contains industrial pipe size and weights. The details of the pipe sizes and loads are shown in the APPENDIX B. The pipe properties and resulting loading was applied in the SAP2000 model as a uniformly distributed (average) dead load on the three main beams in each elevation, referred to as the two side beams and mid-beam and shown in Figure 12.

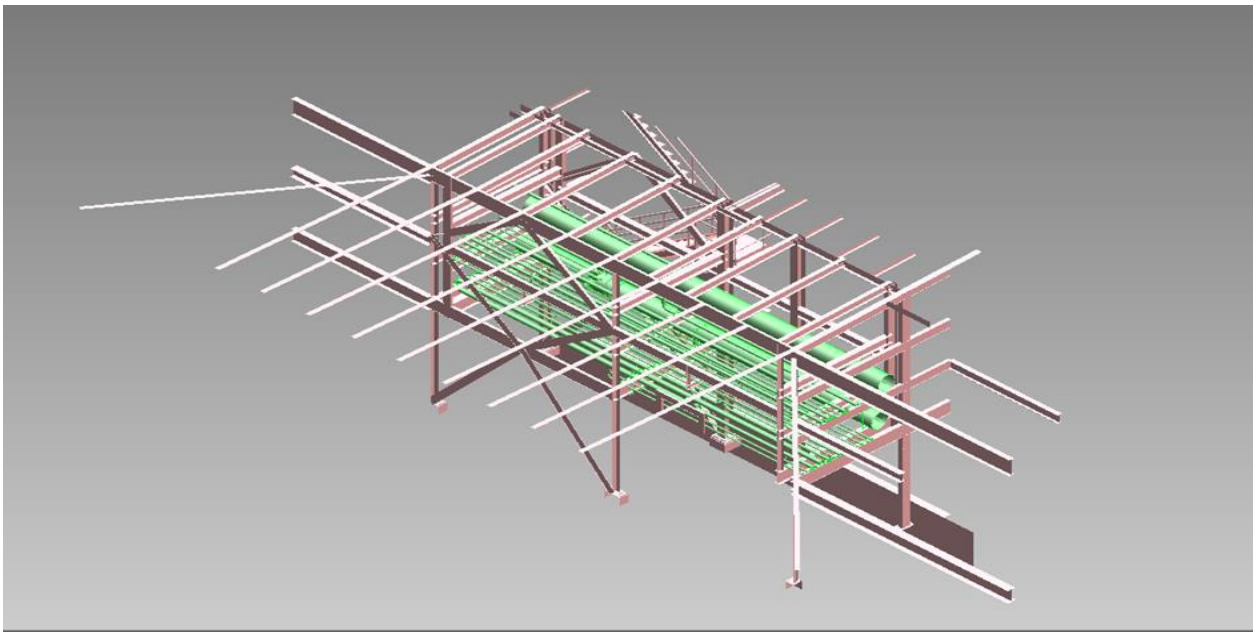

Figure 10: AUTODESK drawing of the industrial piping modular chassis, side view 1

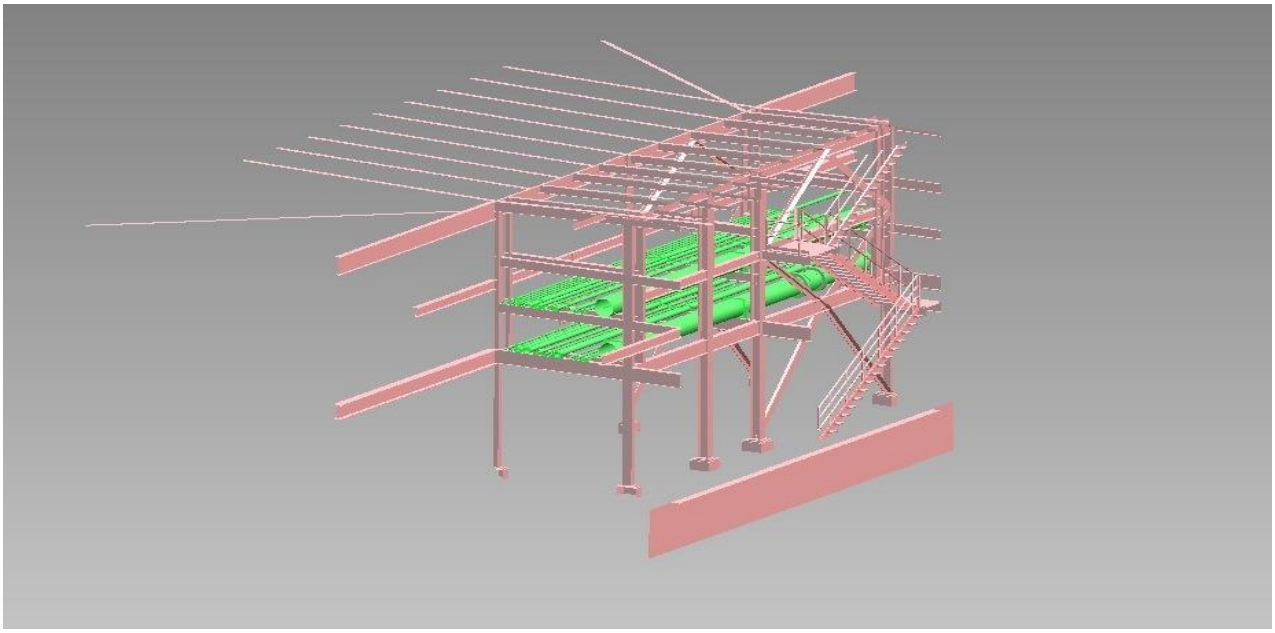

Figure 11: AUTODESK drawing of the industrial piping modular chassis, side view 2

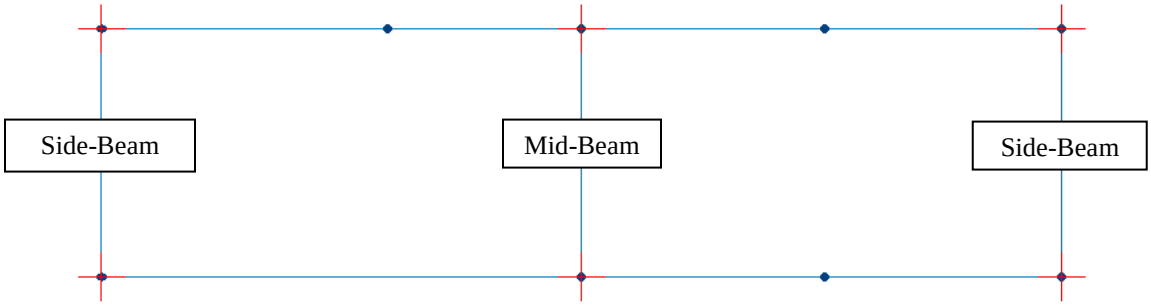

Figure 12: Model plan view-beam location

The assumed loading during transportation and handling was divided into three different categories for load pattern definition:

- Inclined or tilted gravity loads: an inclination angle of 30 deg. from vertical was assumed to represent a worst-case of tilted orientation during handling. It should be noted that this angle may vary for different handling situations and will result in a change in the inclined or tilted gravity load. Separate inclination cases were considered in both vertical planes of the model (XZ and YZ).
- Rapid lateral acceleration/deceleration: lateral forces based on an assumed lateral acceleration of 0.5g were applied to simulate severe braking or acceleration motions. These lateral forces (equal in magnitude to half the total pipe and structural weight) were applied separately in the longitudinal (X) and transverse (Y) directions of the model.
- Vertical acceleration upwards: vertical forces based on an assumed upwards acceleration of 2.0g were applied to simulate severe, rapid vertical acceleration encountered during lifting or when the transport vehicle hit a sharp bump. This vertical force (equal in magnitude to half the total pipe and structural weight) was applied in the Z-direction of the model.

The loading conditions described above were defined in the SAP2000 model using six different load cases as shown in Table 1. Model axis directions are indicated in Figure 9.

Table 1: Module Load Cases

Load Case		**Description**	**Load Patterns Used**
LC_1	Self-weight	Structure self-weight plus pipe dead load	Ds + Dp (vertical)
LC_2	Self-weight: Inclined in YZ plane	Structure plus pipe load inclined at 30 deg. from vertical in YZ plane	(Ds + Dp)cos30 (vertical) (Ds + Dp)sin30 (horiz-Y)
LC_3	Self-weight: Inclined in XZ plane	Structure plus pipe load inclined at 30 deg. from vertical in XZ plane	(Ds + Dp)cos30 (vertical) (Ds + Dp)sin30 (horiz-X)
LC_4	Lateral impact load: transverse direction	Self-weight plus lateral impact loading applied in transverse direction (Y) of module. Assumed lateral impact of 0.5g	Ds + Dp (vertical) 0.5(Ds + Dp) (horiz-Y)
LC_5	Lateral impact load: longitudinal transverse direction	Self-weight plus lateral impact loading applied in longitudinal direction (X) of module. Assumed lateral impact of 0.5g	Ds + Dp (vertical) 0.5(Ds + Dp) (horiz-X)
LC_6	Vertical impact loading	Assumed vertical impact of 2.0g.	2.0(Ds + Dp) (vertical)

Where,

D_s = self-weight of module structure

D_p = self-weight of piping

3.5 A Risk Based Approach to Module Tolerance Specification

This risk based approach to define and optimize tolerance for modular construction was developed using the industrial piping module defined in the preceding sections as a case study. The development process is divided up into seven sections:

1. **Module Design:** The module design using the plans, and BIM drawing was done using the SAP2000 structural design commercial software and has been reviewed in Section 3.3. Figure 9 illustrates the module design of the industrial piping modular chassis.
2. **Load Configuration:** Inclined or tilted gravity loads, lateral acceleration/deceleration, and vertical acceleration upwards are the three load patterns which have been assumed in addition to the structural dead load and pipe load for the load configuration step. The details of these loads have been completely explained in the preceding section (3.4) and APPENDIX A. Table 1 above contains the load patterns and load case details.
3. **Strength/Stability Inspection of the Structures:** This inspection was done using the SAP2000 software, in addition to the Handbook of Steel Construction by the Canadian Institute of Steel Construction. Section 3.5.1 contains the strength/stability inspection of the industrial piping module.
4. **Story Drift Values with Respect the Fabrication Costs:** The fabrication cost function was developed using the initial plan drawings. The section sizes were reduced step by step using the R.S. Means Building Construction Data (Waier, 2009) and strength/stability inspection of the structure was checked at each configuration. Section 3.5.2 contains the details of the 57 fabrication cost function data configuration steps. It should be noted that inelastic /inelastic distortions are also to be checked at this step (Section 3.5.3 through 3.5.5).
5. **Divergent Structure Cost/Risk functions:** The module risk functions are considered to be transportation, alignment, rework, and safety. Sections 3.5.6 and 3.5.7 contain the details of the modular site-fit risk functions.
6. **Total Structural and Site-fit Cost/Risk Function:** Once the module risk functions have been identified, the total structural site-fit risk in terms of cost and fabrication cost function can be developed. This function is generated by adding the site-fit risk functions to the fabrication cost function. Section 3.5.8 contains the details of this function.

7. **Optimal Tolerance Level:** The optimized model represents the lowest total site-fit risk and fabrication cost with respect to the amount of modular reinforcement in terms of story drift value. Sections 3.5.9 and 3.5.10 cover the optimal tolerance level in addition to a generalized risk based approach to module tolerance specification.

Figure 13 illustrates the complete algorithm of this approach.

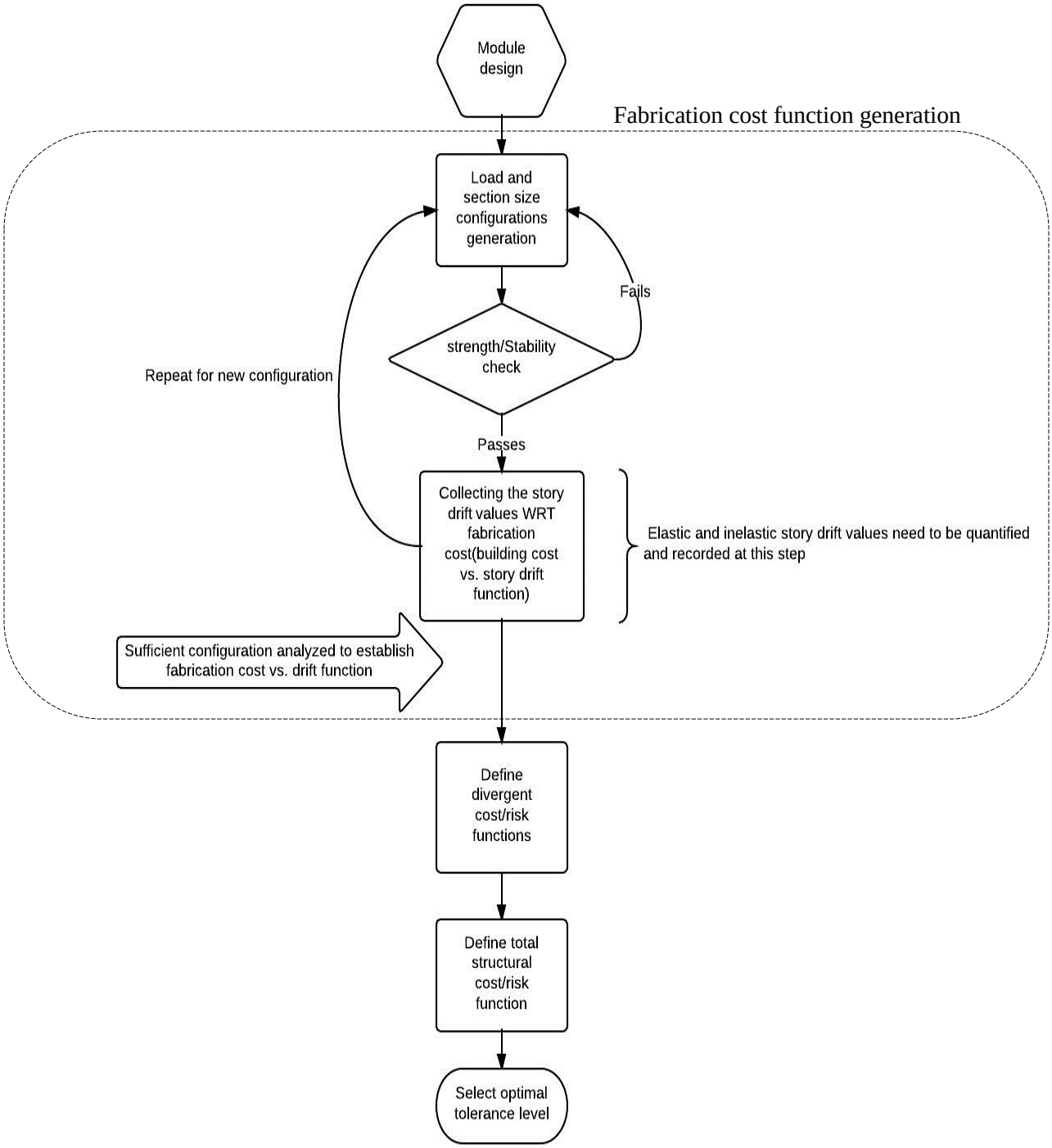

Figure 13: A risk based approach to module tolerance specification algorithm

3.5.1 Strength/Stability Inspection of the Structure

Once the module and load configuration step has been completed, the strength and stability of the structure needs to be verified. The industrial chassis module shown in Figure 9 was subjected to various types of load cases and the adequacy of the design was checked according to the Canadian Institute of Steel Construction (Albert, 2010). The Canadian Code built in the SAP2000 software is referred to as CAN/CSA-S16-01. Once the loads were applied to the module, by means of the steel design/check of the structure, the pipe-rack can be tested for safety and deformations. Figure 14 illustrates the isometric view of the module for the lateral impact load. It should be noted that the lateral impact load (LC_4), and structure+pipe load inclined in the YZ plane (LC_2) were the load cases which caused with the largest modular deformations. The isometric view of these structural deformations for LC_2 is shown in Figure 14. The testing of the industrial chassis module using the SAP2000 software demonstrates that the module survives the defined loading combinations and load patterns. Figure 15 shows the structural adequacy check and section sizes. The spectrum bar of colors shown under the figure displays the degree of member adequacy with respect the defined building code. These colors are labeled with numbers from 0 and 1. If the beams and columns are and far-off from the limit state value, color blue will be shown; values between 0.5 and 0.7 are shown with the colors yellow and green. If the correct calculations and assumptions are used, color orange is typically satisfactory. Red is not safe and means that the member does not meet the design building code requirements for strength and should be replaced with a larger section size.

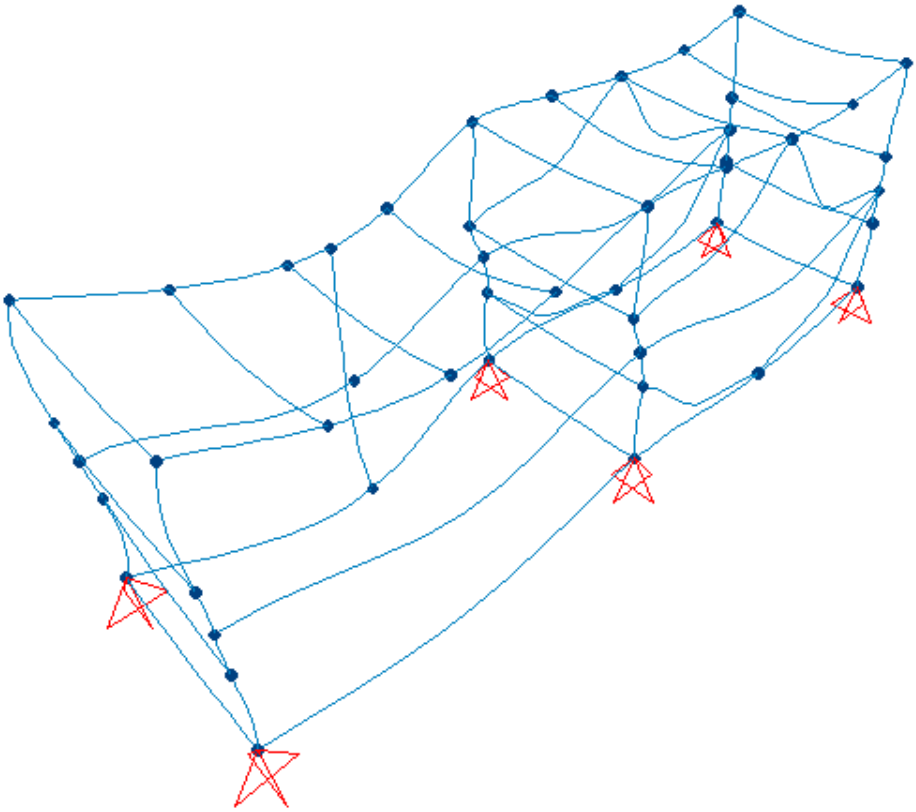

Figure 14: Isometric view of deformations for LC_2

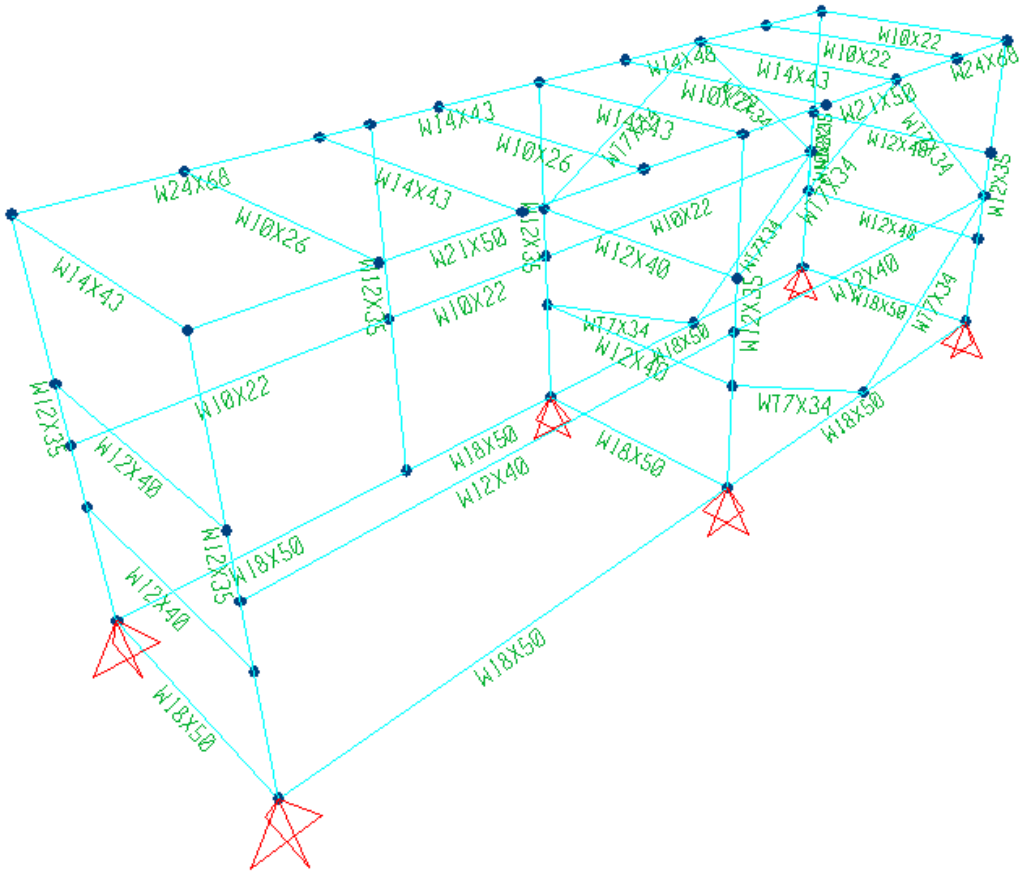

Colors	Degree of Adequacy
	0.0-0.4
	0.5-0.7
	0.7-1.0
	>1.0

Figure 15: Steel design check of the structure

The industrial chassis module has been designed with large section sizes. For this reason, the design check of the structure shows the color blue. This implies that the strength/stability check of the structure is a number between 0.0 and 0.5. The strength indicated may be due to the connection of this module to other sub-modules or the pipe-rack may act the core of an entire assembly of modules. The "far-off from the limit state value" expression could be used due to the explained situation.

To ensure the results of SAP2000 structural analysis, three member were chosen and analyzed using the Handbook of Steel Construction by the Canadian Standard Association (2010). The selected beam and columns are shown in Figure 16.

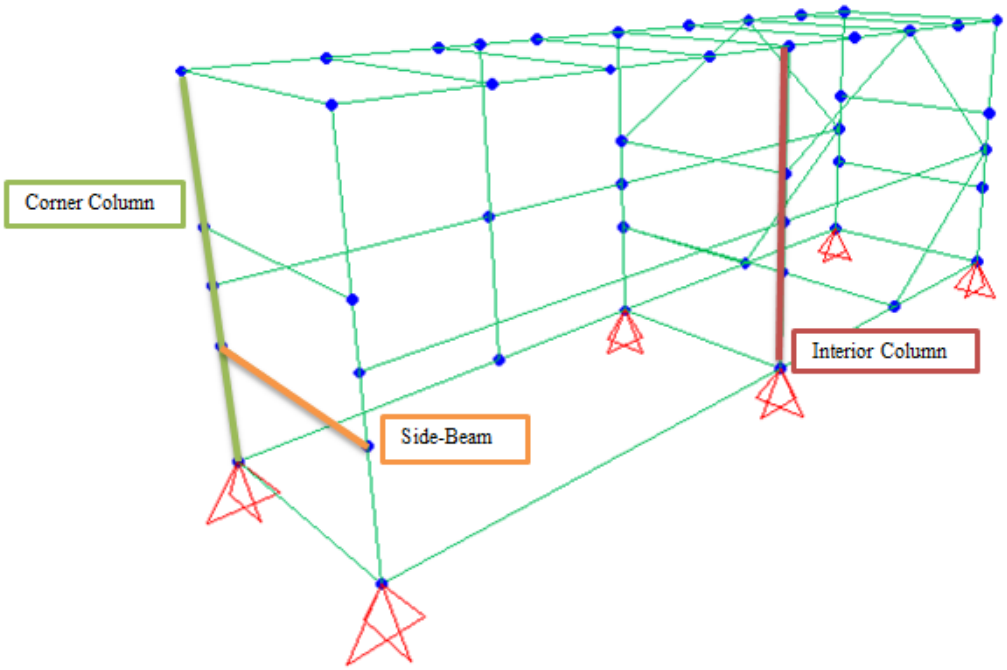

Figure 16 : Selected beam and columns for strength/stability check

Story drift is the $\frac{\Delta}{h}$ value for each member. The "Δ" is the displacement of each joint in feet, and " h" is the height of each joint in feet. with respect to the ground (i.e. first floor beams). The largest story drift values for the critical load cases: lateral impact load (LC_4), and structure+pipe load inclined in the YZ plane (LC_2) belong to the column ends (on the roof) and the beams supporting the pipes. The corner, interior column and the side-beam had the largest story drift of 6.25E-06, 0.0000125, and 0.000004375 ft respectively and were chosen for the strength/stability check hand calculations. The story drift of the

columns were measured at the roof of the module and the height of 16ft. The story drift of the beam was monitored at the joint at which the beam connects to the corner column.These members were analyzed using the member strength and stability code for class one and class two I shaped sections shown in Equation 6 for columns and Equation 7 for the beam (Albert, 2010).

Equation 6: $\frac{C_f}{C_r} + \frac{0.85U_{1x}M_{fx}}{M_{rx}} + \frac{\beta U_{1y}M_{fy}}{M_{ry}} \leq 1.0$

Equation 7 : $\frac{M_{fx}}{M_{rx}} + \frac{M_{fy}}{M_{ry}} \leq 1.0$

The factored force effects, C_f, M_{fy}, and M_{fx}, were computed using S16-01 specified load factors (1.25D+1.5L). The impact loads were taken as live loads with a load factor of 1.5 and the structural+pipe load as the dead load with a load factor of 1.25. The force effects, C_f, M_{fy}, and M_{fx}, were found using the SAP2000 software output.

For columns:

Equation 8: $U_1 = \frac{\omega_1}{1-\frac{C_f}{C_e}}$ and $C_e = \frac{\pi^2 EI}{L^2}$

Equation 9: $C_r = \emptyset A_e F_y (1 + \lambda^{2n})^{-1/n}$:

$\lambda = \sqrt{\frac{F_y}{F_e}}$, n=1.34, $F_e = \frac{\pi^2 E}{(\frac{KL}{r})^2}$, Ø=0.9, $A_e = \emptyset A_g$, L is the unbraced length and K is the ratio of the smaller factored moment to the larger factored moments at the opposite ends of the inbraced length and has been considered to be equal to 1.

Equation 10: $M_{rx} = 1.15\emptyset M_p \left[1 - \frac{0.28M_p}{M_u}\right]$ **(Strong Axis)**

Equation 11: $M_{ry} = \emptyset Z F_y = \emptyset M_p$ **(Weak Axis)**

Equation 12: $M_u = \frac{\omega_2 \pi}{L} \sqrt{EI_y GJ + (\frac{\pi E}{L})^2 I_y C_w}$:

ω_2=1.0 (For loads applied at the level of the top flange)

$M_p, I_y, I_x, C_w, G \text{ and } J$: are known for each section size

For the beam:

Equation 13: $M_r = \emptyset Z F_y = \emptyset M_p$

It should be mentioned that frames are catagorized to braced and non-braced frames and the frame type should be known before using the Handbook of Steel Construction (2010) for the calculations. For this purpose a moderate load of 500 lb was applied to the module at point A and B, which had the the largest story drift values and $K_{sway} = \frac{500+500}{h}$ was measured at point C with and without the braces. These point are shown in Figure 17.

Equation 14: $5 \times K_{Sway}^{Unbraced\ frame} < K_{Sway}^{Braces\ frame}$

Therefore the typical industrial chassis module can be considered as a braced frame and the mentioned equations can be used.

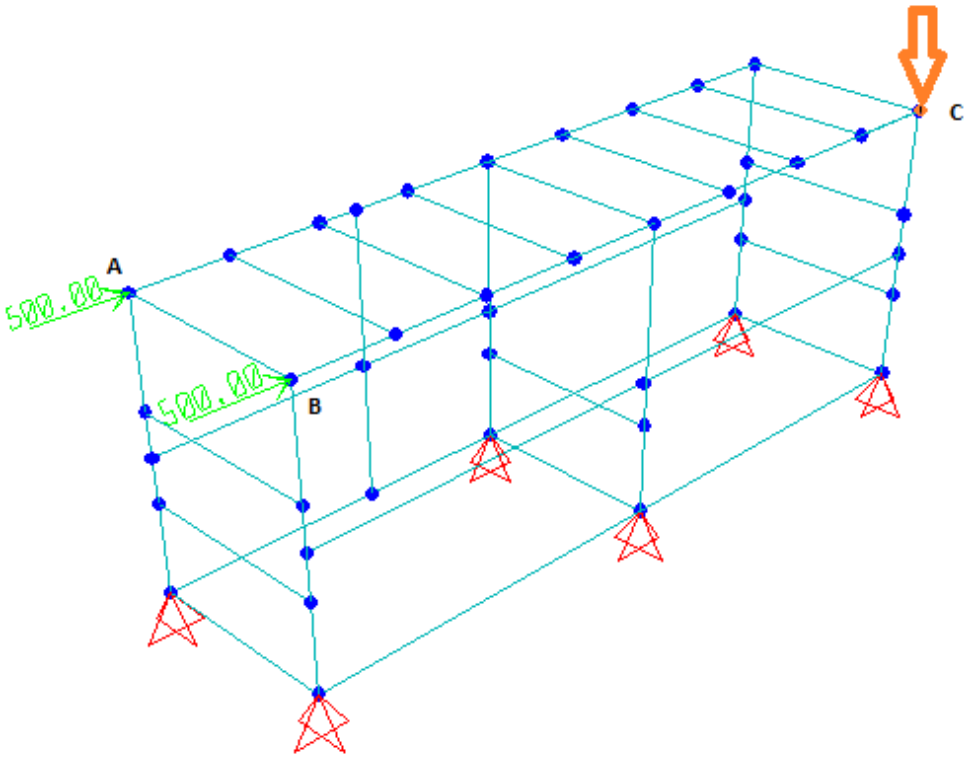

Figure 17: Calculating the K_{sway} value

The results of the design check on the key columns and beam are summarized in Table 2 through Table 4. The last row in each table represent the strength/stability of the specified beam/column. These numbers represent the factored load combinations which was specified in the precedings. As an example:

Equation 15 : LC_4=Ds + Dp (vertical) + 0.5(Ds + Dp) (horiz-Y),

and the factored force effect for this load combination is $C_f = \propto_D [C_{DS}+C_{DP}]+\propto_L [C_{IS}+C_{IP}]$ which is equal to:

1.25×{Self-weight}+1.5×{Impact load at 0.5g}

Equation 16: LC_1=Ds + Dp (vertical),

and the factored load effects for this load combination are:

$C_f = \propto_D [C_{DS}+C_{DP}]$ which is equal to 1.25×{Self-weight},

and $M_f = 1.25\times[M_{DS}+M_{DP}]$

The degree of member adequacy is a value between 0 and 1, since it is a ratio of the nominal strength of each section. These numbers are "far-off from the limit state value". The limit state value is 1 and the values clearly state that the members are far-off from the limit state value of strength and stability. This implies that the module is safe and can withstand its structural weight, pipe and impact loads, therefore it can used to define the fabrication cost function for the industrial pipe-rack module.

Table 2: Strength and stability check of the corner column

Relative elevation from the ground	0	1/4	2/4	3/4	1
L_{C1}	0.15	0.15	0.090	0.080	0.010
L_{C2}	0.25	0.21	0.14	0.10	0.030
L_{C3}	0.21	0.17	0.17	0.050	0.040
L_{C4}	0.10	0.06	0.04	0.030	0.020
L_{C5}	0.18	0.18	0.17	0.050	0.050
L_{C6}	0.29	0.29	0.17	0.16	0.020

Note: These values represent the degree of adequacy of the corner column for the six different load combinations and relative elevation from the ground.

Table 3: Strength and stability check of the interior column

Relative elevation from the ground	0	1/4	2/4	3/4	1
L_{C1}	0.15	0.15	0.090	0.090	0.020
L_{C2}	0.34	0.34	0.17	0.18	0.020
L_{C3}	0.18	0.18	0.060	0.070	0.030
L_{C4}	0.15	0.15	0.080	0.080	0.040
L_{C5}	0.11	0.11	0.050	0.040	0.040
L_{C6}	0.30	0.30	0.18	0.17	0.040

Note: These values represent the degree of adequacy of the interior column for the six different load combinations and relative elevation from the ground.

Table 4: Load combination strength and stability check for the beam

Load Combinations	L_{C1}	L_{C2}	L_{C3}	L_{C4}	L_{C5}	L_{C6}
Strength and stability check	0.033	0.27	0.24	0.25	0.0020	0.060

Note: These values represent the degree of adequacy of the beam for the six different load combinations and relative elevation from the ground.

3.5.2 Defining the Story Drift vs. Fabrication Cost Function

Once the strength and stability of the model has been demonstrated, the overall hypothesis of the proposed research can be verified. The overall hypothesis of the proposed research was that a process can be developed whereby the required tolerances are determined for a particular modular construction application within an overall cost and risk framework. The definition of tolerances would consider a number of inter-related factors, wherein the relationships between the costs of the module structure (material, labour, transportation) as a function of tolerance requirements are compared to the costs and risks associated with site fit or module assembly. Specifically, the proposed research will develop processes to establish the module structure cost function and the site fit cost/risk function, and then solve the optimization problem within established limits based on other project constraints and safety.

The verification of the hypothesis was done by collecting data points which are needed for developing the hypothesised functions. The primary section sizes were known from the plan drawings, therefore those section sizes were used as a starting point. The development of the fabrication cost function was done

using the R.S. Means Building Construction Data (Waier, 2009). The fabrication cost for each section size was computed and added to the other sections. It should be noted that the "fabrication cost" in the fabrication cost function has been developed by taking into account the crews of workers which need to work on each specific section size. Two dissimilar crews of workers from section sizes W6×9 to W16×67, and from W18×35 to W36×302 are required in order to work with each section size. The fabrication costs for the first crews of workers, for the small section sizes include, structure steel foreman, and structure steel workers, crane equipment operator, oiler equipment operator, and a lattice boom 90 Ton crane. However, the second crew of workers, for the larger section sizes, have the same foreman and operators, in addition to the welder, and 300 amp welder gas engines. In practice, only the crew with the larger capacity would be used, however this fact does not significantly impact results of the estimate. It should be noted that material costs per unit ft of each structural member was also added to the above mentioned costs. For calculating the total fabrication cost relative to each section size, overhead and profits which add 10% to bare material and equipment costs, were added to the costs. The R.S. Means Building Construction Data provides all the mentioned information in detail (Waier, 2009).

Once the fabrication cost for the initial model has been identified, the relationship between the fabrication costs and modular drift needs to be identified. Modular drift or story drift value is the lateral displacement (Δ) over the height (h) of the structure. This procedure will assist with defining the fabrication cost function. To do this, the section sizes were reduced incrementally and structural strength and stability of the structure was checked at each step. As expected the reduction of section sizes leads to a larger story drift value at the joints and therefore a greater tolerance limit. The details of this process are shown in Table 5. The first trial, referred to as reduction step 1 is the primary as-designed model and, therefore, has no cost reduction. With the reduction of the sections sizes, labour, material and equipment costs are reduced; therefore, there will be a decrease in the total fabrication cost. The rows in Table 5 show 5 of the total 62 design configuration points.

The joints placed on the roof of the module had the largest story drift values, therefore the connection with the largest $\frac{\Delta}{h}$ (story drift) value was chosen among them. This joint is shown in Figure 18 and is placed at the end point of the back corner column where the column connects to the roof. It should be noted that the other joints were checked at each reduction step to verify that the selected joint has the maximum story drift value. The displacements for each joint are in the X, Y and Z direction. These directions in the SAP2000 software are known as the local axes and are titled U_1, U_2 and U_3. The local

axis is shown in Figure 19. The maximum displacements for the joints in this module were in the direction of each member, referred to as U_1.

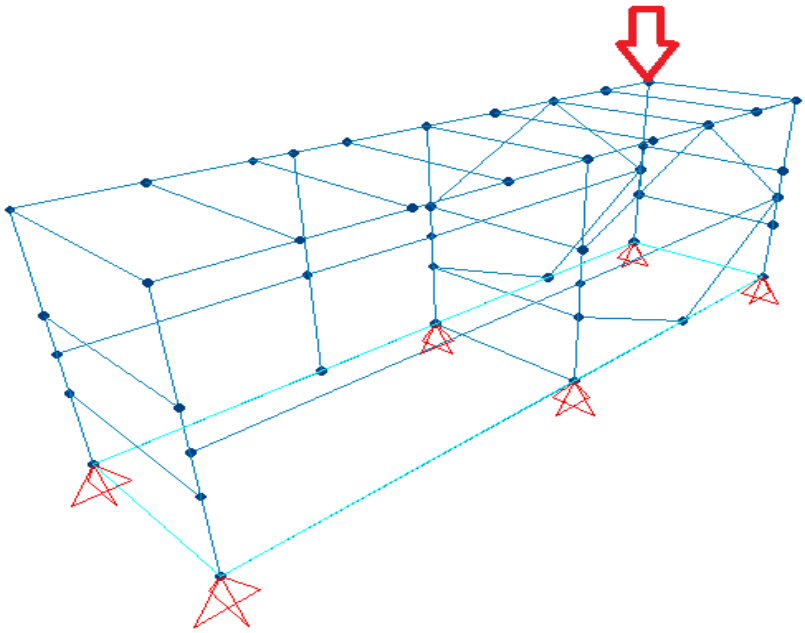

Figure 18: Joint with the maximum story drift

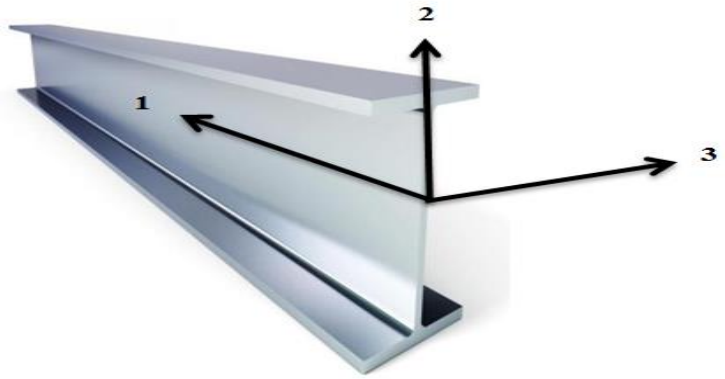

Figure 19: SAP local axis

The colors shown in Table 5 define the section adequacy color. The spectrum bar of colors under the table defines each color number from 0 to 1(limit state value), which defines the interval between the section strength and the limit state value. The portion of each color in the entire module is scaled down by 10. This means that each colored bar in the table represents 10 or less sections in the actual model. As an example, in the second trial 50 or less of the sections were blue (0), 30 or less were green (0.5-0.7) and less that 10 of them were yellow (0.7-0.8). If any of the sections were red (1), this means that the section will fail and its dimensions need to be increased to its previous size. As a case in point, the third trial had 30 or less red sections, this implied that those specific sections should be changed to their previous dimension in the second trial. The algorithm of this procedure is shown in Figure 20. APPENDIX E shows all the 61 configurations. It should be noted that the dominant load cases for the critical joint are the lateral impact load (LC_4), and $\text{structure} + \text{pipe}$ load inclined in the YZ plane (LC_2).

Table 5: Development of the fabrication cost function

Trial	Member Size Reduction Step	Sections Removed	Connections Weakened	Sections										Section Colors/Strength Check	Lateral Displacement(ft)/ Height(ft)	Most critical Joint displacement case	Reduced Cost $
				W12x35 Column	W18x50 Beams 1st floor	W12x40 Beams 2nd floor	W10x22 Beams on roof	W14x43 Beams on roof	W10x26 Beams on roof	W21x50 perimeter beams on roof	W14x48 Perimeter beams on roof	W24x68 Perimeter beams on roof	WT7x34 braces				
1	None	None	None												0.00138	Impact lateral in Y-dir & Structures+Pipe load inclined in the YZ plane	0
2	-1	Braces	None	W12x26 Column	W18x46 Beams 1st floor	W12x35 Beams 2nd floor	W10x15 Beams on roof	W14x34 Beams on roof	W10x22 Beams on roof	W21x44 perimeter beams on roof	W14x43 Perimeter beams on roof	W24x62 Perimeter beams on roof	REMOVED		0.00186	Impact lateral in Y-dir & Structures+Pipe load inclined in the YZ plane	18722
3	-2	Braces	None	W12x22 Column	W18x40 Beams 1st floor	W12x26 Beams 2nd floor	W10x12 Beams on roof	W14x30 Beams on roof	W10x15 Beams on roof	W18x106 perimeter beams on roof	W14x34 Perimeter beams on roof	W24x55 Perimeter beams on roof	REMOVED		0.00535	Impact lateral in Y-dir & Structures+Pipe load inclined in the YZ plane	21822
4	-3	Braces	None	W12x26 Column	W18x40 Beams 1st floor	W12x26 Beams 2nd floor	W10x12 Beams on roof	W14x30 Beams on roof	W10x15 Beams on roof	W18x106 perimeter beams on roof	W14x34 Perimeter beams on roof	W24x55 Perimeter beams on roof	REMOVED		0.00229	Impact lateral in Y-dir & Structures+Pipe load inclined in the YZ plane	20891
5	-4	Braces	None	W12x26 Column	W18x35 Beams 1st floor	W12x22 Beams 2nd floor	W8x48 Beams on roof	W14x26 Beams on roof	W10x12 Beams on roof	W18x86 perimeter beams on roof	W14x30 Perimeter beams on roof	W21x122 Perimeter beams on roof	REMOVED		0.00229	Impact lateral in Y-dir & Structures+Pipe load inclined in the YZ plane	18904

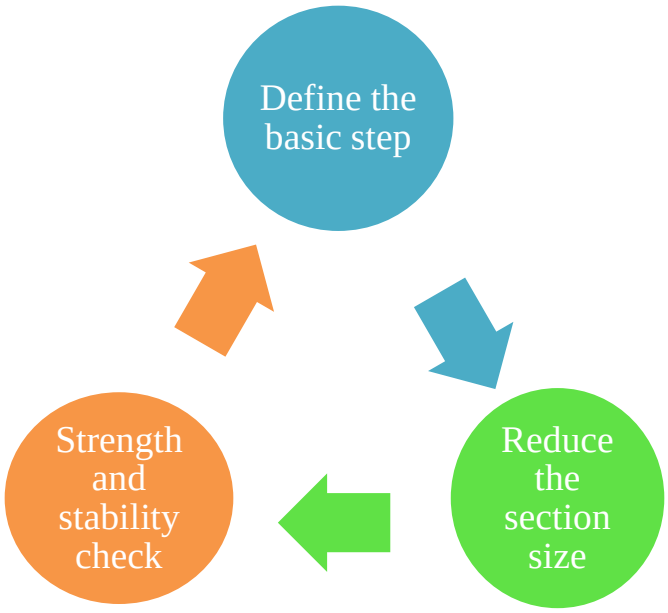

Figure 20: Fabrication cost vs. story drift value data collection procedure

Once the fabrication cost data for each of the 61 design configurations was determined, each data point was plotted with respect to its joint displacement for that design configuration. It should be noted that using the RS means building construction cost data book, after each reduction step, the fabrication costs (material, labour and equipment) of all the structural sections were added in order to generate the fabrication cost of each reduction step (Waier, 2009). The calculation details of four of the total of 61 data points are shown in APPENDIX E. The fabrication (material, labour and equipment) of each section can be calculated by a simple multiplication shown in Equation 17.

Equation 17: $[(\boldsymbol{Labour\ work\ rate}\$) \ / \ (\boldsymbol{Unit\ length\ ft.})] \times (\boldsymbol{Total\ section\ length\ ft.})$

The joint displacement (Δ) of the column containing the maximum joint displacement value shown in Figure 18 has been identified for the critical load cases/patterns (lateral impact load, and structure + pipe load inclined in the YZ plane). This Δ value has been identified for each reduction step; therefore fabrication costs can be plotted with respect to the story drift values ($\frac{\Delta}{h}$).

Figure 21 illustrates this relationship and justifies that fabrication costs decline with lowering the section sizes at each step. It should also be noted that due to the plotted function, the Pareto optimal boundary/set of non-inferior solutions of the fabrication-story drift function can be chosen. This boundary is shown in

Figure 21. The ”pareto optimal” boundary term has been named after Vilfredo Pareto (1848-1923). This boundary defines the best state of allocation of the data points and there is no better point (lower fabrication cost) that can be defined without making a worse decision. This implies that the Pareto optimal boundary shown contains the least amount of fabrication costs with respect to the largest acceptable story drift values and no other point with a lower fabrication cost which can be chosen without making at least 1 worse decision (higher fabrication cost shown with a diamond shape). Once the data points have been found, they need to be tested in the next sections, in order to be qualified for the definition of the site- risk function.

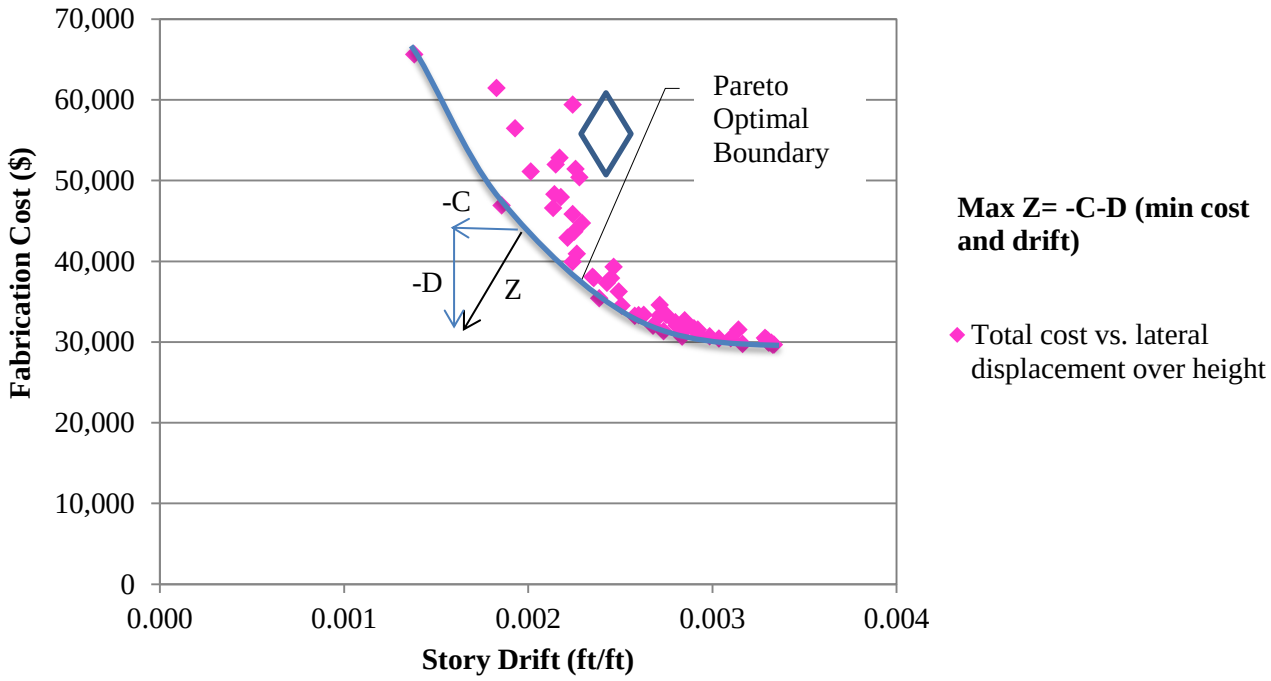

Figure 21: Total fabrication cost vs. story drift

The preceding analysis to develop the fabrication cost versus story drift function was based on linear elastic behavior. That is, the drift values are computed an elastic response, and would be recovered (return to zero) when the loading is removed. In some cases, the loading on a module may induce plastic or permanent deformations in some members or connections, resulting in permanent drift. Another scenario that might result in a permanent drift is that or loosely bolted connections in the module. In this case,

some amount of applied load would be resisted by the connection, after which the connection could slip, resulting in a permanent linear or rotational displacement at the connection in question, and contributing to a permanent (plastic) drift in the module. In each of these scenarios, the total drift of the module could be increased, resulting in a modified fabrication cost versus story drift function.

3.5.3 Elastic and Inelastic Distortions of a Test Frame

An initial fabrication cost versus story drift function was established in the preceding section using linear elastic story drift values. In order to determine whether plastic or non-recoverable drift values could occur in the module, additional analysis were performed to account for yielding of members and connections, and for loosely bolted connections.

The contribution of plastic or inelastic deformations to the total drift of the module is illustrated in Figure 22 and Figure 23. Joint displacements have a total displacement value for each load case (Δ_T) that includes an elastic distortion that recovers when the load is removed (Δ_e), and an inelastic displacement which is permanent and remains the same after the load is removed (Δ_i). Figure 23 shows the elastic/inelastic displacements on an idealized force-displacement curve (p-Δ). It should be noted that "P" in Figure 23 represents the horizontal force (H) in lb., which is applied to the model in Figure 22. In addition, once the applied horizontal load is removed from the model, three cases may happen: (a) the model is in an elastic displacement range and recovers fully once the load has been removed. (b) the model has exceeded the elastic range, however partially recovers from the permanent displacement caused by the inelastic distortions (dashed line (1) in Figure 23), and (c) the model exceeds the elastic range and does not recover from the permanent distortions caused by the inelastic joint displacements (dashed line (2) in Figure 23).

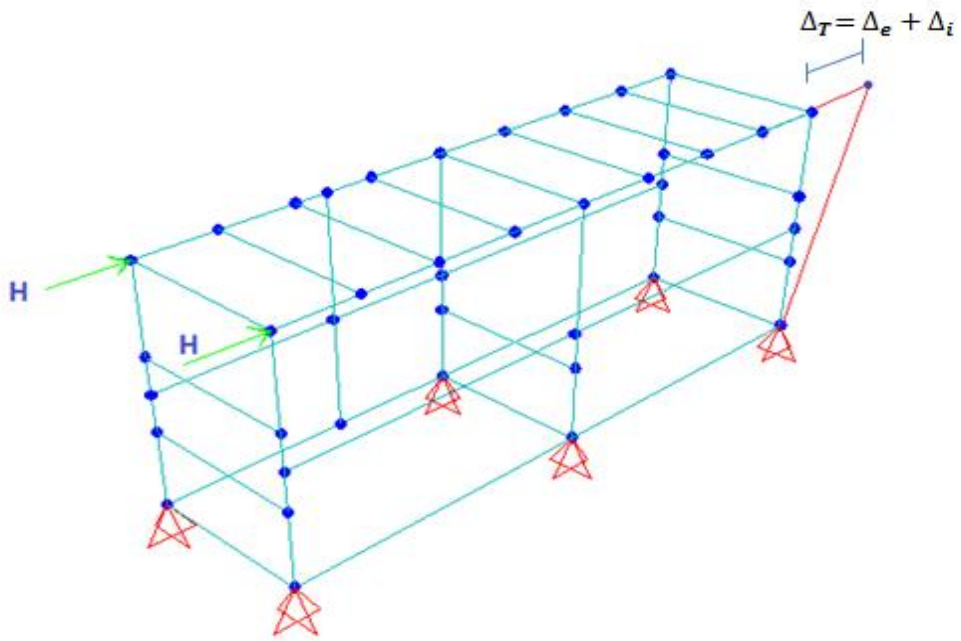

Figure 22: Joint displacement

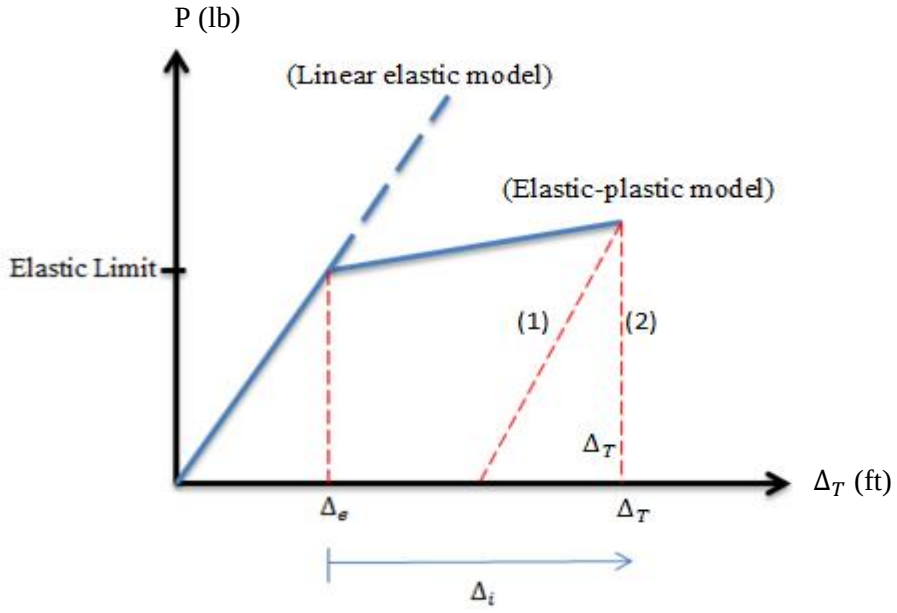

Figure 23: Force-displacement curve

Elastic/plastic, stiffening, and loosely bolted connections are the three various types of connections which may be used in practice. Each of these connections was modeled and analyzed using the built-in tools in the SAP2000 software. Once the elastic and plastic deformations were defined, the effect of these connections types was reviewed as a basis for modeling various types of connections.

Prior to implementing the plastic connection types in the structural analysis model of the module, the plastic hinge capabilities of SAP2000 were studied using a simple frame model. Figure 24 illustrates this simple frame. The dimensions of this frame are L_b=24 ft and L_c=12 ft. This frame was used for understanding the elastic-plastic behavior of frames. For this motive, one of the built in joint modelling properties in SAP2000 must be used. Link/support properties and hinges are the two options that can be defined and monitored for a single point. Links in SAP2000 are designed for defining a specific property for a point inside a section; however the SAP2000 hinge analysis option is best for assigning to a specific joint. The built-in hinge property in the SAP2000 software can model the elastic/plastic deformations of the connections. Torsional, moment and coupled hinges are the three kinds of hinges that are definable in SAP2000. The hinge properties for each of the six degrees of freedom of each joint can be uncoupled or specified as a coupled-force/bi-axial-moment. Coupled hinges are typically best, as they capture both moment and axial force. P-M2-M2 (PMM) and PM hinges are the two types of coupled hinges (Wilson & Emeritus, 2013). For this simple frame a PM, 2D hinge was sufficient for modeling purposes. Since the direction of the horizontal force is in the direction 3 of the local coordinate system, a P-M3 hinge was selected. The frame is 1° indeterminate; thus it only needs one hinge to be determinate (i.e., to form a collapse mechanism). Additional hinges will make the structure unstable and are unsatisfactory. It should be noted that if the joint displacement-force graph is modeled correctly, the unstable phase would be an accurate reflection of the performance until the hinges stiffened. The hinge should always have some (small) stiffness or SAP2000 solver may not converge for producing the joint displacement-force diagram output. This hinge was placed at the point where the horizontal load was applied, as shown in Figure 24.

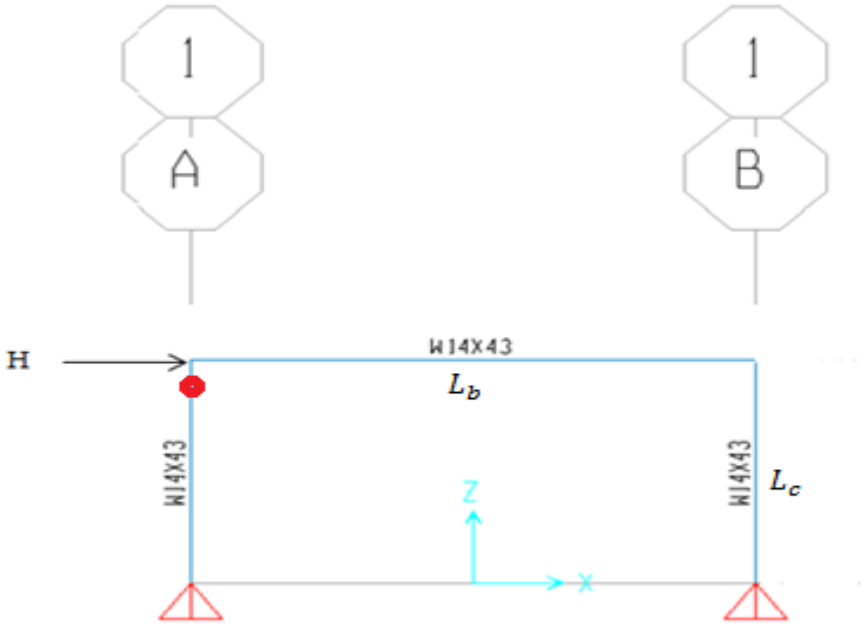

Figure 24: Test frame with hinge (top left column)

The horizontal load H needs to be sufficiently large to produce plastic behaviour in the hinge. Therefore some basic structural analysis was used to define the horizontal load to exceed the plastic moment,M_p of the column. The sections sizes for both the beams and columns are W14×43; therefore the M_p=102.5 k-ft.

M_p=102.5 k-ft
$P_{Column} \cong 0$
$M = H \times 72$

$$H_p = \frac{M_p}{72} = 1.42\ kip$$

Thus, H greater than H_p is needed to activate the hinge and enter the plastic distortion range; therefore a horizontal load of 2 kip was chosen. In order to verify the assumptions and plastic hinge response, the response of the simple frame was analyzed by first treating the elastic and plastic contributions separately (two analyses), and then using the plastic hinge features to capture the full plastic behavior in one analysis. In the first approach, the frame was analyzed without a hinge (n = 1, indeterminate) and subject to an applied lateral load of H = 1.42 kips, taking the frame to the limit of elastic behavior. The frame

model and resulting bending moment diagram are shown in Figure 24. The second step was to assume that a frictionless hinge had formed at the top of the column (member end release inserted at the top of the column), and then to apply the remaining increment of applied load (ΔH = 2.00 – 1.42 = 0.58 kips) to the now statically determinate frame. The frame model and resulting bending moment diagram are shown in Figure 25. The superposition of these two bending moment diagrams produces the elastic-plastic response shown in Figure 26.

The second model approach was to insert a plastic hinge (M_p = 102.5 k-ft) at the top of the column, and to apply the full load of H = 2.0 kips. The resulting bending moment diagram is shown in Figure 27, and matches the superposed diagram from the first analysis as shown in Figure 26. This confirmed the modelling assumptions and specified hinge properties.

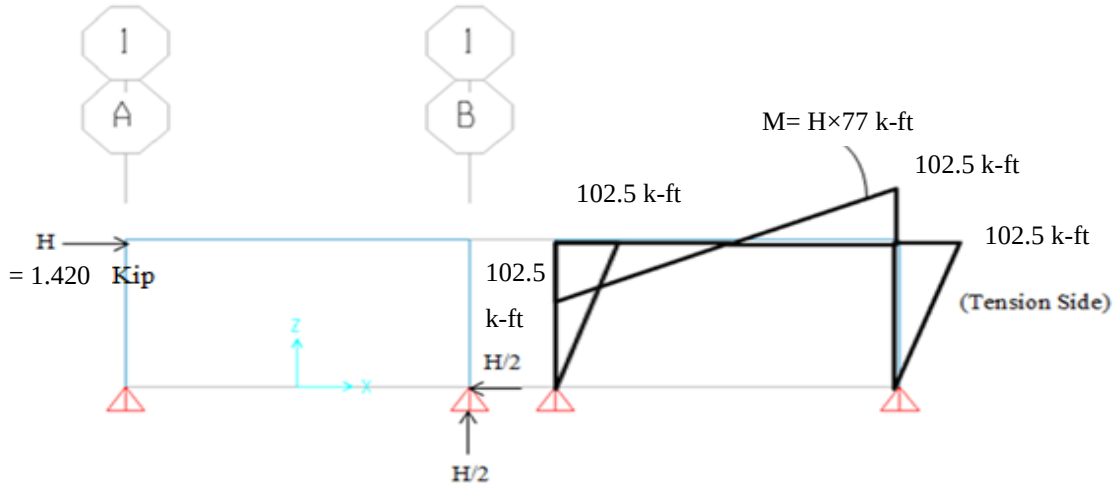

Figure 25: Bending moment diagram of the frame with n=1(degrees of indeterminacy), H=1.42 kip and M_p=102.5 k-ft

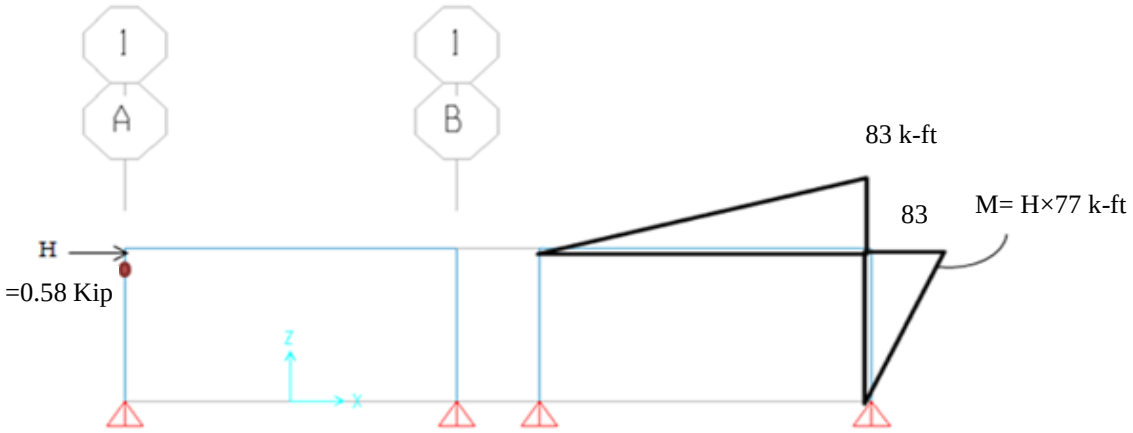

Figure 26: Bending moment diagram of the hinged frame with n=0(degrees of indeterminacy), ΔH=0.58 kip and $\Delta M = 83$ k-ft

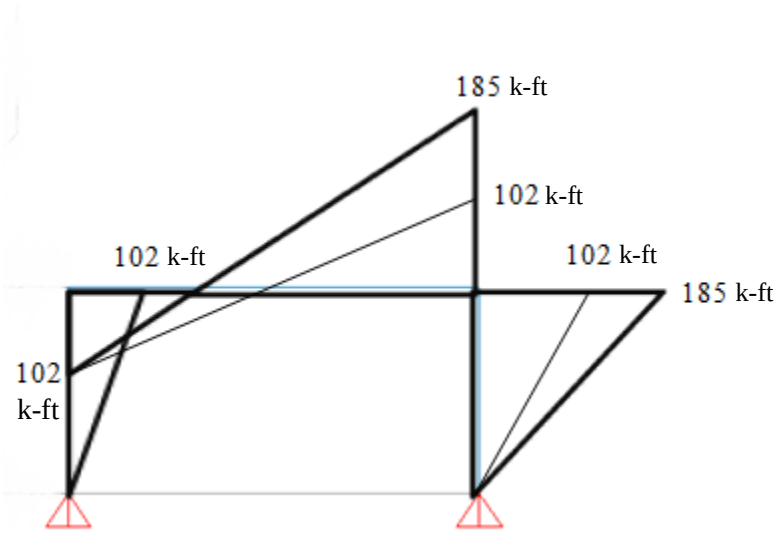

Figure 27: Total bending moment diagram of the hinged frame with H=2 kip (elastic-plastic response)

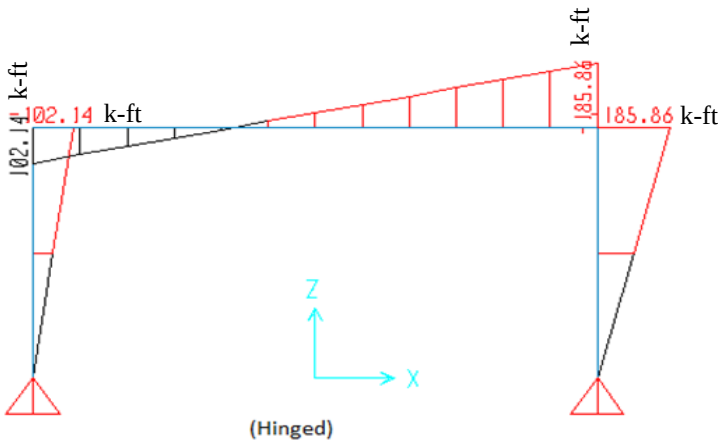

Figure 28:SAP2000 BMD of the test frame, with H=2 kip

Once the basic functioning of the plastic hinges in SAP2000 was verified, various types of connections were tested on the simple frame model in order study other construction behaviours. Connection details in the SAP2000 software were defined as hinges and categorized as, plastic (elastic-plastic), stiffening, and loosely bolted connections/hinges. The plastic (elastic-plastic) hinge models connections are engaged when subjected to force/bending moment larger than the sectional nominal strength of that connection. Once plastic behaviour begins, the connections may displace, rotate, or bend continuously with the load increments. The stiffening hinge model connections continuously displace, rotate, or bend up to a specified strength (specified in terms of a moment value), after the specified strength limit, they will "stiffen". This means that force-displacement or moment-rotation behaviour will stiffen. The third connection type is the loosely bolted connection which will be modeled at the end of this section. Not all the connections in practice are perfectly bolted with the exact nominal strength, for this reason loosely bolted connections should be modeled as well. Once the initial steps are clarified, Section 3.5.5 will go into more depth on the loosely bolted connections. Most of the connections in practice are stiffening type connections, since each connection is placed in a group of assemblies and will not be able to rotate freely with load increments.

Firstly, the non- hinged frame was modeled and considered as a linear elastic model. This was done by simply applying the H=2 kip horizontal force to the frame. For defining the elastic/plastic and stiffening connections in SAP2000, two curves need to be specified in SAP for each hinge, the moment rotation curve and the P-M3 interaction curve. APPENDIX C shows the details of the data for each curve. The P-M3 interaction curve data used was the same for both hinges, since the section sizes remain the same. The P-M3 curve was defined using the M_{px}=205 k-ft and P_y=500 kip which are known for the W14×34 section. This curve needs 5 defined points; therefore multipliers from 0.1 to 0.5 will be used. Figure 29 shows the interaction curve data and Table 6 illustrates the P-M3 curve.

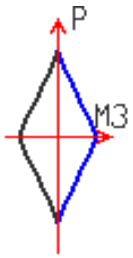

Figure 29: P-M3 curve

Table 6: P-M3 interaction curve data

Multiplier	M(k-ft)	P(kip)
0.1	20.50	50.00
0.2	41.00	100.0
0.3	61.50	150.0
0.4	82.00	200.0
0.5	102.5	250.0

The second curve needed to define the P-M3 hinge is the moment-rotation. For a plastic (elastic–plastic) hinge, the moment/yield moment should vary from 0 to 1. It should be noted that the moment is defined as a fraction of the yield moment and the rotation value is defined in radians. This hinge will only activate if the defined plastic moment has been exceeded, therefore it will be 0 if the moment is not large enough and 1(activate) when the defined limit stated has been exceeded. In the test frame, the plastic hinge will active after the moment value has exceeded the M_p=102.5 value and the moment will be equal 1. The rotation values could remain the same as what SAP has defined. Figure 30 illustrates the moment-rotation curve and its data.

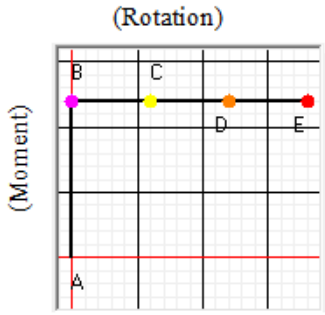

Point	Moment/Yield Mom	Rotation/SF
A	0.	0.
B	1.	0.
C	1.	2.
D	1.	4.
E	1.	6.

Figure 30: Plastic hinge (elastic-plastic model) moment-rotation curve

The stiffening hinge will have the same pre-defined rotation values; although, the moment values will change. This hinge will act almost the same as the plastic hinge; however, after the stepped load has passed a certain limit, the hinge will change its path in the force-joint displacement curve and accept smaller rotational/displacement values and "stiffen". This implies that the hinge will not activate once the moment value is 0 (point A), will start to slip (rotate) once half of the yield moment value is achieved (point B and C), and will "stiffen", and almost stop rotating once the yield moment value has been achieved (point D and E). It should be noted that the rotation values may seem to be increasing even in the last two points, however the model has been designed in a way that it would never reach points D and E. This implied that the model will stop rotating, or at least rotating significantly after 50% of the yield moment value has been exceeded. Figure 31 shows the moment-rotations curve and its data.

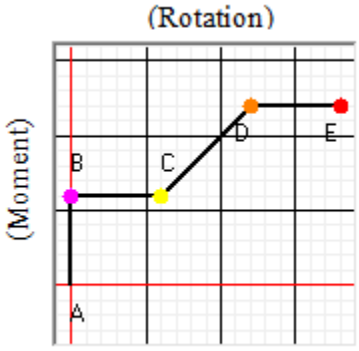

Point	Moment/Yield Mom	Rotation/SF
A	0.	0.
B	0.5	0.
C	0.5	2
D	1.	4
E	1.	6

Figure 31: Stiffening hinge moment-rotation curve

Once the two types of hinges have been defined, the force-joint displacement graph needs to be generated in order to justify that each hinge is functioning correctly and has the expected outcomes. It should be noted that the horizontal load case (H=2 kip) has been defined as a "stepped load" and will be applied to the defined point in 10 steps, therefore 10 joint displacement values can be obtained during the 10 loading steps. Figure 32 displays the frame with no hinge and with plastic and stiffening hinge. The hinge results confirm that the hinges are working correctly and the joints deformations are in a plastic stage. Figure 33 illustrates the activation of the stiffening and plastic hinges with the no hinge frame. The colored bar under the figure displays the deformation measures referred to as IO (immediate occupation), LS (life safety), and CP (collapse prevention). These measures are reported in the analysis results and assist with a performance base result; therefore, they do not have any effect on the behavior of the structure. Figure 34 displays the deformation measures. Point A, B, C, D, E, and F on this curve are intended for pushover analysis and earthquake load modeling. These letters respectively stand for the origin, yielding, ultimate capacity, residual pushover strength and total failure (Wilson & Emeritus, 2013). The sample test frame shaped a better understanding of the hinge types and their behavior; hence the same procedure can be applied to the industrial chassis module.

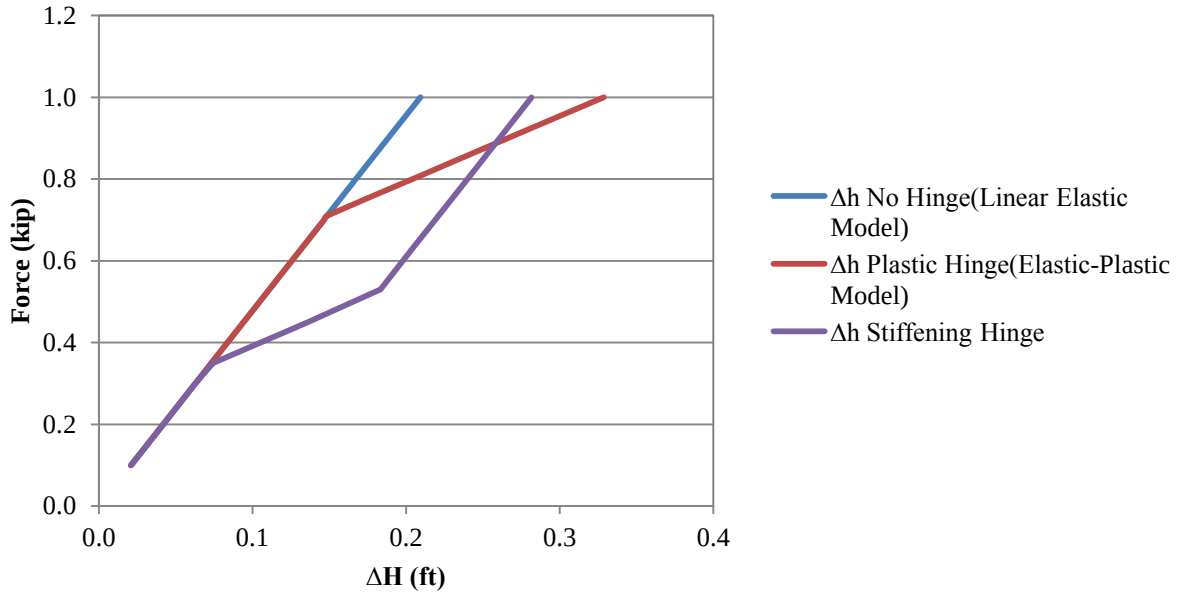

Figure 32: Force-Joint displacement graph of the indeterminate test-frame, determinate plastic hinge and stiffening hinge frame

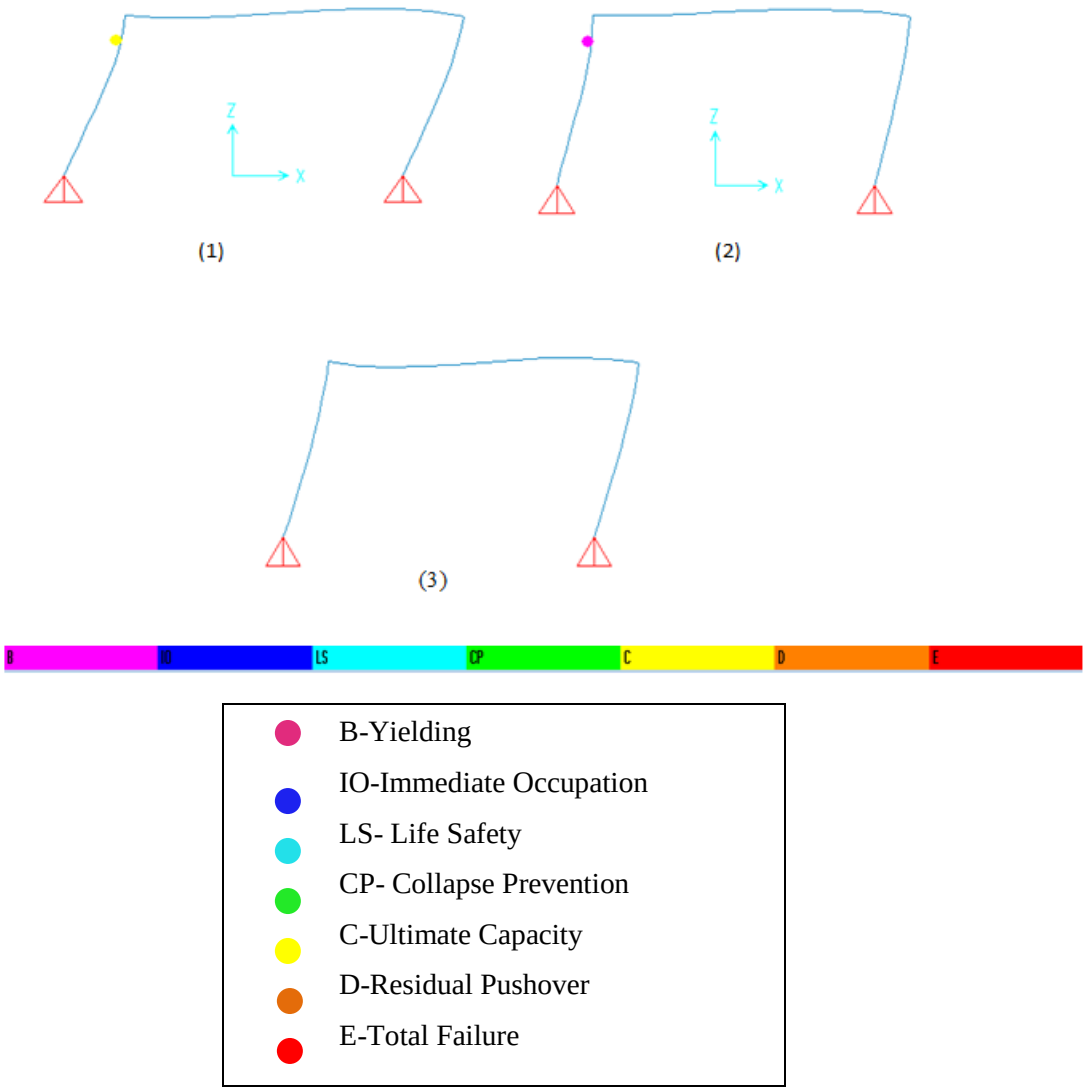

Figure 33: Test frame with (1) Stiffening hinge, (2) Plastic hinge and (3) no hinge

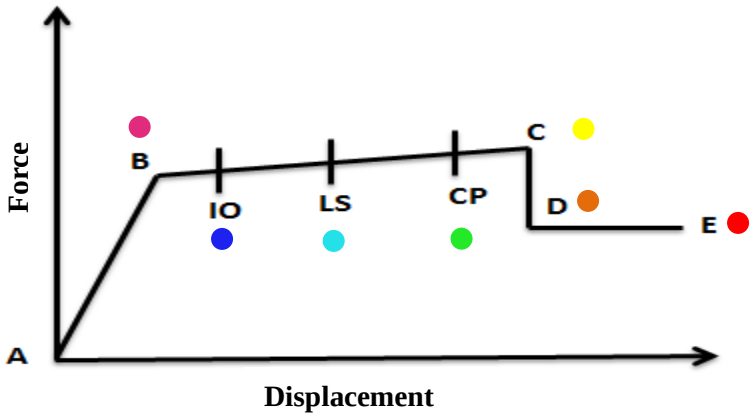

Figure 34 : Force-displacement graph for various deformation measures (Wilson & Emeritus, 2013)

3.5.4 Elastic and Inelastic Distortions of the Industrial Chassis Module

The effect of the plastic hinge types described in the preceding section on the joint displacements and distortions of the pipe-rack module are discussed in this section. Since this module is much more complex than the simple frame, the placement of the hinges is extremely important. Figure 35 shows the frames which will be containing the hinges. The chosen frames were the main frames of the module, which were holding the pipes and most of the dead load of the structure; therefore they are more critical and will be modeled including hinges. The hinges will be placed at the end of each column and at the two ends of the beams in the three frames. As explained in the last section, each hinge will release one degree of indeterminacy (DOI) and needs to be placed at connections that are not already pinned.

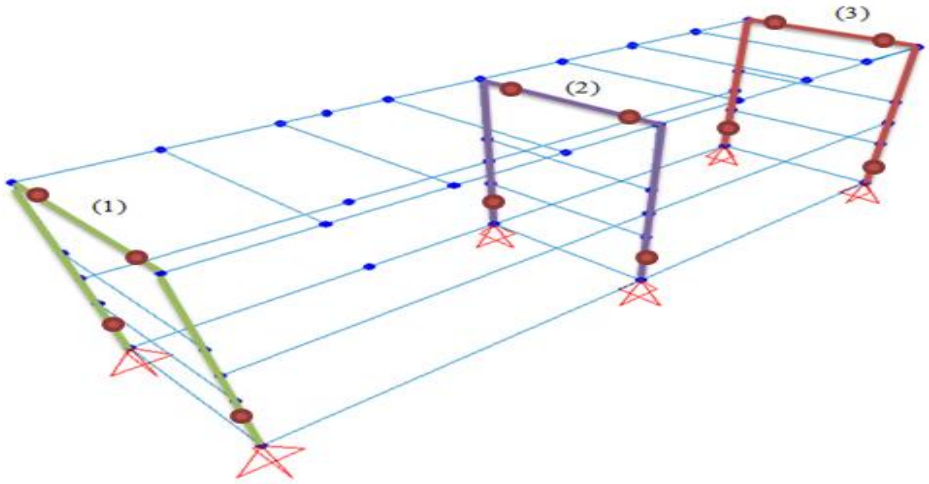

Figure 35: Hinged frames

The procedure of the hinge definition has been reviewd in the last section; therefore, the declared steps will be followed. The industrial chassis module is a 3D frame and consequently has moments about axis (2) and (3). Figure 19 shows the local 3D axis. The plastic moment and axial force need to be identified for each section and divided into 5steps (similar to Table 6) in order to define the interaction curve (P-M2-M3) data, which is shown in Figure 36. This figure is representing the three dimensional (P-M2-M3), interaction diagram in the SAP2000 software for the hinges shown in Figure 35. APPENDIX D contains the details of the hinge data. It should be noted that M3 was assumed to be equal to M2.

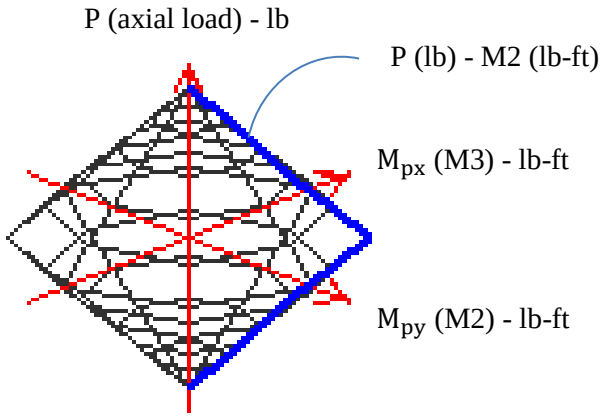

Figure 36: P-M2-M3 interaction curve(as output by SAP2000)

This module has been built as a part of a larger modular system or as a core of a entire system and has stiff and large member sizes. For this reason the impact loads and additional load combinations will not cause large amounts of deformations in the module, therefore hinges will not be activated. As as example, the top beam on the third frame shown in Figure 35 has M_{px}(M3)=90828.66 lb-ft, M_{py}(M2)=22875, and lb-ft P_y=324000. The largest load cases/combination applied to this beam/module are the structure and pipe load inclined in the YZ plane and the inclined impact load in the Y direction . The largest M2, M3 and P value for the lateral impact load was respectively 2347, -1936 lb-ft, and -312lb. For the Structure and pipe load inlcined in the YZ plane those values were correspondingly 285 lb-ft, and 2345 lb-ft, and -1,463 lb. These values are much smaller than the plastic limit states, therefore 10% of the actual plastic moment value will be used for the analysis in an attempt to induce plastic behaviour in the connections. Below is the detail of the calculations :

$$Min\ M_p = M_{py}\ and\ M_{py} = 22875(roof\ beam\ on\ the\ third\ hinged\ frame),$$

$$10\%\ of\ the\ plastic\ moment\ will\ be\ used$$

$$Min\ M_p = \ 0.1 \times \ M_{py} = 0.1 \times \ 22875 = 2286$$

Similar to the test frame, 5 data point need to be defined for the P-M2-M3 interactions curve and M3 was assumed to be equa to M3. APPENDIX D shows the detailes of the hinge data.

The moment rotation curve data remains the same as the plastic hinge curve shown in Figure 30. Three different hinges were defined for the module. The six columns had the same section sizes. The beam on the first and second frame and the beam on the third frame had different section sizes, and therefore had different P_y values. The moment values were the same for all sections and equal to 1000 lb-ft. Once the hinges have been defined, they will be assigned to the related beam or column. It should be noted that due to the unsymmetrical shape of the original module one column and the braces were removed, in order to capture the correct joint displacement values. Figure 37 illustrates the removed section with the color red.

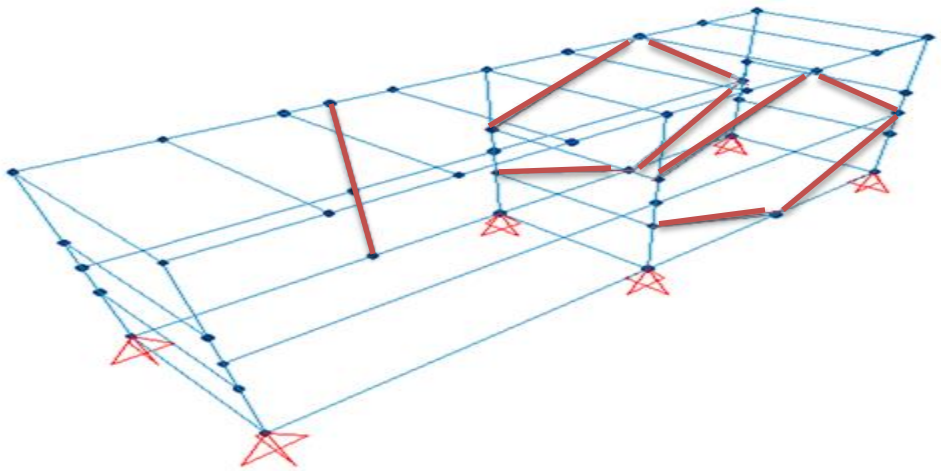

Figure 37: Removed sections for the hinge analysis

The final step once the hinges have been defined for each section is applying the hinges to the model. By selecting the beams and columns, under the define tab dropdown menue in SAP2000 software, frame, and hinges will be seleccted and assigned to each section at distance 0 and 1 for the beams and 1 for the columns. This number represents the distance of the hinge from the starting point of the section. For the columns, considering the 0 distance represents the top of the column (connection to the roof) and 1 is at the column supports, hinges are placed at the first floor column connection. For the beam distances 0 and 1 represent each of the beam ends connecting to the module and this implies that for each beam two hinges are placed at the two beam ends (supports). Once the hinges have been defined under the analyze tap in SAP2000 software the run analysis will be selected and the output of the hinged frame will be created.

Figure 38 illustrates the industrial chassis module with the defined hinges. The SAP2000 model output for $LC_2$and LC_4(critical load cases) shows that all of the hinges are in the color purple; this implies that yielding with no deformation has occurred at the joints. Only plastic deformations beyond point B (Figure 34) will be exhibited by the hinge. The results of this analysis justify that joint displacement in the typical industrial chassis module are not close to the limit state value or plastic (permanent) displacements. For ensuring the results of this analysis, 10 more reduction steps of the fabrication cost function have been tested in a similar way and have justified the fact that joint displacements are in the safe zone, with non-permanent displacements and can be used for defining the cost/risk functions in the next section. This may imply that the braces were never necessary for this module, however it should be mentioned that this

module may act as a core of an entire system, and be attached to a system of modular assemblies. For this reason braces may be necessary for this module due to its serviceability. It should be noted that the story drift values in the fabrication vs story drift function, were collected using a linear elastic analysis. This implies that all joint displacement were in an elastic range, however this procedure will assist with other divergent models that behave differently from the industrial pipe-rack module and need to be analyzed and checked with both elastic and plastic deformations. The industrial pipe-rack module has been checked and none of the defined hinges had plastic displacement values to be added to the linear elastic story drift values which were collected before. Therefore, the story drift values in the fabrication cost function can be used for future analysis, and the definition of the site-fit risk function.

In addition to this described hinge analysis, there could be a possibility that the connections are loosely bolted, and therefore are able to move more freely. For this reason the next section will describe loosely bolted connections and examine the behaviour of the module associated with loosely bolted connections.

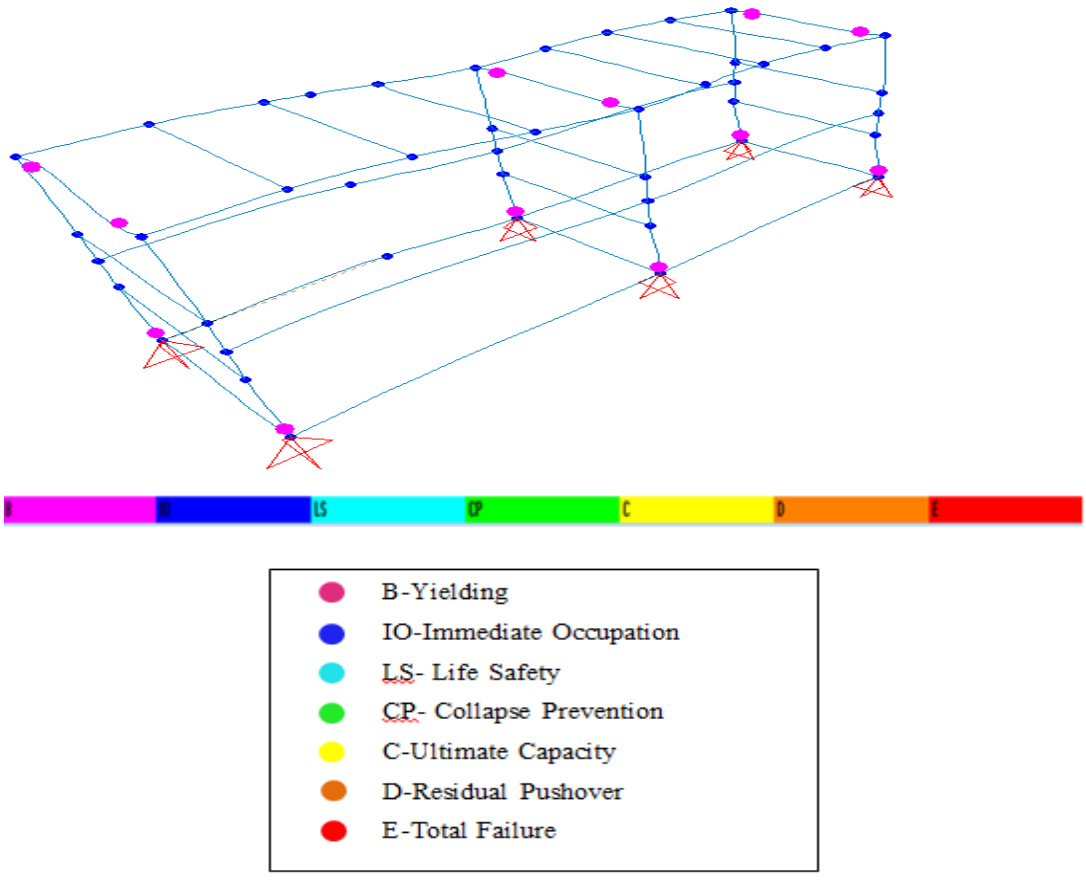

Figure 38: SAP2000 output of the industrial chassis module with defined hinges

3.5.5 Loosely connected bolts

The hinges described in the preceding section, model the behaviour of a tightly (correctly) connected bolted connection. However there could a possibility that the bolt is connected insecurely and with inaccuracy sometimes intentionally to allow alignment on site. The loosely connected joints are to be modeled on the industrial pipe rack module in this section. For modeling a loosely bolted connection, the identical frames which were described in Figure 35 will be used and the similar procedure will be followed. The critical load cases/combinations remain the same as well. However, the plastic moment values and axial force values will decrease, due to the loosely bolted connections. 10% of the M_p and $P_y$values were used for the P-M2-M3 diagram. This value will be multiplied by the multiplication factor of 0.1, 0.2, 0.3, 0.4 and 0.5 in order to be definable for the SAP interaction curve (P-M2-M3). Once again M2 and M3 were assumed to have equal values for defining the interaction curve. M2 as the smaller moment value was chosen for the interaction diagram. Figure 39 illustrates the P-M2-M3 interaction diagram of the loosely bolted connection in the SAP2000 software.

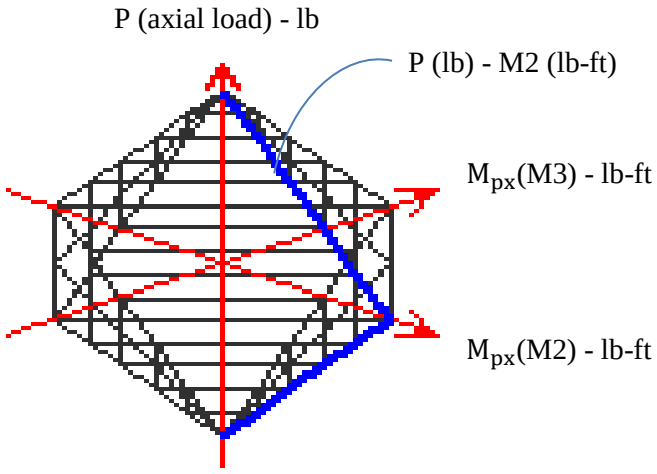

Figure 39: P-M2-M3 interaction curve of the loosely bolted connection (as output by SAP2000)

Figure 40 illustrates the moment-rotation diagram of the loosely bolted connection at the critical joint which was shown in Figure 18. It should be noted the end point (colored red) of the diagram illustrated in Figure 40, has to be identified for the SAP2000 analysis, this number has been chosen as 5. However, this joint rotation value will not be achieved due to the large moment value identified as 100 lb-ft. The rationale behind this decision is that loosely bolted connections can have two dissimilar behaviours: (a)

Once the load is applied to the joint, the joint/connection displaces a certain amount, then keeps displacing and distributes the load to the sections and causes deflections and distortions as well, and (b) once the load is applied to the joint, the joint displaces a certain amount, then stops displacing and distributes the remaining amount of the load to the other members and causes deflections and distortions. Figure 41 shows a simple beam to column loosely bolted connection and Figure 42 illustrates the magnified display of two types of connection behaviours in the simple loosely bolted connection which (a) stop displacing after a certain amount of angular rotation and (b) continue displacing. It should be noted that rotation value for the 16 ft industrial module has been considered to be 1°(0.0175 rad). A larger joint rotation value could be chosen, however due to the tolerance escalation, deflection, and distortions of the entire module, a single joint displacement of 1° would be reasonable.

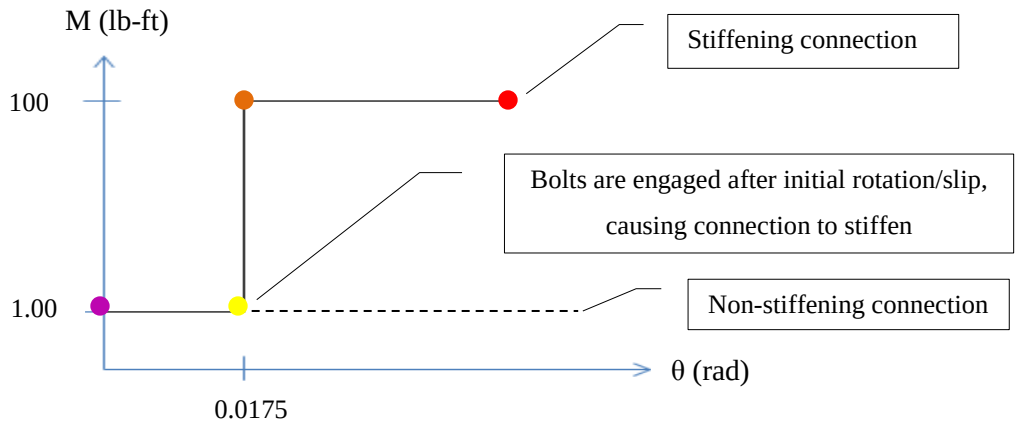

Figure 40: Moment-rotation diagram of the loosely bolted hinge

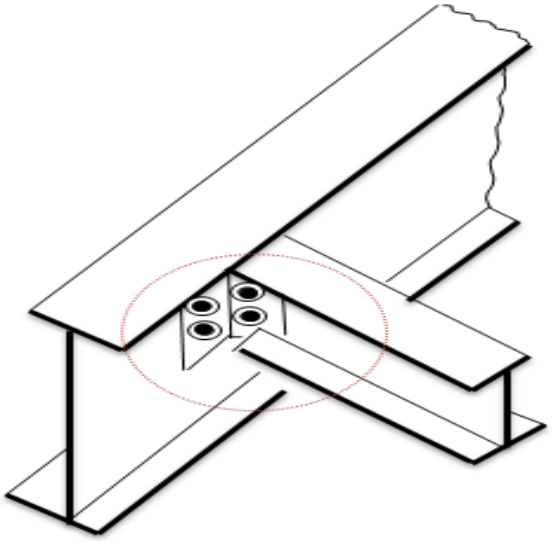

Figure 41: Simple beam to column connection

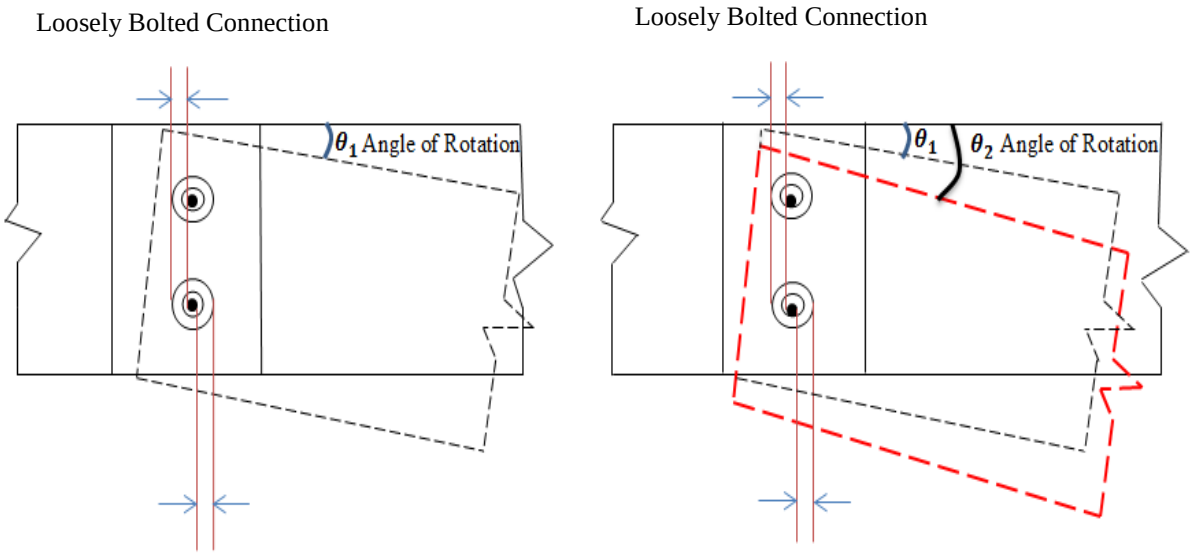

(a) Stiffening Connection: Connected piece rotates initially and then contacts bolts causing stiffening.

(b) Non-Stiffening Connection: Connected piece rotates without contacting bolts, therefore does not stiffen.
Total rotation/slip > Stiffening connection

Figure 42: Connection behaviour types

The loosely bolted connection defined for the critical joint/column, is a type (a) connection. This implies that the defined connection will continue to deflect until it has reached the rotation value of 0.0175 rad. or 1° . After this rotational value, the forces will be distributed in the beams and columns associated with the joint. The defined moment number of 100 lb-ft is a very high number, therefore will not be achieved during the SAP2000 analysis. This number represents the gross sectional failure, for this reason it will not be reached during the SAP2000 analysis. This procedure assists with defining a type (a) connection. The type (b) hinge has been defined in the previous section and referred to as the "elastic-plastic" hinge. Any type of hinge/connection that continues to displace (slip) or rotate due to the defined moment-rotation curve is a type (b) hinge. The plastic hinge/connection described in the previous section could be considered as type (b) hinge as well. Once the connection types, moment-rotation curve, and P-M2-M3 interaction diagram for the critical connection has been identified, the hinges can be modeled on the defined frame and the model can be analyzed.

Figure 43 illustrates the SAP2000 analysis of the module with the defined hinges. It should be noted that that lateral impact load in the Y direction (LC_4) and $\text{structure} + \text{pipe}$ load inclined in YZ plane (LC_2) were the critical load combinations with the maximum story drift values. The lateral structural weight in the Y direction (inclined), and lateral pipe load in the Y direction (inclined) are the two dominant load cases in the mentioned load combinations. The largest load case value in both load combinations is the pipe load which was applied to the module in the Y direction. This load has been applied to the module in the Y direction to the main beams which were supporting the pipes (Figure 12), in the base, 1st and 2nd floor (the roof of the module had no pipe load). For this reason the joint of interest shown in Figure 43 was analyzed under the pipe load inclined in the y-direction load case. The 3D local and global axis is also shown in this figure and assists with understanding the direction of the inclined pipe load. The numbers in front of each global axis represents the local axis. The module has been displaced in the direction of the applied load and hinges have been activated. All of the hinges are in the color yellow; this implies that due to the defined moment-rotation (Figure 40) curve all the hinges are at a rotational value of 0.0175 rad. This implies that the type (b) behaviour (Figure 42) has been achieved.

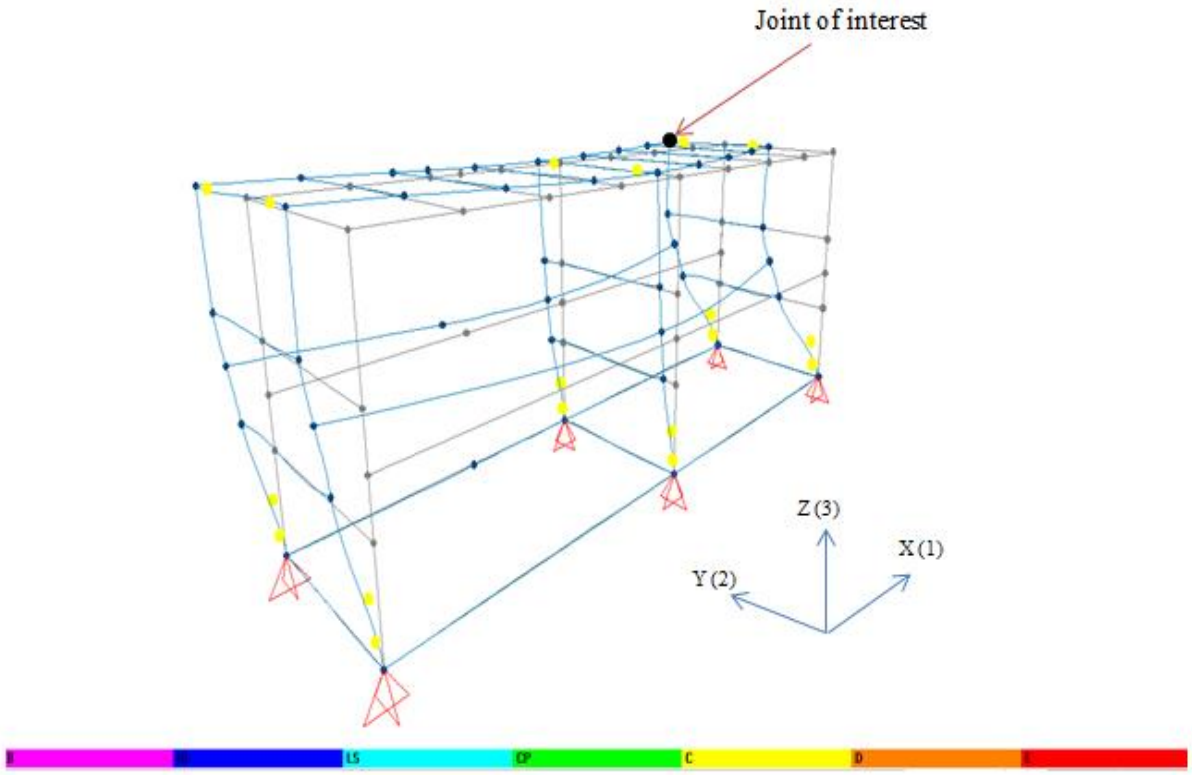

Figure 43: Hinge analysis of the loosely bolted connection

Once the model had been analyzed, further examination needs to be done on verifying the force-displacement and force-rotation diagrams of the specified joint. Figure 44 and Figure 45 respectively illustrated the applied force (lb)-joint rotation (rad) and applied force (lb)-joint displacement (in) diagrams. It should be noted that the joint rotation/displacement values shown are at the joint of interest (Figure 43) which is adjacent to the location where the hinge (loosely bolted connection) is placed.

The lateral structural weight inclined in the Y direction (LC_4), and lateral pipe load inclined in the Y direction (LC_2) are the two dominant load cases in the mentioned load cases. Therefore the non-linear stepped load case in the SAP2000 was applied to the two mentioned load cases, in order to monitor the structural behaviour in 10 definable steps. It should be noted that more or less steps could be defined for the non-linear load definition in SAP; however a minimum of 10 steps was enough for monitoring the behaviour of this industrial pipe-rack module. The displacements (U_2) and rotation (R_1) of the stated joint with the maximum story drift were measured for the lateral pipe load which was applied to the module in the y-direction. The load was applied to the module in the y-direction; therefore the maximum joint displacement value would be in the direction which is parallel to the y-axis (U_2). For the joint

rotation values, there will not be a large rotational value in the y-direction (R_2) since the applied load is parallel to the y-axis, and in the z direction (out of plane rotation) due to the direction of the applied force. The largest rotation value is about the x axis and is shown byR_1. For this reason the force-R_1 and force-U_2 values have been graphed respectively in Figure 44 and Figure 45.

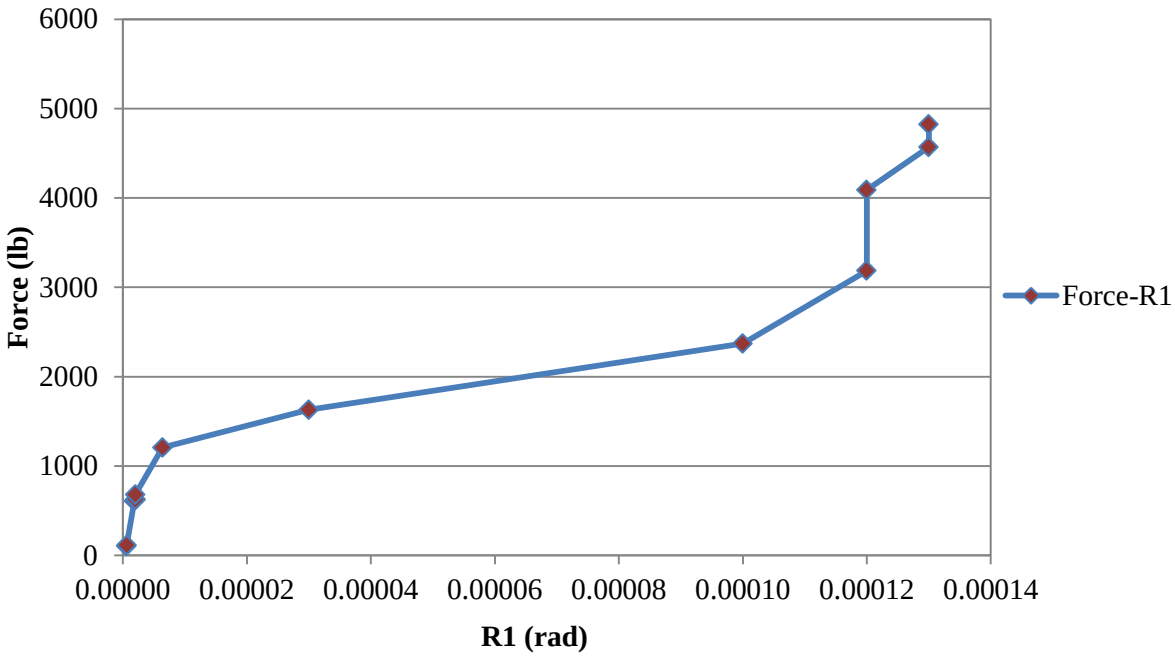

Figure 44: Force-rotation curve of the joint of interest (adjacent to the loosely bolted connection)

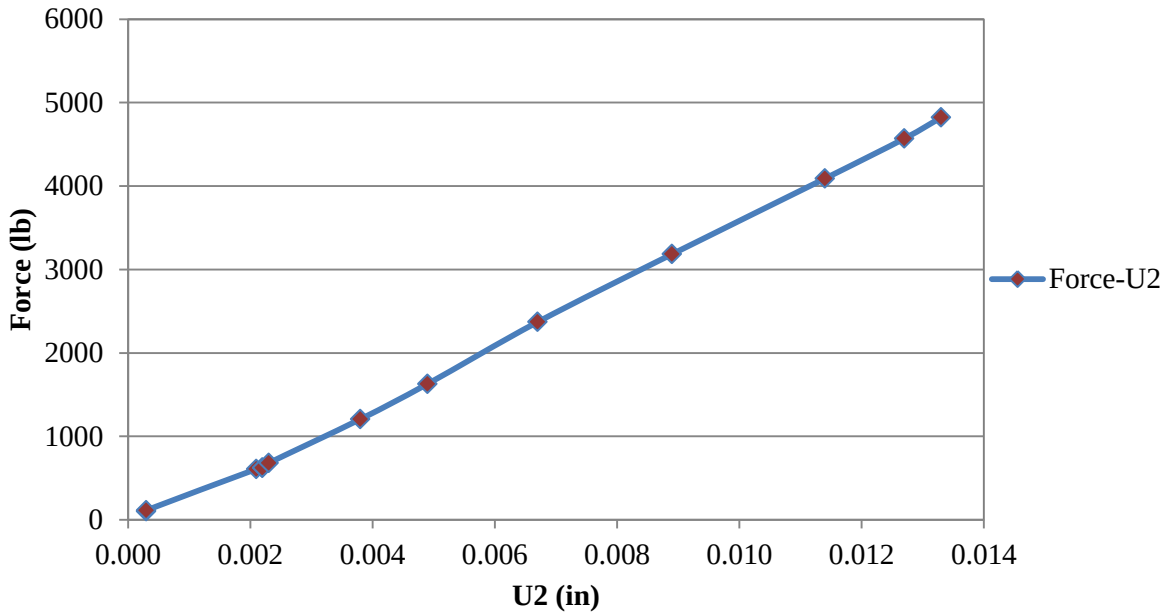

Figure 45: Force-displacement curve of the joint of interest (adjacent to the loosely bolted connection)

The joint rotations and displacements are useful to examine the overall response of the structure and the influence of the loosely bolted connection (plastic hinge). The applied force (lb)-joint rotation (rad) graph shows a maximum rotational value of 0.00014 rad, which is almost two orders of magnitude smaller than plastic hinge rotation value of 0.0175 rad. It should be noted that the magnitude of the plastic hinge rotation is considerably larger than the maximum joint rotation since the hinge rotation is the relative angle change at the hinge, while the joint rotation is the overall rotation at the joint in global coordinate; they are not the same measurement. Figure 46 illustrates the joint and hinge rotations. The shape of the force-rotation curve (Figure 44) is as expected. Loading steps 7 to 11 had a relatively higher R_1value, this implies that these steps are where the hinge activates and the plastic deformation phase occurs. Table 7 displays the loading steps and their relative force,R_1 and U_2 values.

Table 7: Displacement data at joint of interest (adjacent to the loosely bolted connection)

Loading Step	F (lb)	U_2 (in)	R_1 (rad)
1	102.390	0.000300	0.000000587
2	114.770	0.000300	0.000000608
3	608.610	0.00210	0.00000183
4	622.550	0.00220	0.00000207
5	625.370	0.00220	0.00000206
6	**680.180**	**0.00230**	**0.00000201**
7	**1206.23**	**0.00380**	**0.00000640**
8	**1628.93**	**0.00490**	**0.0000300**
9	**2370.44**	**0.00670**	**0.000100**
10	**3184.12**	**0.00890**	**0.000120**
11	**4089.82**	**0.0114**	**0.000120**
12	4569.35	0.0127	0.000130
13	4820.97	0.0133	0.000130

Plastic Deformation Steps

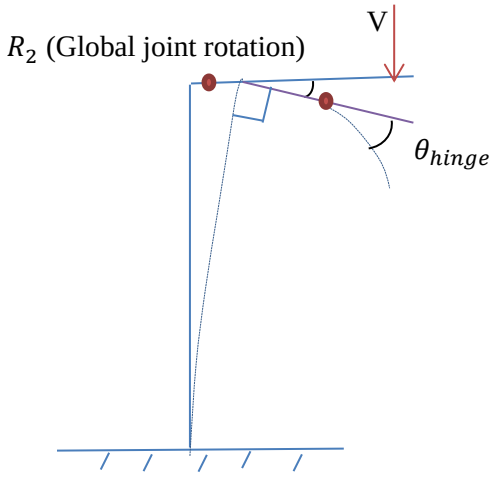

Figure 46: Joint of interest and hinge rotations

The force-displacement diagram of the adjacent point to the loosely bolted connection is a straight line. However, this diagram should have a similar shape as the force-rotation diagram. Since it is capturing the behaviour of an elastic-plastic hinge, there should be a region in the curve which shows the activation of the hinge and the plastic deformation values. However, the plastic deformations may be small and not affect the shape of the curve. Figure 47 illustrates the elastic and plastic deformations in a column. Part (a) of the figure illustrates a column with a perfectly elastic behaviour and a linear force-displacement diagram. One the other hand part (b) of the figure illustrates a column with both elastic and plastic deformations, which should have a force-displacement diagram similar to the force-rotation diagram shown in Figure 44. In the specified joint of the industrial pipe-rack module, plastic and elastic deformations will be caused due to the activation of the hinge; however, the plastic displacements values maybe small and not affect the total displacement value. This could cause a relatively straight force-displacement diagram.

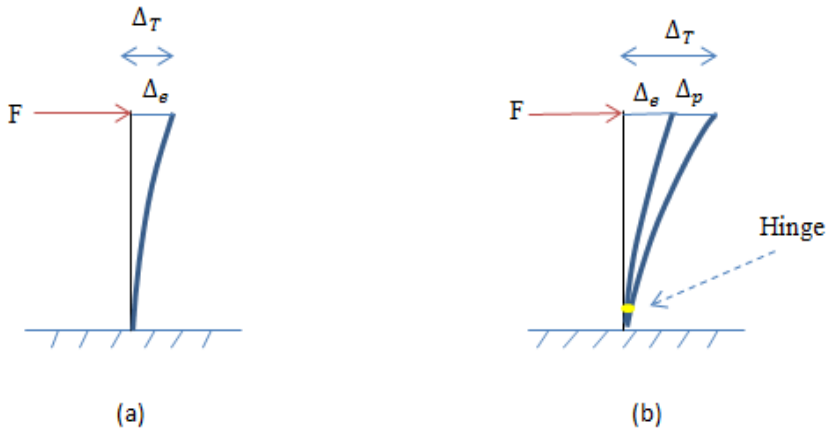

Figure 47: Elastic and inelastic distortions

Various hinge models were developed to describe connection options for modules to be shipped to site. While a loosely bolted connections model intentional flexibility for site plumbing and alignment that has not been used for module fabrication, it does illustrated a type of behaviour that might be considered acceptable or even intentional for some joints in a resilient modular system design. Elastic, plastic and stiffening joints modeled as hinges may represent other strategies or combinations of materials. For simplicity, and in order to develop a workable framework for a broader model of resilient design for

modular systems the linear elastic analysis which was done during the story drift data collection phase will be trusted and used for developing the divergent module risk functions. The next sections will describe the procedure of defining the module risk functions, which is the major contribution of this research.

3.5.6 Factors Affecting a Module Risk Function

To this point, a module design cost function has been developed as a function of expected drift, and the module's structural behaviour based on various fabrication strategies has been modeled. To complete the objectives of this thesis, a module risk function expressed in units of dollars must be developed. Such a function is depended on the control of tolerances and associated fabrication, transportation, and erection risks. The tolerances are categorized as manufacturing, interfacing and erection tolerances, and practical. Tolerance level determination is based on actual project applications. The characteristics of expected variations (e.g., dimensional, positional, orientation, etc.) associated with each tolerance type will affect the risk data. Risks are expressed as dollars. These variations and diverse tolerance classifications will be used to develop the tolerance accumulation or escalation relationships. The tolerance escalation relationships will be used in the development of the site risk function. The fabrication cost function was developed in the last sections. The risk functions which will lead to the formation of the site-fit risk function will be developed in this section. It should be noted that four dissimilar risk functions will be added to the fabrication cost function. Rework, transportation, alignment, and safety risk are the four functions that have been designed in order to capture the risk associated with the module at each construction phase.

Four critical modular construction phases have been analyzed in order to form the risk functions which are illustrated in Figure 48. The first function is the rework function which occurs after the fabrication phase has been completed and the module is ready to be transported to the construction site or once it has arrived on the construction site. Any fabrications errors, miss-alignment, and out-of-tolerances caused during the fabrication phase will be checked and fixed at this stage. The second risk function is the transportation function, which is designed to evaluate the transportation costs and risks generated during transportation phase of the module from the fabrication shop to the construction site. This function captures the transportation costs in addition to the transportation risks due to the shipping insurance, and risks of dimensional degradation due to the reduction of the reinforcement in the fabrication cost function. The third function is the alignment risk, which occurs during the on-site erection phase and computes risks and known costs which are associated with the module during the on-site erection phase. This

function represents the on-site erection costs and additional risks associated with the reduction of reinforcement in the fabrication cost function. The safety risk function, is the fourth risk function which accounts for the safety of the workers during the extra hours associated with fixing the fabrication errors (rework function), in addition to the Workers Compensation (WC) Insurance cost. The WC covers any injuries caused during the labour working hours, in addition to the medical costs which are associated with the injury.

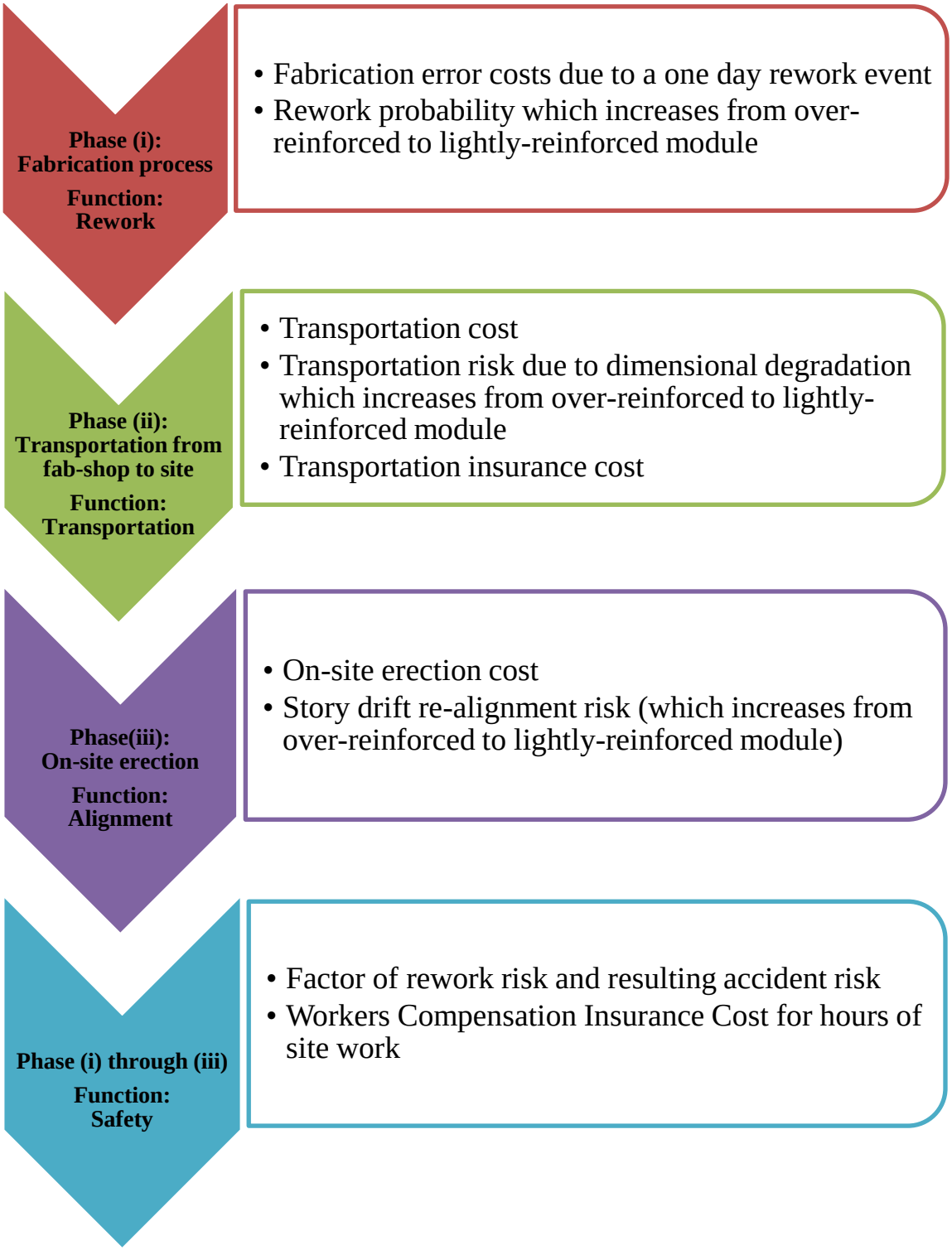

Figure 48: Diverse risk functions from the fabrication shop to on-site erection

Each of the stated functions has inputs which form the independent variables of the function, and an output which represents the cost associated with each construction phase risk function. Table 8 summarizes each of these functions and their input and output data. Once the four risk functions in addition to the fabrication cost function have been verified, the next section will describe the details of each of the risk function.

Table 8: Inputs and outputs for the four cost/risk functions

Rework	Transportation	Alignment	Safety
• **Input**: Rework event, and rework probability range from over-reinforced to lightly-reinforced module • **Output**: Amount of the rework event needed in order to fix the fabrication errors on the module with respect to the amount of reinforcement	• **Input:** Fabrication cost function, transportation insurance cost, and dimensional degradation probability from over-reinforced to lightly-reinforced module • **Output:** Total transportation costs/risks from the fabrication shop to the site with respect to the amount of reinforcement	• **Input:** On-site erection hours, $ rate per hour, and story drift re-alignment risk values from over-reinforced to lightly-reinforced module • **Output:** Total alignment costs for on-site erection with respect to the amount of reinforcement	• **Input:** Factor of rework risk and resulting accident risk, Workers Compensation Rate for hours of site work, and total labour hours from over-reinforced to lightly-reinforced module • **Output:** Risk associated with the safety of the workers with respect to the amount of reinforcement

3.5.7 Development of the Module Risk Function

This function will demonstrate the interaction of the tolerance types and analyzes the trade-offs between the diverse risks and structural cost functions. The story drift value is the controllable variable (through design) that drives fabrication costs as well as offsetting module risks. In this section, the four types of diverse risk functions will be described in detail and added to the fabrication cost function values. Rework, transportation, alignment, and safety cost/risk are the four diverse types of systematic risks that have been considered for developing the site-fit risk functions. Each of these functions will be described in detail.

3.5.7.1 Rework Risk Function

This function will represent any type of rework caused due to the miss-alignments occurring during fabrication that are not detected before transportation to the site, or which occur on site due to handling, miscommunication, or poor planning. The rework risk function was developed by creating a typical rework event. Handling a joint on the construction site generally takes 3 times as long as doing it in a fabrication shop. As an illustration, welding a 28"-7/8" wall p91 pipe on the construction site normally takes about 36 hours. In addition, cutting and beveling of the same pipe took about 2 days of 5 people, working 12 hours per day on the construction site (Innovations in Mechanical Construction Productivity-RT252). An industrial pipe-rack module is less complex than such a pipe. For this reason the rework that needs to be done on this 45×16×14 ft^3(length, height and width), 104315 lb module chassis is considered to be a crew of workers, working 8 hours for 1 day at a rate of $^{125\$}/_{hr}$ Each. It should be noted that researchers with vast industrial experience have stated that the labour cost per hour for rework on such modules is approximately $^{125\$}/_{hr}$. This will be:

$$5 \times \frac{8\ hr}{day} \times \frac{\$125}{hr} = \$5000\ per\ day$$

However, there is a probability that this 1 day rework will occur due to the modular reinforcement values (story drift). If the module is over-reinforced (e.g., the first reduction steps in the fabrication cost function) due to the specified load cases/combinations, less joint displacement will occur and therefore less rework is expected. As the story drift value increases, larger joint displacements may cause distortions and deformations. This will lead to a larger probability of experiencing the 1 day rework event. For this reason a probability range from 0.01 to 0.8 has been used for this event that increases with 0.014 increments over the acceptable story drift range. This increment has been chosen in a way to reach a

probability of 0.8 at the last step of the fabrication vs. story drift cost function shown in Figure 20. The rationale behind this decision was that the last data point in the tolerance fabrication cost data (56th point) had the largest story drift value and this will lead to an 80% probability of a rework event. It should be noted that 5 of the 61 data points had sections that were colored red (failed), therefore those 5 data points were eliminated from the total points and 56 of them were chosen as the acceptable story drift values with respect to the fabrication costs. Table 9 displays the probability rates and rework risk of 10 configurations. APPENDIX F contains the site-fit risk function data of all the 56 data points. Some may argue that the probability value of 1 could be chosen for a 100% probability of rework on the module. However, the collected data points which had a failed section due to the strength and stability codes were eliminated from the data sets of the fabrications cost function. For this reason the maximum probability of rework was chosen as 0.8 and not 1.

Figure 49 illustrates the rework risk curve of the design configurations ordered by story drift values. This curve illustrates the expectation that lightly-reinforced modules have a higher risk of being out-of-tolerance or miss-aligned during the fabrication phase due to their flexibility. In other words the probability of rework needed for repairing the fabrication errors increases, as the story drift values increase.

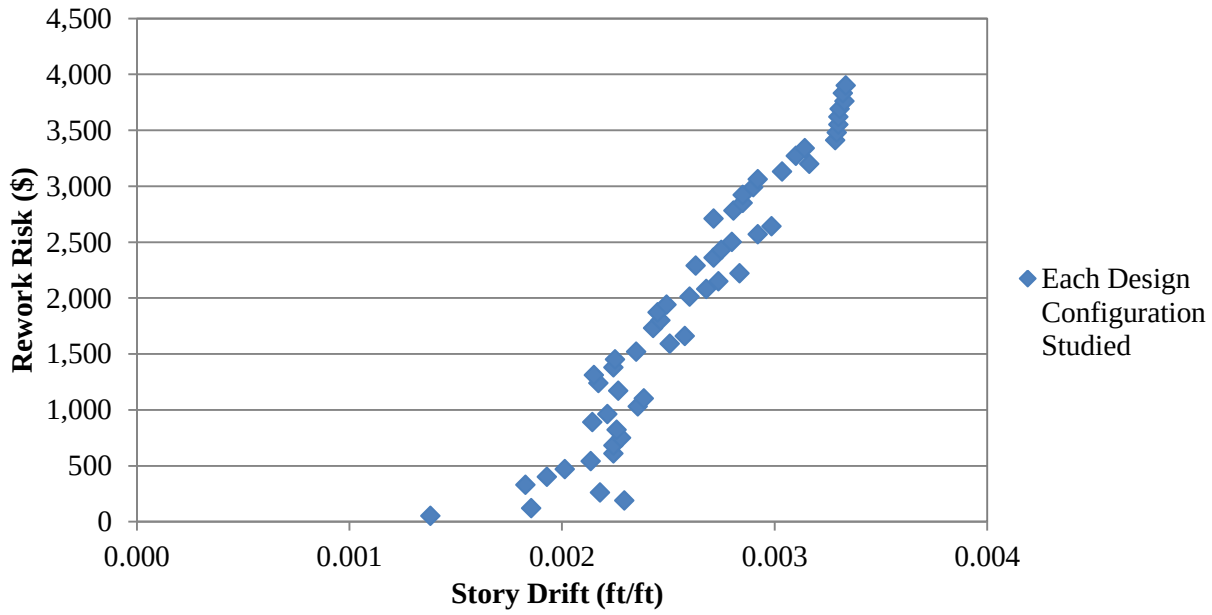

Figure 49: Rework event probability curve as a function of story drift

Equation 18 represents the rework risk function:

Equation 18: $\boldsymbol{Rework\ risk = Rework\ probability \times Rework\ event\ cost}$

$$= \boldsymbol{Rework\ probability} \times \$\mathbf{5000}$$

3.5.7.2 Transportation Risk Function

The next defined function is the transportation risk function. This function estimates the transportation costs associated with the module during the transportation phase from the fabrication site to the construction site. The transportation risk consists of three different parts: shipping cost, shipping insurance and dimensional degradation risk. The transportation cost is generally about 10% of a total cost of a product (Rodrigue & Notteboom, 1998). In this case, the transportation cost has been considered to be 16% of the total fabrication costs, which is $0.01 per lb. A larger value than the 10% was chosen for the analysis because of the high volume to weight ratio of a typical module. The modular weight of each story drift value in the fabrication cost function was considered to be reduced by 10% at each fabrication cost function step (point). It should be noted that the modular reinforcement was reduced at each fabrication cost function step, for this reason modular weight decreased as well. The total structural weight was 104315lb for reduction step 0(actual model) and reduced to 12388 lb at the 56th step. These values correspond to the actual weight of the module for each increment of the story drift, which reduced by 10% at each incremental step. Given the structural weight and transportation unit price per lb, the transportation costs were calculated.

The second part of the transportation risk function is the shipping insurance costs. The insurance rate for transporting the module was assumed to be 0.05% of the total fabrication costs. It should be mentioned that the Standard Freight Insurance and Policy Terms and Conditions clearly state that insurance costs generally cover collision, derailment, fire, hurricane, earthquakes, lightening, sinking, stranding and etc. , however loss of or damage arising out or resulting from unexplained mysterious disappearance, mechanical or electrical derangement, and changes in climate conditions are not covered by the insurance company. In this case the insurance would be beneficial if it covers the all-risk and basic risk conditions. Basic risk conditions cover collision; earthquake, cyclones and etc., while the all risk coverage include all risks (partial and total loss) cause by physical loss or damage caused during the door to door transit. (Freight Insurance Coverage Terms & Conditions, 2003). Insurance types and the amount of coverage that each type has, is dependent on the transportation system, product, destination, insurance company, etc.

Based on the above mentioned information and supposing that some distortions are not covered by the insurance company, the risk of damage to be assumed by the fabricator must be added to the transportation function. The risk of damage referred to as the "Dimensional Degradation Cost" for the transportation function has the similar probability values that were explained in the rework function Section 3.5.7.1 and Figure 49. The rework that has been multiplied by the dimensional degradation probability values is the total fabrication cost and not the rework event that was defined earlier. The rationale behind this decision is that deformations caused during transportation phase are unlike the misalignments that may be caused in the design phase. These deformations could be more severe, and therefore cause section failure and out-of-tolerance issues, which will lead to replacing the failed sections. For this reason the probability of damage caused by transportation should be multiplied by the total fabrication costs which include labour, material and equipment. This implies that rework in the transportation function includes cost of labour, equipment and material for changing a specific section (damage probability).

As tolerance values increase (designed in story drift increases), more displacements are likely to occur in transportation, thus there is a higher probability that sections have to be replaced. The last data point (story drift value) in the fabrication cost data has an 80% chance of failure and damage, since it has the highest story drift value. This indicates that the probability of section replacement will increase with the story drift increase and that all the sections in the last reduction step of the fabrication cost vs. story drift function could fail and exceed the tolerance limitations (all sections are misaligned and distorted). In this case most of the entire module would need to be replaced, and the rework cost equates the 80% of the entire fabrication cost of the module, which is 0.8 × $29000. Equation 19 shows the transportation risk function. It should be noted that 0.05 is the insurance rate per total fabrication cost.

Equation 19:

$$\boldsymbol{Total\ transportation\ \ cost/risk} = \boldsymbol{Transportation\ risk} + \boldsymbol{Transportation\ cost}$$

In which

$$\boldsymbol{Transportation\ risk} = \boldsymbol{Total\ fabrication\ cost} \times (\boldsymbol{Insurance\ rate} + \boldsymbol{Dimensional\ degradation\ probability})$$

$$\boldsymbol{Tranportation\ cost} = \boldsymbol{Modular\ weight}\ (\boldsymbol{lb}) \times \boldsymbol{Transportation\ cost}\ (\$/\boldsymbol{lb})$$

It should be stated that that the above mentioned shipping cost refers to the module shipping costs from the fabrication shop to the construction site. Figure 50 illustrates the supply chain of the raw material to the steel fabricator, fabrication shop and site for a mixed modular and conventional project. In the stick built construction systems the material is transported from the steel fabricator directly to the site; however, in the modular construction system, the material is transported from the steel fabricator to the fabrication shop, then to the site. The transportation cost function above refers to the transportation of the module from the fabrication shop to the site.

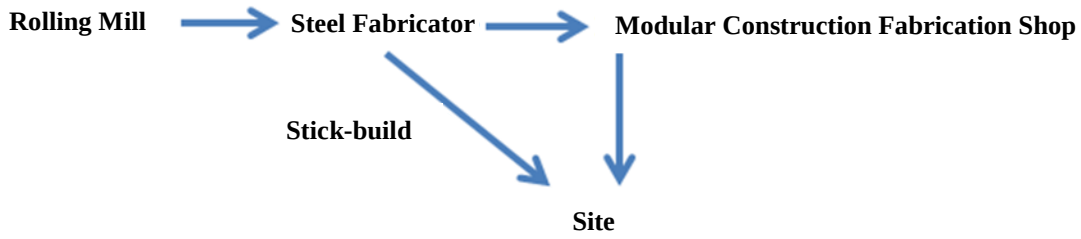

Figure 50: Supply chain for steel in a mixed modular and conventional project

The dimensional degradation probability in the transportation risk function varies from 0.01 to 0.8 with respect to the fabrication cost decrements. The transportation risk values thus can be plotted with respect to the fabrication costs for a better understanding of the transportation risk with respect to designed story drift for each configuration considered. Figure 51, probability of impact of transportation event, illustrates this relationship and justifies that with the reduction in fabrication costs (lightly-reinforced module) the probability of dimensional degradation increases. Therefore, there is a risk that the sections in the module may distort/deflect and need to be replaced, re-aligned, etc.

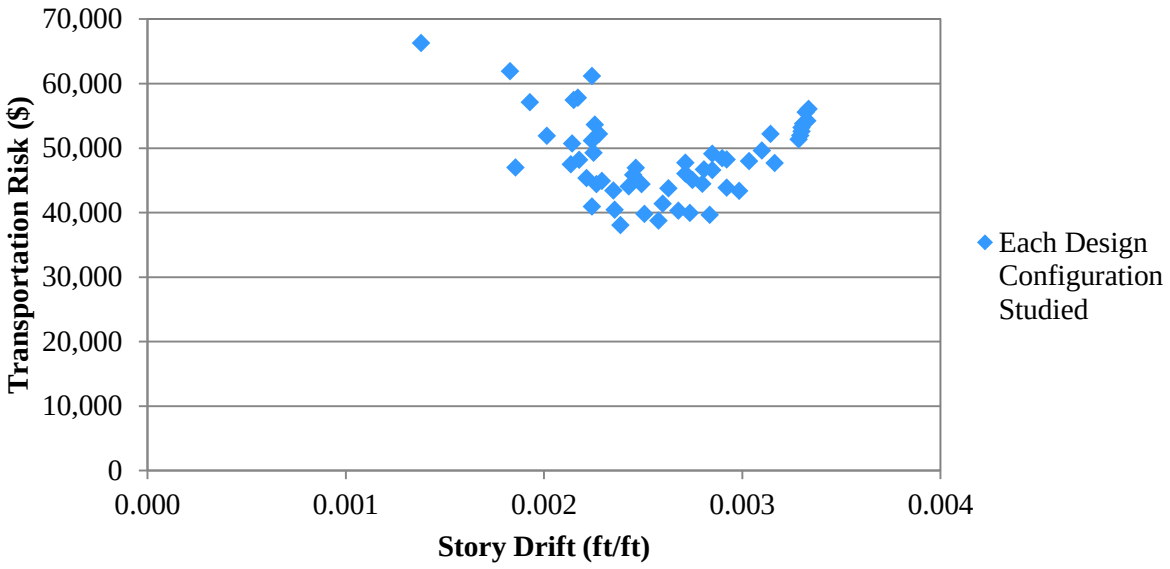

Figure 51: Dimensional degradation probability vs. fabrication cost

3.5.7.3 Alignment Risk Function

Once a module is fabricated in the factory, it will be erected and aligned in order to form the initial module, however after the module has been transferred to the construction site additional alignment needs to be done in order to erect the module on the construction site (e.g., connected to other modules, a superstructure, a foundation, or assembly parts). The alignment risk function refers to the on-site erection and not the assembly and erection process in the fabrication shop. This function consists of two parts: (1) on-site erection alignment costs and (2) alignment risk. The first part of the function includes the on-site erection hours, and the total labour dollars per hour based on crew configuration. The second part of the function consists of the story drift values from over-reinforced to lightly-reinforced modules. On-site erection costs can be evaluated by multiplying the erection labour hours by unit cost per hour. However, it should be noted that researchers with vast industrial experience have stated that alignment is typically 25% of the total on-site erection labour hours; therefore the alignment cost function is multiplied by 0.25. The on-site erection alignment cost for this module has been estimated to be 100 hours $\times$ \$125/hr$\times$ $0.25 = \$3125$. These values were chosen based on the labour hours and unit costs used by industry experts to build such modules.

As the story drift ($\Delta/_h$) value increases there is a larger risk of misalignment and distortions. For this reason the alignment risk function accounts for the story drift values, in order to capture the risks associated with the module behaviour. The alignment cost of $3125 has been assumed to increase from over-reinforced to lightly-reinforced modules in the fabrication cost function. As story drift increases, modular reinforcement decreases, and there will be more distortion and misalignments in the module. For this reason more time will likely be spent on the module during the on-site erection phase and the alignment costs will be higher than $3125. In the first fabrication function step, the module is heavily-reinforced and therefore the alignment cost function will remain at the base level ($3125); however as design configurations increase, story drift values increase, and deformations are expected to increase. This implies that a multiplication factor is needed for the alignment cost function, in order to account for the expected incremental deformations. Equation 20 displays the alignment risk function which properly scales the incremental story drift value impacts on the alignment cost function.

Equation 20: $\boldsymbol{Alignment\ risk = 0.85 + 100 \times Story\ drift}$

This function has been designed in a way to have no effect on the alignment cost function ($3125) when the module is heavily-reinforced (1st step in the fabrication cost function). The 1st configuration step has a story drift of 0.0015 and in order to add no alignment risk to the heavily reinforced module (1st configuration step); two scale factors have been chosen. The first scale factor is 100 which will be multiplied by the drift value of 0.0015 and result in a multiplier of 0.15 for the alignment risk function. In order to have a risk multiplier of 1 for the 1st configuration step (over-reinforced module), 0.85 was added to 0.0015×100, to form a risk multiplier value of 1 for the first configuration step. These scale factors will remain the same in the alignment function and add "no risk" to the first confirmation step by forming a multiplier of 1. For this reason, the two scale factors of 0.85 and 100 have been used. When the fabrication cost function, declines (higher story drift), this factor will start to grow and reflect the risk caused due to the deformation of the module. The effect of the alignment risk function is illustrated below with a series of examples:

$$(1)\ 0.85\ +\ 100 \times 0.0015 = 1$$

$$(2)\ 0.85 + 100 \times 0.0019 = 1.02$$

$$(3)\ 0.85 + 100 \times 0.0023 = 1.08$$

$$\vdots$$

$$(56)\ 0.85 + 100 \times 0.0034 = 1.19$$

The output of this function is expected total alignment costs for on-site erection with respect to story drift. Equation 21 is the complete form of the alignment risk function:

$$Alignment\ risk\ function = \ Alignment\ cost\ function\ \times\ Alignment\ risk\ function$$

In which:

$Alignment\ cost\ function = \ 0.25 \times Total\ onsite\ erection\ labour\ hours\ \times 125\ \left(^{\$}/_{hr}\right)$, and

$Alignment\ risk\ function = [Scale\ factor_1 + Scale\ factor_2 \times story\ drift]$

Equation 21:

$$\boldsymbol{Alignment\ cost\ function = \ 0.25 \times 100 \times 125\ \left(^{\$}/_{hr}\right) \times [0.85 + 100\ \times Story\ drift]}$$

3.5.7.4 Safety Risk Function

This function represents the safety risk associated with workers due to the rework function and the total hours of labour work. The total hours of daily work in RS Means Building Construction Data (Waier, 2009), is computed by dividing the crew daily working hours by the daily output. It should be noted that the total labour daily hours include two dissimilar crews of workers from section sizes W6×9 to W16×67, and from W18×35 to W36×302. The labour hours for the first crews of workers, for the small section sizes include structural steel foreman, and structural steel workers, crane equipment operator, and an oiler equipment operator. However, the second crews of workers, for the larger section sizes, have the same foreman and operator, in addition to the welder (Waier, 2009). This explanation provides a better understanding of the "total labour hours" definition. The first part of the risk function (rework risk) is the same function that was developed in Section 3.5.7.1., referred to as the rework risk function. The second part of the safety risk function is the product of the total design hours, unit cost per hour, and the workers compensation insurance multiplier.

A high multiplier (WC) is 50% of the average weekly wage (AWW) and is used here to calculate an injured employee's temporary or permanent benefits in the worst case. This insurance rate varies for different trades. This rate is about 10% of the "total labour hours" for the oilers and equipment operators, and 15.5% for skilled worker. As mentioned earlier in the fabrication cost function section, a crew of 4 workers are required for assembling the light section sizes, and a crew of 5 workers for the heavy sections. These two crews should work simultaneously in order to assemble both light and heavy sections. It should be noted that in practice, the crew with the larger capacity would be used, which in this case is the crew of 5 workers required for assembling the heavy section sizes. For this reason, assuming this WC rate is 10% for each craft worker; it will add up to a total worker compensation insurance rate of 50% for the entire crew to work on light and heavy section sizes (Waier, 2009). For this reason the WC multiplier has been considered to be 50% of the total labour hours. The complete form of this equation is shown below:

Equation 22:

$$\boldsymbol{Safety\ risk\ function = WC \times Total\ labour\ hours \times 125(^{\$}/_{hr}) + Rework\ risk\ function}$$

Table 9 below displays each fifth configuration of the 56 data points. APPENDIX F shows the complete 56 data points. This table covers information regarding the rework, transportation, alignment, safety risk/cost, and the total structural fabrication cost. It should be noted that the first fabrication cost function data represents the actual (initial) braced module, and all the other data points are for the unbraced modular frame. The last added data point (57^{th}) represents the module with the loosely bolted connections, defined in Section 3.3.5. The loosely bolted connections for the same defined frames (Figure 35), and the 1% of the nominal moment and axial force values for the selected beams and columns have also been analyzed for the last fabrication cost function step (56^{th} step). The moment-rotation and P-M2-M3 interaction diagram data for this configurations step (56^{th}) has been illustrated in APPENDIX D. This added configuration (57^{th}) has the maximum story drift value and models a case which analyzes the module as a "shock absorber" during the transportation phase and assumes that the structure is slightly collapsed. For this case, the modular behaviour in terms of the story drift value, site-fit risks, and fabrication costs shown are as shown in the 57^{th} configuration step.

The connections in this model behave similar to an earthquake fuse on an earthquake resilient steel structural connection. One type of a steel structural fuse is a pin-fuse joint. The behaviour and shape of a pin-fuse joint respectively, are shown are Figure 52 and Figure 53. These connections will rotate under

seismic forces and will come back to their initial place once the aftershocks are finished (Skidmore, Owings, & Merrill, 2009). The behaviour of the loosely bolted connection modeled in the 57th configuration, with a story value of 0.00575 is similar to the pin-fuse during the transportation phase. However, this module chassis, if displaced more than the specified tolerance limit for deflections, may need the entire rework event of $5,000 for alterations, alignments, etc. Significant distortions, and a 100% probability of occurrence of each alteration event, will also lead to cost increments in the transportation, and safety risks. For this reason the loosely bolted connections have a site-fit risk value of 100% due to the slightly collapsed module and this may cause significant cost increments in the risk functions. The story drift of the loosely bolted connection (0.00575) was found by defining the connection in the SAP2000 model, applying the connection as a hinge to the module, and running the analysis for the critical load cases (LC_2 and LC_4) as explained in earlier. Assuming the loosely bolted connection has a risk value of 1 and entering this number in each of the risk functions, the risk in terms of costs associated with a loosely bolted connection can be identified (e.g., $5000 alteration risk). It should be noted that this configuration step has not been shown in the site-fit risk function plots, since it is modeled differently from the other 56 data points. However, adding it in this section assists with comparing the results of the hinged frame with loosely bolted connections with the actual fabrication cost model data.

Figure 52: Pin-fuse joint behaviour during and after the earthquake shock (Skidmore, Owings, & Merrill, 2009)

Figure 53: Pin-fuse joint (Skidmore, Owings, & Merrill, 2009)

Once the configuration of the divergent site-fit risk functions and their relationship with the loosely bolted connection has been identified; the fabrication cost data will be plotted in terms of story drift values.

Figure 54 illustrates the fabrication, rework; transportation, alignment, and safety cost versus the story drift values.

Table 9: Site-fit risk function data

Configuration Step	Lateral Displacement(ft) /Height(ft)	Total Fabrication Cost ($)	Probability of rework	Rework Risk ($)	shipping Cost ($)	Transportation Risk ($)	Total Design Hours (hr)	Alignment Risk ($)	Safety Risk ($)	TOTAL ($)
1	0.00138	65632	0.01	50.00	1044	4982.0	61.4	3088	3887	77639
5	0.00183	62094	0.07	330.0	894.0	8097.0	48.9	3228	3384	77133
10	0.00224	59638	0.14	680.0	737.0	11829	47.0	3358	3616	79121
15	0.00236	37920	0.21	1030	607.0	10314	65.6	3393	5124	57781
20	0.00224	45815	0.28	1380	500.0	15436	49.1	3358	4448	70437
25	0.00243	37322	0.35	1730	412.0	15191	47.2	3416	4676	62335
30	0.00268	31995	0.42	2080	340.0	15249	46.4	3494	4977	57795
35	0.00275	33357	0.49	2430	280.0	18159	48.1	3516	5435	62897
40	0.00281	32052	0.56	2780	231.0	19654	48.0	3534	5777	63797
45	0.00304	30432	0.63	3130	190.0	20762	48.2	3605	6142	64071
50	0.00329	30353	0.70	3480	157.0	22800	48.4	3686	6505	66824
55	0.00332	29880	0.77	3830	129.0	24511	48.2	3695	6842	68758
57	0.00575	29667	1.0	5000	124.0	31274	48.2	4454	8012	78407

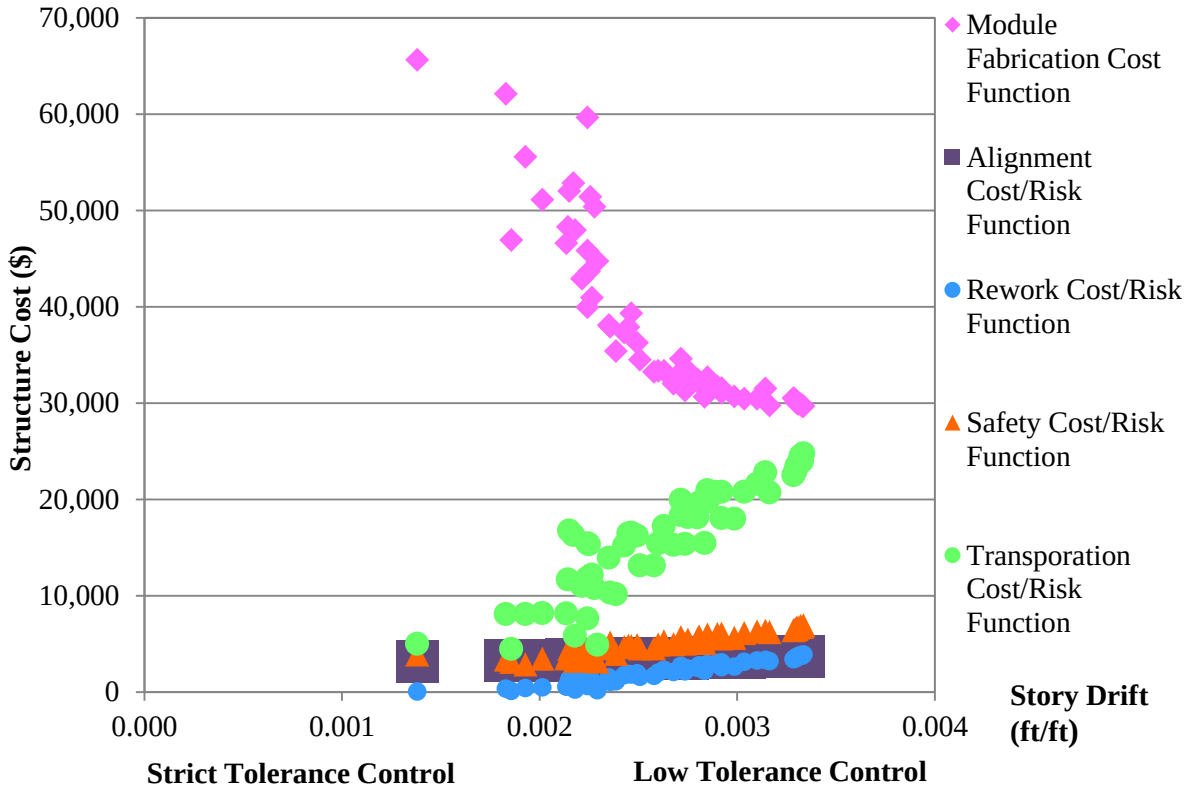

Figure 54: Divergent site-fit risk functions

Each of the colors illustrated in the curve, match the colors provided in Table 9.Figure 54 illustrates that module fabrication, transportation, and safety risk respectively are estimated to have the highest impact on the structural cost and site-fit risk function. The alignment, and rework risk functions are estimated to have the lowest impact with respect to the other functions. This implies that fabrication, and transportation costs and risks are the most influential factors for controlling the total costs. The remaining factors are important as well due to their relative cost and impact. The rework, safety, alignment risk/cost function have cost values between 0 and $9,000, however the transportation costs vary from $5,000 to $30,000, and fabrication costs from $30,000 to $69,000. The transportation and fabrications cost and risk functions vary within a larger range, therefore reduction of the reinforcements will affect the total costs by a large amount. The range of variation from heavy to lightly-reinforced modules vary, about $39,000

for the fabrications costs, $25,000 for the transportation function, and about $9000 for the alignment, rework, and safety risk functions.

Once the divergent site-fit risk functions have been identified, optimization of the costs for the aim of configuring the lowest total cost of combined fabrication cost and transportation, rework, alignment, safety risks will be presented.

3.5.8 Risk Analysis Performance

As discussed in the introduction chapter, the decision that needs to be made regarding the strength of a module is not straight forward one; therefore this section will discuss how to balance the site-fit risks, realignment and over-reinforcement costs in modular design. Modules can be heavily-reinforced and over-designed, from a structural point of view, and it will require no or little adjustment when they arrive on the construction site. A module can be designed for that loading which is associated with the permanent and end-use conditions, mainly ignoring the higher loads that modules will experience during the transportation phase. Once the fabrication costs are reduced, there is a higher probability that the module will need significant alterations in order to correct the sustained damage during transportation. This risk function will provide the possibility to estimate the optimal trade-off between over-design and significant expected alterations, as well as assessing potential impact of techniques for module resiliency.

Figure 55 illustrates the total cost which includes the structural fabrication costs. This function represents rework, transportation, alignment, safety and fabrication costs that were assessed in the preceding section. The analysis of the data sets will be done in the next section.

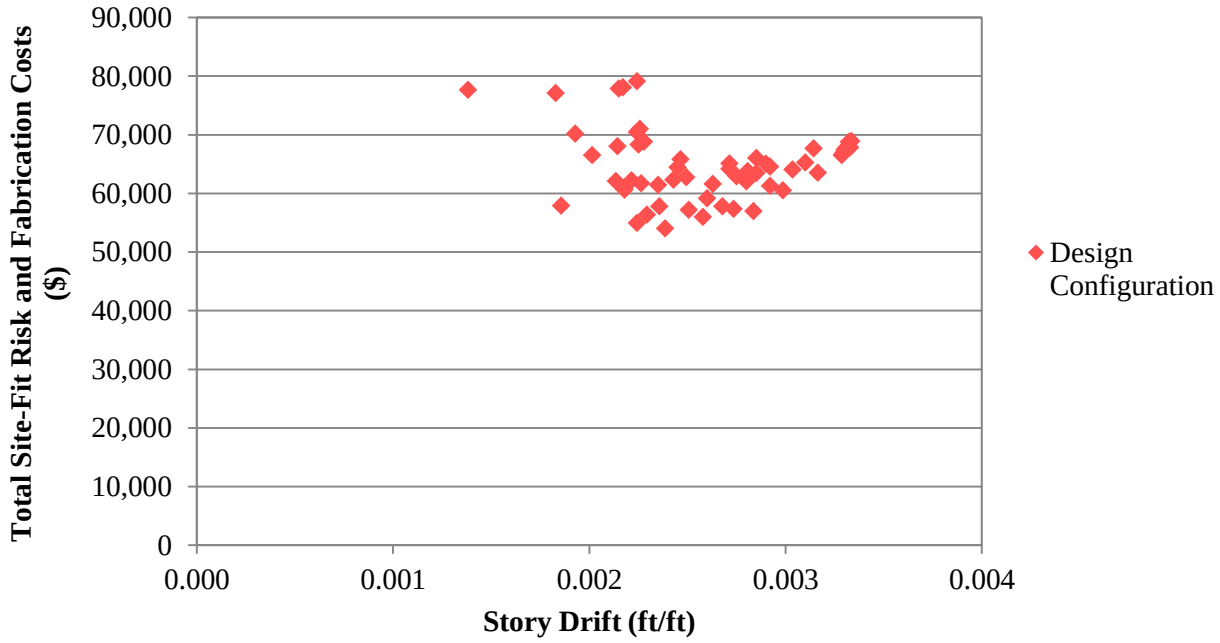

Figure 55: Total site-fit risk and fabrication costs for each considered design configuration ordered by story drift

3.5.9 A Module Design Principle

Since the site-fit risk and fabrication cost functions have been developed, analysis needs to be done on how to optimize the trade-off between the risk of realignment and cost of over reinforcement. Figure 56 illustrates the Pareto optimal boundary of the total site-fit risk functions in addition to the fabrication cost function. This boundary illustrates the minimum amount of construction cost/risk associated with the smallest allowable distortions and deformations.

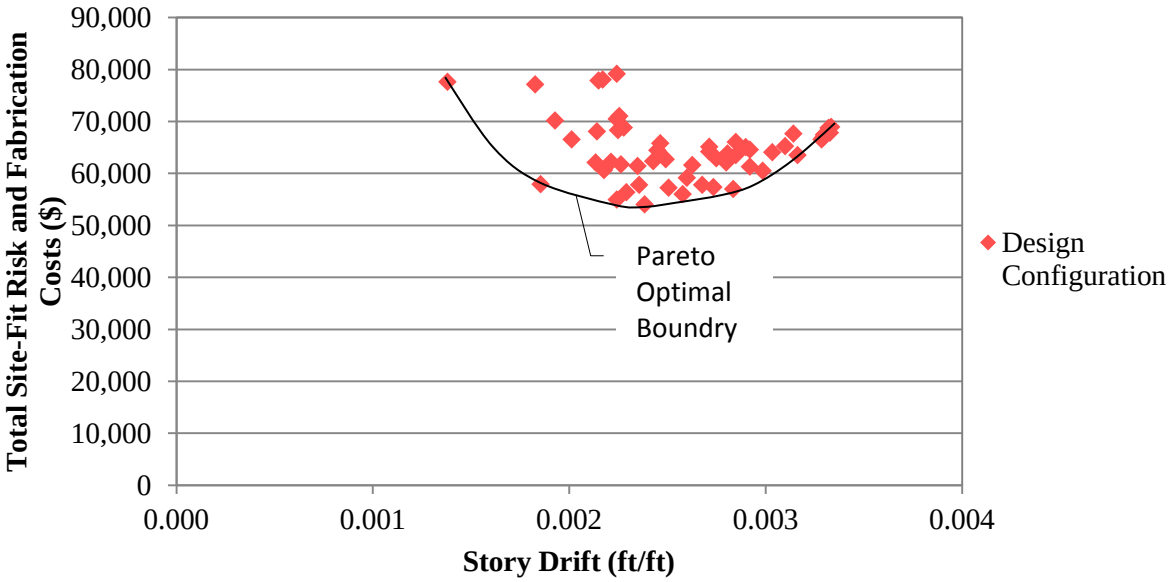

Figure 56: Pareto optimal boundary for design configurations

It should be noted that once a certain amount of distortion is caused due to the reduction of reinforcement, risks begin to out-weight the benefits of a lighter and less expensive fabrication design. Figure 57 illustrates the optimum designed critical story drift value which occurs at a total cost of $54,000 and a story drift value of 0.0024. There is a large cost variation, among design configurations examined, about the mentioned story drift value of 0.0024 with a cost variation from $54,000 to $8,0000. This indicates that once the story drift values reaches the critical story drift value of 0.0024, cost variations may increase with deviations from that specific story drift value. Once the story drift values exceed the critical story drift value, total site-fit risk and fabrication costs increase significantly.

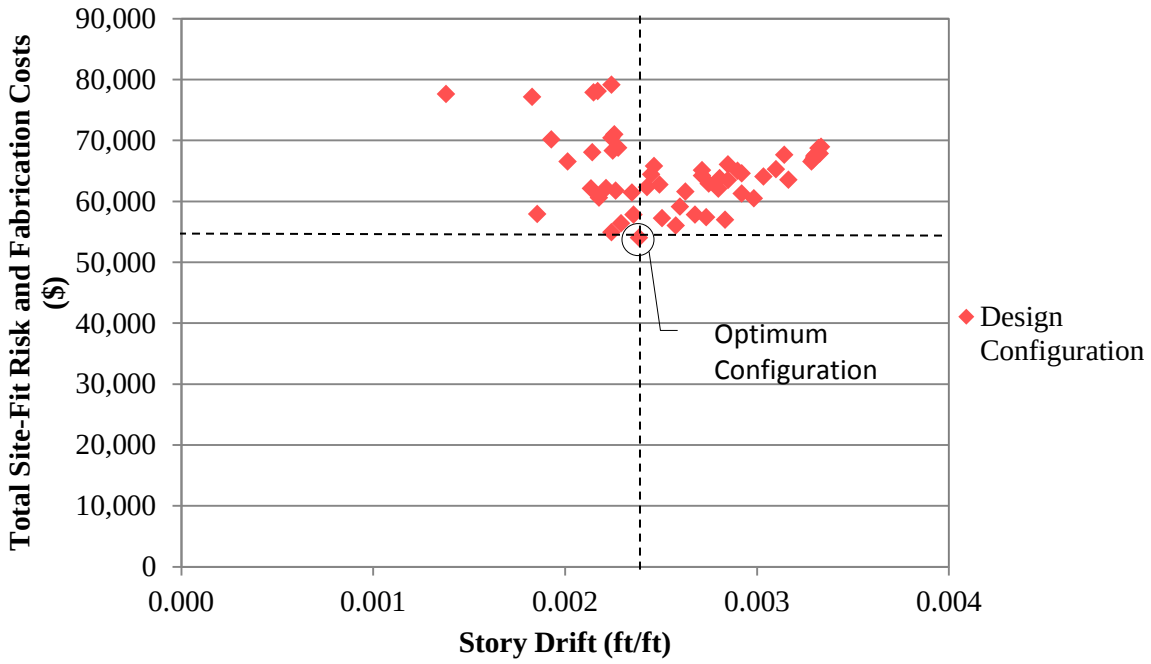

Figure 57: Critical story drift value

It may be concluded that there should be a trade-off between the risk of realignment and the cost of over-reinforcement. Reduction of reinforcement may cause additional risks and lead to unexpected costs. Therefore lightly and over-reinforced modular systems is not an option for respectively reducing fabrication costs, or neglecting alignment costs. Lightly-reinforced modules will increase the risks associated with rework, alignment, safety and transportation.

3.5.10 A More Generalized Module Design Principle

Methods to reduce module site-fit risks are not limited to stiffer structural designs. They may include flexible fixtures for fitting tie-in points of modules to superstructures, foundations or other modules. They may also include enhanced shop fabrication controls. These methods typically increase fabrication costs with the intent of reducing site-fit risks. The analysis presented in this thesis can be generalized to include this wider set of methods. For example, each option can be evaluated according to their:

1. Designed cost of fabrications, and
2. Site-fit risk

The design with the lowest total expected cost can be selected (Figure 58). Each shape represents a configuration step. Once the fabrication cost (1) is added to the site-fit risk (2) the final answer (1) + (2) will represent the total site-fit risk and fabrications cost. In practice 57 configuration steps will not be analyzed, this generalized module design principle shows a risk based approach to module tolerance specification with 4 configuration steps. As a brief conclusion, heavily-reinforced modules may reduce the risks of alignment, safety and rework, however will have increasing costs due to the fabrication and transportation costs. The conclusions and recommendations of the proposed methodology will be reviewed in the last chapter.

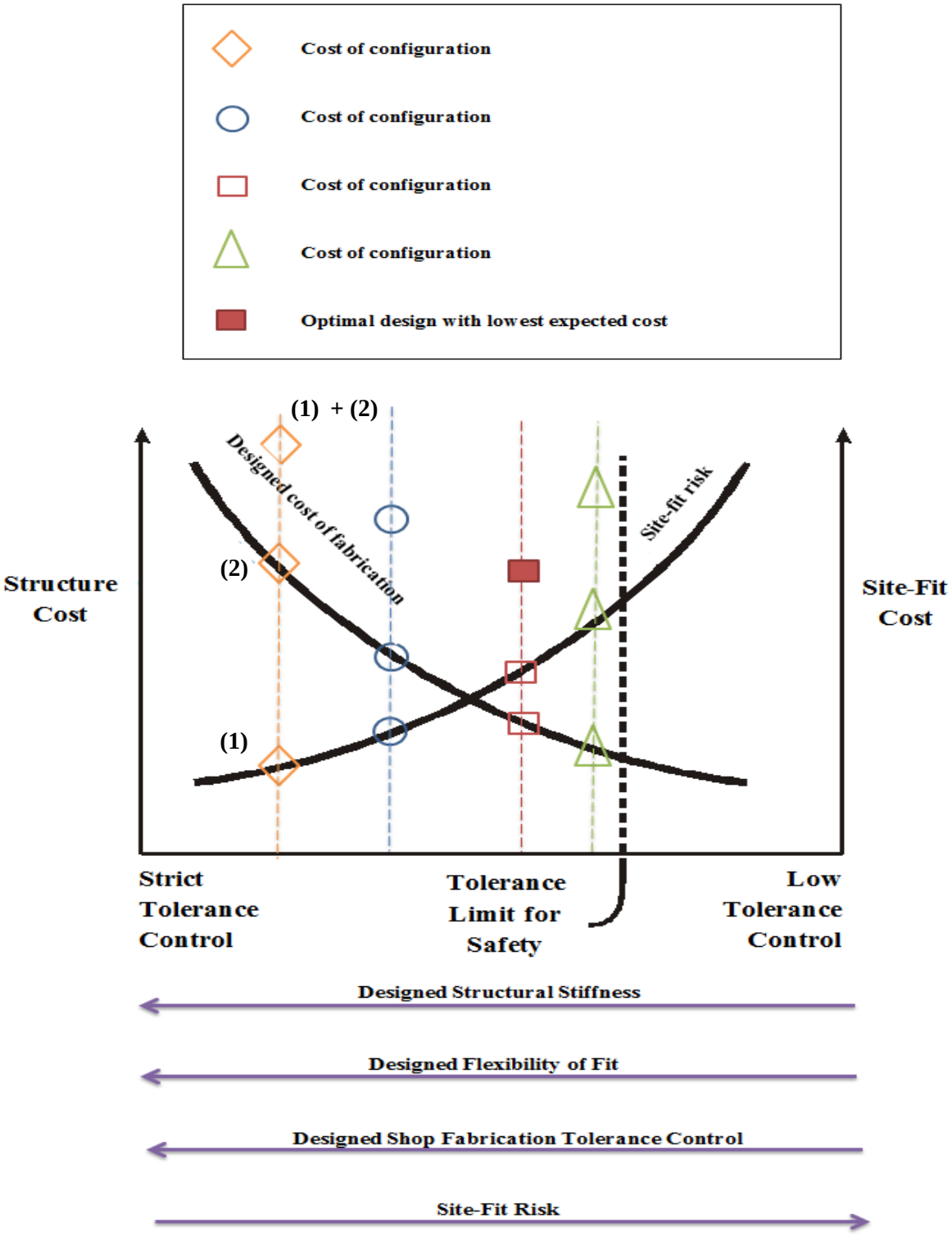

Figure 58: Design with the lowest expected cost

Chapter 4
Conclusions and Recommendations

4.1 Conclusions

The methodology for tolerance definition in modular construction is project specific, and therefore may be specified differently for various types of modular systems. This approach provides information about optimizing the trade-off between the risk of site-fit costs due to realignment and the cost of over-reinforcement. The story drift values, generated in the fabrication cost function are in an acceptable range with regards to strength and stability codes, however each data point has an associated total site-fit risk and fabrication cost that is specific to that certain story drift value. Reduction of modular reinforcement will lead to a reduction in fabrication costs. However, on-site alteration risks will increase. With reducing the module reinforcement, alteration risks due to re-alignments, rework, transportation, and safety risks will increase. However, alteration costs are low and do not have a high impact on the total structural costs (fabrication costs and site-fit risks), for this reason it is beneficial to reduce modular reinforcements, as long as site-fit risks are closely monitored. This reduction in the total structural cost caused by the reduction in reinforcement will endure up to a specific story drift value and will begin to add large amounts of cost increments to the total site-fit risk function after the critical story drift value has been achieved. It should be noted that, in practice, 56 different structural models will not be analyzed for optimizing site-fit risks, and fabrication. This methodology is attainable with analyzing a few fabrication cost reduction models as explained in Section 3.5.10.

This methodology concludes that there should be a balance between site-fit risks and over-reinforcement. The step by step reduction of section sizes in a structural system will reduce fabrication costs. Nevertheless, the site-fit risk function will effect in significant cost increases due to alterations that may lead to section replacement and total loss. In this case study once the story drift value exceeds an amount of $0.0024\frac{\text{ft}}{\text{ft}}$, the module is subjected to significant cost increases up to about $80,000. This is approximately adding $26,000 to the optimal total fabrications and site-fit risk cost of $54,000. This leads to the fact that fabrication cost reduction by itself cannot be a solution to reduce the building expenses, and site-fit risk functions are a much more influential factor once the structural system has achieved its critical story drift or distortion value. On the other hand over-reinforcement (over-design) of the structural system may result in few or no adjustments on the construction site. Nevertheless, the material, labour, and transportation for this over-designed module will be much higher. A module can be designed with

only considering its end condition and ignoring the large amounts of loads that will be applied to the module during the transportation phase. A risk based approach to module tolerance specification will make it possible to determine the optimal solution with regard to fabrication, transportation, rework, and safety costs. The potential impacts of optimal tolerance definition can also be verified.

Based on the presented case study, the following conclusions are drawn:

1. The fabrication cost function has the largest impact in the total structural cost, due to the material, labour, and equipment costs.
2. Transportation risks are having the second greatest impact, since they include the transportation cost, risks due to dimensional degradation, and insurance costs. The rework costs for the dimensional degradation in the transportation function have the highest impact since they are considered to be costs caused by section replacement due to severe displacements/distortions.
3. Safety risk has the third greatest impact among the site-fit risk functions. This is caused due to the factor of rework risk and resulting accident risk, labour average weekly wage, and the workers compensation insurance cost for hours of site work which do not have a relatively high value with respect to the other risk functions.
4. Alignment cost values have a moderate to low impact on the site-fit risk function. The rationale behind this conclusion is that story drift re-alignment risk, and on-site erection costs are the influential factors in this function.
5. Rework risk function has the lowest impact; hence this function has been formed with multiplying a rework probability by a 1 day rework event that will be used to alter minor miss-alignments, distortions and displacements.

The presented research shows that that the influential factors of the site-fit risk functions are respectively fabrication, transportation, safety, alignment, and rework costs. In addition the presented generic module design procedure is a methodology, which is adaptable to properly account for trade-off between over-design and significant alterations. The sit-fit risk influential factors may vary for different modular systems. This optimal tolerance resilience strategy is easy to follow for a design engineer and shows that over-designed modular systems are not a solution for reducing the rework costs and mitigating risks and neither are lightly-reinforced modules for reducing fabrication costs. Both of the mentioned cases can lead to a drastic cost increase. Therefore, a site-fit risk function is the best way of finding the balanced point between the amount of necessary reinforcement and produced risks. The maximum allowable

modular out-of-tolerance value, which requires the minimum amount of cost with respect to fabrication, transportation, rework, safety, and alignment costs, can be verified using this methodology.

4.2 Recommendations for Future Research

Little has been published describing a procedure for defining tolerance limits, since most of the guidelines contain information regarding tolerance specification values for various types of building systems. The tolerance specification handbooks and guidelines contain numbers and limits for various types of sections and structural systems. However, there is a limited information on the how to specify tolerance limits. For this reason, further research on a methodology for module resiliency could lead to a new approach for defining tolerance limits and finding the optimal trade-off between various risk types and structural costs. Future research my therefore include the following:

1. Analysis on various types of risks that are associated with transportation, rework, alignment, fabrication, and safety costs that may not have been considered in this research.
2. Considering a more flexible module for obtaining the risk based approach to module tolerance specification and also comparing the results to an over-reinforced modular system.
3. Analyzing a multistory building for generating a systematic or progressive tolerance drift function for multistory buildings.
4. Developing an automated system with the use of MATLAB or any other similar commercial software in addition to the SAP2000 software. This model could receive structural design, construction site, and structural serviceability specifics as in input and output the maximum allowable module out of tolerance value that requires the minimum amount of cost. It should be noted that the design and structural testing phase of the module should be done manually. However, generating the fabrication and site-fit risk functions with respect the originated data points on SAP2000 could be done automatically with the use of MATLAB or other similar commercial software.
5. Generating a new methodology for modular systems, with different soft wares and functions could assist with building a diverse frame work for defining tolerance specifications.
6. Further analysis on the loosely bolted connection behaviour and their definition on SAP2000
7. Calibrating all of the preceding functions with real data

Appendix A:

Load Pattern Definition and Load Cases in SAP2000

The following load patterns were applied to the module: α_s and α_c are the SIN and COS of the assumed load angle, which was 30°. D_s and D_p are respectively the structural dead load and pipe load.

$\boldsymbol{Lp_1 = D_s}$: Structure self-weight (vertical)-Gravity

$\boldsymbol{Lp_2 = D_p}$**:** Pipe load (Vertical)-Gravity

$\boldsymbol{Lp_3 = \alpha_s D_s}$**:** Structure self-weight (lateral)-Y direction in SAP2000**.** This was assumed to be inclined 30 degrees in the YZ plane with respect to the Z axis

$\boldsymbol{Lp_4 = \alpha_s D_p}$**:** Pipe load (lateral)-Y direction in SAP2000. This was assumed to be inclined 30 degrees in the YZ plane with respect to the Z

$\boldsymbol{Lp_5 = \alpha_c D_s}$**:** Structure self-weight (vertical)-Gravity. This was assumed to be inclined 30 degrees with respect to the Z axis (vertical × cos30).

$\boldsymbol{Lp_6 = \alpha_c D_p}$**:** Pipe load (vertical)-Gravity. This was assumed to be inclined 30 degrees with respect to the Z axis (vertical × cos30).

$\boldsymbol{Lp_7 = \alpha_s D_s}$**:** Structure self-weight (lateral)-X direction in SAP2000. This was assumed to be inclined 30 degrees in the XZ plane with respect to the Z axis (vertical × sin30)

$\boldsymbol{Lp_8 = \alpha_s D_p}$**:** Pipe load (lateral)-X direction in SAP2000**.** This was assumed to be inclined 30 degrees in the XZ plane with respect to the Z axis (vertical × sin30)

The following load cases were considered:

$\boldsymbol{LC_1 = Lp_1 + Lp_2}$**:** Structure and pipe weight (vertical)-Gravity

$\boldsymbol{LC_2 = Lp_{3+}Lp_4 + Lp_5 + Lp_6}$**:** Structure and pipe weight (inclined in the YZ plane)

$\boldsymbol{LC_3}$=$\boldsymbol{Lp_{3+}Lp_4 + Lp_7 + Lp_8}$ **:** Structure and pipe weight (inclined in the XZ plane)

$\boldsymbol{LC_4}$=$\boldsymbol{LC_1 + Lp_3 + Lp_4}$**:** Impact lateral (0.5g)-Y direction in SAP2000

$\boldsymbol{LC_5}$=$\boldsymbol{LC_1 + Lp_7 + Lp_8}$**:** Impact lateral (0.5g)-X direction in SAP2000

$\boldsymbol{LC_6}$=$\boldsymbol{2LC_1}$**:** Impact vertical (2g)-Gravity

Load patterns and load case specific

	L_P & L_C- Dir.	D_S	D_P	$\alpha_S D_S$	$\alpha_S D_P$	$\alpha_c D_s$	$\alpha_c D_p$
Load Patterns	Lp_1-Z						
	Lp_2-Z						
	Lp_3-Y						
	Lp_4-Y						
	Lp_5-Z						
	Lp_6-Z						
	Lp_7-X						
	Lp_8-X						
Load Combinations	LC_1-Z						
	LC_2-YZ						
	LC_3-XZ						
	LC_4-Y						
	LC_5-X						
	LC_6-Z						

Appendix B:

SAP Loading Details and Strength/Stability Structural Configuration

Piping details on the first and third floor

Actual OD(inch)	Determined OD(inch)	Determined thickness(inch)	Weight lb/ft	Weight lb/ft filled with water	# of pipe
32.4	24.0	1.21	297	455.2	1
6.37	8.62	0.500	43.4	63.10	3
2.73	2.87	0.270	7.60	9.400	7
4.01	4.50	0.330	15.0	20.00	2

Piping details on the second floor

Actual OD(inch)	Determined OD(inch)	Determined thickness(inch)	Weight lb/ft	Weight lb/ft filled with water	# of pipe
22.14	24.0	1.21	297	455.2	1
4.130	4.50	0.330	15.0	20.00	6
3.440	3.50	0.300	10.2	13.00	1
2.730	2.87	0.270	7.60	9.400	8

Pipe Load distribution on the main beams

Total pipe load (lb/ft)	Length of each beam	Total length of each floor (ft)	Load on mid-beam (lb/ft)-UDL	Load on the two side beams (lb/ft)-UDL	Floor
750.3	14	45	1205.83	602.91	1st
663.4	14	45	1066.17	533.08	2nd
750.3	14	45	1205.83	602.91	3rd

Impact load distributions

Pipe UDL load on mid-beam LATERAL-Y and X Dir. (lb)	PIPE UDL load on the two side beams LATERAL-Y and X Dir. (lb)	PIPE UDL load on mid beam VERTICAL- Z Dir. (lb)	PIPE UDL load on the two side beams VERTICAL- Z Dir. (lb)	Floor
602.91	301.45	1044.28	522.14	1st
533.08	266.54	923.330	461.66	2nd
602.91	301.45	1044.28	522.14	3rd

Factored moment resistance

	Corner Column	Interior Column
M_u (lb-ft)	36037.64	87637.22
λ	1.920000	1.640000
Cr	69958.12	145483.3
M_r(Strong Axis)X (lb-ft)	17982.89	69277.29
M_r (Weak Axis)Y (lb-ft)	25920.00	45360.00

Corner column strength and stability check for L_{P1}: Dead Load

Relative elevation from the ground	0	1/4	2/4	3/4	1
C_r (lb)	69958.2	69958.2	69958.2	69958.2	69958.1
U_{1x} (ft)	-4.74613E-08	-4.74600E-08	-4.74600E-08	-4.74613E-08	-4.70000E-08
U_{1y} (ft)	-5.17948E-07	-5.17900E-07	-5.17900E-07	-5.17948E-07	-5.20000E-07
C_f(Detrimental in lb)	2122.50	2122.50	1691.25	1188.75	833.750
M_f(Strong Axis)X (lb-ft)	1235.00	102.240	829.880	190.140	1391.00
M_f (Weak Axis)Y (lb-ft)	52.7000	72.1100	1.97000	72.1500	77.7000
M_r (Strong Axis)X (lb-ft)	17982.9	17982.9	17982.9	17982.9	17982.9
M_r (Weak Axis)Y (lb-ft)	25920.0	25920.0	25920.0	25920.0	25920.0
Strength Check	0.0303310	0.0303360	0.0241760	0.0169926	0.0119200

Interior column strength and stability check for L_{P1}: Dead Load

Relative elevation from the ground	0	1/4	2/4	3/4	1
C_r (lb)	145483.3	145483.3	145483.3	145483.3	145483.0
U_{1x} (ft)	-7.285020E-09	-7.285000E-09	-7.285000E-09	-7.285020E-09	-7.300000E-09
U_{1y} (ft)	-1.019900E-07	-5.179000E-07	-5.179000E-07	-5.179480E-07	-5.200000E-07
C_f(Detrimental in lb)	5926.250	5926.250	4836.250	4086.250	2943.750
M_f(Strong Axis)X (lb-ft)	328.0000	201.0000	12.0000	167.0000	308.0000
M_f (Weak Axis)Y (lb-ft)	210.3700	705.0000	613.0000	831.0000	169.0000
M_r (Strong Axis)X (lb-ft)	69277.29	69277.29	69277.29	69277.29	69277.30
M_r (Weak Axis)Y (lb-ft)	45360.00	45360.00	45360.00	45360.00	45360.00
Strength Check	0.04073492	0.04073500	0.03324300	0.02808700	0.02023400

Corner column strength and stability check for L_{P2}: Pipe load (vertical)

Relative elevation from the ground	0	1/4	2/4	3/4	1
C_r (lb)	69958.2	69958.2	69958.2	69958.2	69958.2
U_{1x} (ft)	-4.74613E-08	-4.74613E-08	-4.74600E-08	-4.74600E-08	-4.74600E-08
U_{1y} (ft)	-5.17948E-07	-5.17948E-07	-5.17900E-07	-5.17900E-07	-5.17900E-07
C_f(Detrimental in lb)	8132.50	8132.50	4307.50	4303.75	24.7000
M_f(Strong Axis)X (lb-ft)	138.000	7.00000	61.0000	27.0000	58.0000
M_f (Weak Axis)Y (lb-ft)	681.000	1094.000	1988.000	1167.000	303.000
M_r (Strong Axis)X (lb-ft)	17982.9	17982.9	17982.9	17982.9	17982.9
M_r (Weak Axis)Y (lb-ft)	25920.0	25920.0	25920.0	25920.0	25920.0
Strength Check	0.116249	0.116249	0.0615725	0.0615189	0.000353100

Interior column strength and stability check for L_{P2}: Pipe load (vertical)

Relative elevation from the ground	0	1/4	2/4	3/4	1
C_r (lb)	145483.3	145483.3	145483.3	145483.3	145483.3
U_{1x} (ft)	-7.285020E-09	-7.285020E-09	-7.285000E-09	-7.285000E-09	-7.285000E-09
U_{1y} (ft)	-1.019900E-07	-5.179480E-07	-5.179000E-07	-5.179000E-07	-5.179000E-07
C_f(Detrimental in lb)	16240.00	16240.00	8612.500	8616.250	45.00000
M_f(Strong Axis)X (lb-ft)	7498.000	5360.000	917.0000	648.0000	625.0000
M_f (Weak Axis)Y (lb-ft)	57.00000	29.00000	29.00000	2.500000	0.7000000
M_r (Strong Axis)X (lb-ft)	69277.29	69277.29	69277.29	69277.29	69277.29
M_r (Weak Axis)Y (lb-ft)	45360.00	45360.00	45360.00	45360.00	45360.00
Strength Check	0.1116271	0.1116271	0.1116271	0.1116271	0.1116271

Corner column strength and stability check forL_{P3}: Structure self-weight (lateral)-Y direction

Relative elevation from the ground	0	1/4	2/4	3/4	1
C_r (lb)	69958.2	69958.2	69958.2	69958.2	69958.2
U_{1x} (ft)	-4.74613E-08	-4.74600E-08	-4.74600E-08	-4.74613E-08	-4.70000E-08
U_{1y} (ft)	-5.17948E-07	-5.17900E-07	-5.17900E-07	-5.17948E-07	-5.20000E-07
C_f(Detrimental in lb)	1876.50	1876.50	606.000	1153.50	474.000
M_f (Strong Axis)X (lb-ft)	21.0000	35.0000	66.0000	42.0000	23.0000
M_f (Weak Axis)Y (lb-ft)	3154.00	2926.00	705.00	1340.00	1157.00
M_r (Strong Axis)X (lb-ft)	17982.9	17982.9	17982.9	17982.9	17982.9
M_r (Weak Axis)Y (lb-ft)	25920.0	25920.0	25920.0	25920.0	25920.0
Strength Check	0.0268230	0.0268230	0.00866200	0.01648800	0.00677500

Interior column strength and stability check for L_{P3}: Structure self-weight (lateral)-Y direction

Relative elevation from the ground	0	1/4	2/4	3/4	1
C_r (lb)	145483.3	145483.3	145483.3	145483.3	145483.3
U_{1x} (ft)	-7.285020E-09	-7.285000E-09	-7.285000E-09	-7.285020E-09	-7.300000E-09
U_{1y} (ft)	-1.019900E-07	-5.179000E-07	-5.17900E-07	-5.179480E-07	-5.200000E-07
C_f(Detrimental in lb)	6285.960	6285.960	3636.135	3640.500	1452.000
M_f(Strong Axis)X (lb-ft)	9106.00	782.0000	4921.000	4908.000	4960.000
M_f (Weak Axis)Y (lb-ft)	9.000000	221.0000	361.0000	199.0000	88.0000
M_r (Strong Axis)X (lb-ft)	69277.29	69277.29	69277.29	69277.29	69277.29
M_r (Weak Axis)Y (lb-ft)	45360.00	45360.00	45360.00	45360.00	45360.00
Strength Check	0.04320700	0.04320700	0.02499300	0.02502300	0.009981000

Corner column strength and stability check for L_{P4}: Pipe load (lateral)-Y direction

Relative elevation from the ground	0	1/4	2/4	3/4	1
C_r (lb)	69958.2	69958.2	69958.2	69958.2	69958.2
U_{1x} (ft)	-4.74613E-08	-4.74613E-08	-4.74600E-08	-4.74600E-08	-4.74600E-08
U_{1y} (ft)	-5.17948E-07	-5.17948E-07	-5.17900E-07	-5.17900E-07	-5.17900E-07
C_f(Detrimental in lb)	2722.50	81.0000	712.500	7.06500	7.50000
M_f(Strong Axis)X (lb-ft)	42.0000	75.0000	87.0000	26.0000	26.0000
M_f (Weak Axis)Y (lb-ft)	7923.00	7600.00	315.000	3300.00	558.000
M_r (Strong Axis)X (lb-ft)	17982.9	17982.9	17982.9	17982.9	17982.9
M_r (Weak Axis)Y (lb-ft)	25920.0	25920.0	25920.0	25920.0	25920.0
Strength Check	0.0389161	0.00115771	0.0101847	0.000100900	0.000107200

Interior column strength and stability check forL_{P4}: Pipe load (lateral)-Y direction

Relative elevation from the ground	0	1/4	2/4	3/4	1
C_r (lb)	145483.3	145483.3	145483.3	145483.3	145483.3
U_{1x} (ft)	-7.285020E-09	-7.285020E-09	-7.285000E-09	-7.285000E-09	-7.285000E-09
U_{1y} (ft)	-1.019900E-07	-5.179480E-07	-5.179000E-07	-5.179000E-07	-5.179000E-07
C_f(Detrimental in lb)	9793.500	9793.500	3381.000	4285.500	1122.000
M_f(Strong Axis)X (lb-ft)	22448.00	6332.000	3649.000	13093.41	3776.000
M_f (Weak Axis)Y (lb-ft)	47.00000	411.0000	376.0000	189.0000	81.00000
M_r (Strong Axis)X (lb-ft)	69277.29	69277.29	69277.29	69277.29	69277.29
M_r (Weak Axis)Y (lb-ft)	45360.00	45360.00	45360.00	45360.00	45360.00
Strength Check	0.06731702	0.06731702	0.02323980	0.02945700	0.007712200

Corner column strength and stability check for L_{P5}: Structure self-weight (vertical)-Gravity

Relative elevation from the ground	0	1/4	2/4	3/4	1
C_r (lb)	69958.3	69958.3	69958.3	69958.3	69958.1
U_{1x} (ft)	-4.74613E-08	-4.74600E-08	-4.74600E-08	-4.74613E-08	-4.70000E-08
U_{1y} (ft)	-5.17948E-07	-5.17900E-07	-5.17900E-07	-5.17948E-07	-5.20000E-07
C_f(Detrimental in lb)	4393.50	4393.50	3901.50	1713.00	1348.50
M_f(Strong Axis)X (lb-ft)	473.000	316.000	708.000	363.000	375.000
M_f (Weak Axis)Y (lb-ft)	24.0000	47.0000	4.00000	44.0000	28.0000
M_r (Strong Axis)X (lb-ft)	17982.9	17982.9	17982.9	17982.9	17982.9
M_r (Weak Axis)Y (lb-ft)	25920.0	25920.0	25920.0	25920.0	25920.0
Strength Check	0.0628019	0.0628010	0.0557691	0.0244861	0.0192800

Corner column strength and stability check for L_{P5}: Structure self-weight (vertical)-Gravity

Relative elevation from the ground	0	1/4	2/4	3/4	1
C_r (lb)	145483.3	145483.3	145483.3	145483.3	145483.0
U_{1x} (ft)	-7.285020E-09	-7.285000E-09	-7.285000E-09	-7.285020E-09	-7.300000E-09
U_{1y} (ft)	-1.019900E-07	-5.179000E-07	-5.179000E-07	-5.179480E-07	-5.200000E-07
C_f(Detrimental in lb)	16876.50	16876.50	8950.500	8955.000	46.50000
M_f(Strong Axis)X (lb-ft)	6493.000	4641.000	793.0000	4093.000	541.0000
M_f (Weak Axis)Y (lb-ft)	283.0000	641.0000	358.0000	581.0000	111.0000
M_r (Strong Axis)X (lb-ft)	69277.29	69277.29	69277.29	69277.29	69277.30
M_r (Weak Axis)Y (lb-ft)	45360.00	45360.00	45360.00	45360.00	45360.00
Strength Check	0.1160031	0.1160031	0.06152250	0.06155347	0.000320000

Corner column strength and stability check for L_{P6}: Pipe load (vertical)-Gravity

Relative elevation from the ground	0	1/4	2/4	3/4	1
C_r (lb)	69958.2	69958.2	69958.2	69958.2	69958.2
U_{1x} (ft)	-4.74613E-08	-4.74613E-08	-4.74600E-08	-4.74600E-08	-4.74600E-08
U_{1y} (ft)	-5.17948E-07	-5.17948E-07	-5.17900E-07	-5.17900E-07	-5.17900E-07
C_f(Detrimental in lb)	8451.00	8451.00	4476.00	4323.00	27.0000
M_f(Strong Axis)X (lb-ft)	120.000	6.00000	66.0000	24.0000	50.0000
M_f (Weak Axis)Y (lb-ft)	590.000	916.000	61.0000	1002.00	263.000
M_r (Strong Axis)X (lb-ft)	17982.9	17982.9	17982.9	17982.9	17982.9
M_r (Weak Axis)Y (lb-ft)	25920.0	25920.0	25920.0	25920.0	25920.0
Strength Check	0.120801	0.120801	0.0639811	0.0617941	0.000385900

Interior column strength and stability check for L_{P6}: Pipe load (vertical)-Gravity

Relative elevation from the ground	0	1/4	2/4	3/4	1
C_r (lb)	145483.3	145483.3	145483.3	145483.3	145483.3
U_{1x} (ft)	-7.28502E-09	-7.28502E-09	-7.28500E-09	-7.28500E-09	-7.28500E-09
U_{1y} (ft)	-1.01990E-07	-5.17948E-07	-5.17900E-07	-5.17900E-07	-5.17900E-07
C_f(Detrimental in lb)	16876.5	16876.5	8950.50	8955.00	46.5000
M_f(Strong Axis)X (lb-ft)	6493.00	6317.00	794.000	5605.00	541.000
M_f (Weak Axis)Y (lb-ft)	49.0000	26.0000	25.0000	3.00000	0.600000
M_r (Strong Axis)X (lb-ft)	69277.3	69277.3	69277.3	69277.3	69277.3
M_r (Weak Axis)Y (lb-ft)	45360.0	45360.0	45360.0	45360.0	45360.0
Strength Check	0.116004	0.116004	0.0615225	0.0615535	0.000319600

Corner column strength and stability check forL_{P7}: Structure self-weight (lateral)-X direction

Relative elevation from the ground	0	1/4	2/4	3/4	1
C_r (lb)	69958.2	69958.2	69958.2	69958.2	69958.1
U_{1x} (ft)	-4.74613E-08	-4.74600E-08	-4.74600E-08	-4.74613E-08	-4.70000E-08
U_{1y} (ft)	-5.17948E-07	-5.17900E-07	-5.17900E-07	-5.17948E-07	-5.20000E-07
C_f(Detrimental in lb)	3583.50	3583.50	3582.00	714.000	717.000
M_f(Strong Axis)X (lb-ft)	170.000	588.000	190.000	127.000	151.000
M_f (Weak Axis)Y (lb-ft)	5.00000	4.00000	11.0000	12.0000	14.0000
M_r (Strong Axis)X (lb-ft)	17982.9	17982.9	17982.9	17982.9	17982.9
M_r (Weak Axis)Y (lb-ft)	25920.0	25920.0	25920.0	25920.0	25920.0
Strength Check	0.0512236	0.0512235	0.0512021	0.0102062	0.0102500

Interior column strength and stability check for L_{P7}: Structure self-weight (lateral)-X direction

Relative elevation from the ground	0	1/4	2/4	3/4	1
C_r (lb)	145483.3	145483.3	145483.3	145483.3	145483.0
U_{1x} (ft)	-7.28502E-09	-7.28500E-09	-7.28500E-09	-7.28502E-09	-7.30000E-09
U_{1y} (ft)	-1.01990E-07	-5.17900E-07	-5.17900E-07	-5.17948E-07	-5.20000E-07
C_f(Detrimental in lb)	3259.50	3259.50	1305.00	1311.00	670.500
M_f(Strong Axis)X (lb-ft)	8.00000	17.0000	27.0000	35.0000	14.0000
M_f (Weak Axis)Y (lb-ft)	298.000	2422.00	680.000	1146.00	360.000
M_r (Strong Axis)X (lb-ft)	69277.3	69277.3	69277.3	69277.3	69277.3
M_r (Weak Axis)Y (lb-ft)	45360.0	45360.0	45360.0	45360.0	45360.0
Strength Check	0.0224047	0.0224047	0.00897010	0.00901134	0.00461000

Corner column strength and stability check for L_{P8}: Pipe load (lateral)-X direction

Relative elevation from the ground	0	1/4	2/4	3/4	1
C_r (lb)	69958.2	69958.2	69958.2	69958.2	69958.2
U_{1x} (ft)	-4.74613E-08	-4.74613E-08	-4.74600E-08	-4.74600E-08	-4.74600E-08
U_{1y} (ft)	-5.17948E-07	-5.17948E-07	-5.17900E-07	-5.17900E-07	-5.17900E-07
C_f(Detrimental in lb)	6670.50	6670.50	6685.50	1744.50	1711.50
M_f(Strong Axis)X (lb-ft)	660.000	2141.00	1910.00	1352.00	1048.00
M_f (Weak Axis)Y (lb-ft)	38.000	100.000	413.000	145.000	48.0000
M_r (Strong Axis)X (lb-ft)	17982.9	17982.9	17982.9	17982.9	17982.9
M_r (Weak Axis)Y (lb-ft)	25920.0	25920.0	25920.0	25920.0	25920.0
Strength Check	0.0953491	0.0953499	0.0955643	0.0249363	0.0244646

Interior column strength and stability check forL_{P8}: Pipe load (lateral)-X direction

Relative elevation from the ground	0	1/4	2/4	3/4	1
C_r (lb)	145483.3	145483.3	145483.3	145483.3	145483.3
U_{1x} (ft)	-7.285020E-09	-7.285020E-09	-7.285000E-09	-7.285000E-09	-7.285000E-09
U_{1y} (ft)	-1.019900E-07	-5.179480E-07	-5.179000E-07	-5.179000E-07	-5.179000E-07
C_f(Detrimental in lb)	6274.500	6274.500	1000.500	1012.500	1746.000
M_f(Strong Axis)X (lb-ft)	52.00000	580.0000	664.0000	1022.000	213.0000
M_f (Weak Axis)Y (lb-ft)	490.0000	4286.000	4315.000	2782.000	750.000
M_r (Strong Axis)X (lb-ft)	69277.29	69277.29	69277.29	69277.29	69277.29
M_r (Weak Axis)Y (lb-ft)	45360.00	45360.00	45360.00	45360.00	45360.00
Strength Check	0.04312867	0.04312863	0.006877000	0.006959500	0.01200140

Strength and stability check of the corner column

Relative elevation from the ground	0	1/4	2/4	3/4	1
L_{C1}	0.147	0.147	0.0857	0.0785	0.0123
L_{C2}	0.241	0.212	0.139	0.103	0.0265
L_{C3}	0.213	0.175	0.166	0.0517	0.0416
L_{C4}	0.0961	0.0583	0.0430	0.0336	0.0188
L_{C5}	0.179	0.179	0.171	0.0521	0.0466
L_{C6}	0.294	0.294	0.172	0.158	0.0245

Strength and stability check of the interior column

Relative elevation from the ground	0	1/4	2/4	3/4	1
L_{C1}	0.153	0.154	0.0924	0.0873	0.0205
L_{C2}	0.343	0.343	0.172	0.178	0.0183
L_{C3}	0.177	0.177	0.0641	0.0705	0.0343
L_{C4}	0.152	0.152	0.0815	0.0826	0.0379
L_{C5}	0.107	0.107	0.0491	0.0441	0.0368
L_{C6}	0.305	0.305	0.185	0.175	0.0411

Load pattern strength and stability check for the beams supporting pipes

Load Patterns	L_{P1}	L_{P2}	L_{P3}	L_{P4}	L_{P5}	L_{P6}	L_{P7}	L_{P8}
M_f(Strong Axis)-lb-ft	511.260	6742.58	41150.1	12018.0	389.200	5839.24	11.1800	13.6900
M_r(Strong Axis)-lb-ft	213840	213840	213840	213840	213840	213840	213840	213840
Strength Check	2.39086 E-08	3.15301 E-07	1.92435 E-06	5.62009 E-07	1.82006 E-08	2.73066 E-07	5.22821 E-05	6.40198 E-05

Load combination strength and stability check for the beams supporting pipes

Load Combinations	L_{C1}	L_{C2}	L_{C3}	L_{C4}	L_{C5}	L_{C6}
Strength and stability check	0.034	0.28	0.25	0.26	0.0025	0.068

Appendix C:

Test Frame Hinge Data

Joint displacements of the test frame with no hinge, plastic and stiffening hinge

Loading Steps-kip	Δh No Hinge (Linear Elastic Model)-ft	Δh Plastic Hinge (Elastic-Plastic Model)-ft
0.10	0.020	0.02
0.20	0.040	0.04
0.30	0.060	0.06
0.40	0.080	0.08
0.50	0.10	0.10
0.60	0.13	0.13
0.70	0.15	0.15
0.71	0.15	0.15
0.81	0.17	0.21
0.91	0.19	0.27
1.0	0.21	0.33

Loading Steps-kip	Δh Stiffening Hinge-ft
0.10	0.020
0.20	0.040
0.30	0.060
0.35	0.070
0.45	0.14
0.53	0.18
0.63	0.20
0.73	0.23
0.83	0.25
0.93	0.27
1.0	0.28

Appendix D:

Industrial Chassis Module Hinge Data

Section plastic moment and axial force for the initial model

	M_{px}-M3 (lb-ft)	M_{py}-M2 (lb-ft)	P_y (lb)
TWO ROOF BEAMS on first and second frame	261000.0	64875	633600
ONE ROOF BEAM on third frame	90828.66	22875	324000
SIX COLUMNS on the three frames	192000.0	43125	518400

P-M interaction curve data of the roof beams on the first and second frame of the initial model

Multipliers	M_{px}-M3 (lb-ft)	M_{py}-M2 (lb-ft)	P_y (lb)	(M_{px}-M3)×0.5 (lb-ft)	(M_{py}-M2)×0.5 (lb-ft)
0.1	100	100	63360.0	50.0	50.0
0.2	200	200	126720	100	100
0.3	300	300	190080	150	150
0.4	400	400	253440	200	200
0.5	500	500	316800	250	250

P-M interaction curve data of the roof beam on the third frame of the initial model

Multipliers	M_{px}-M3 (lb-ft)	M_{py}-M2 (lb-ft)	P_y (lb)	(M_{px}-M3)×0.5 (lb-ft)	(M_{py}-M2)×0.5 (lb-ft)
0.1	100	100	32400.0	50.0	50.0
0.2	200	200	64800.0	100	100
0.3	300	300	97200.0	150	150
0.4	400	400	129600	200	200
0.5	500	500	162000	250	250

P-M interaction curve data of the six columns on the three frames of the initial model

Multipliers	M_{px}-M3 (lb-ft)	M_{py}-M2 (lb-ft)	P_y (lb)	(M_{px}-M3)×0.5 (lb-ft)	(M_{py}-M2)×0.5 (lb-ft)
0.1	100	100	51840.0	50.0	50.0
0.2	200	200	103680	100	100
0.3	300	300	155520	150	150
0.4	400	400	207360	200	200
0.5	500	500	259200	250	250

Section plastic moment and axial force for the 56th configuration step

	M_{px}-M3 (lb-ft)	M_{py}-M2 (lb-ft)	P_y (lb)
TWO ROOF BEAMS on first and second frame	191.45	41.879	1368
ONE ROOF BEAM on third frame	191.45	41.879	1368
SIX COLUMNS on the three frames	1331.9	306.38	3816

P-M interaction curve data of the roof beams on the first and second frame for the 56th configuration step

Multipliers	M_{px}-M3 (lb-ft)	M_{py}-M2 (lb-ft)	P_y (lb)	(M_{px}-M3)×0.5 (lb-ft)	(M_{py}-M2)×0.5 (lb-ft)
0.1	19.1	4.20	136.8	9.60	2.10
0.2	38.3	8.40	273.6	19.1	4.20
0.3	57.4	12.6	410.4	28.7	6.30
0.4	76.6	16.8	547.2	38.3	8.40
0.5	95.7	20.9	684.0	47.9	10.5

P-M interaction curve data of the roof beam on the third frame for the 56th configuration step

Multipliers	M_{px}-M3 (lb-ft)	M_{py}-M2 (lb-ft)	P_y (lb)	(M_{px}-M3)×0.5 (lb-ft)	(M_{py}-M2)×0.5 (lb-ft)
0.1	19.1	4.20	136.8	9.60	2.10
0.2	38.3	8.40	273.6	19.1	4.20
0.3	57.4	12.6	410.4	28.7	6.30
0.4	76.6	16.8	547.2	38.3	8.40
0.5	95.7	20.9	684.0	47.9	10.5

P-M interaction curve data of the six columns on the three frames for the 56th configuration step

Multipliers	M_{px}-M3 (lb-ft)	M_{py}-M2 (lb-ft)	P_y (lb)	(M_{px}-M3)×0.5 (lb-ft)	(M_{py}-M2)×0.5 (lb-ft)
0.1	133.2	30.60	381.60	66.60	15.3
0.2	266.4	61.30	763.20	133.2	30.6
0.3	399.6	91.90	1144.8	199.8	46.0
0.4	532.7	122.6	1526.4	266.4	61.3
0.5	665.9	153.2	1908.0	333.0	76.6

Appendix E:

Fabrication vs. Story Drift and Site-Fit Risk Function Data

Trial	Member Size Reduction Step	Sections Removed	Connections Weakened	Sections										Section Colors/Strength Check	Lateral Displacement(ft)/ Height(ft)	Most critical Joint displacement case	Reduced Cost $
1	None	None	None	W12x35 Column	W18x50 Beams 1st floor	W12x40 Beams 2nd floor	W10x22 Beams on roof	W14x43 Beams on roof	W10x26 Beams on roof	W21x50 perimeter beams on roof	W14x48 Perimeter beams on roof	W24x68 Perimeter beams on roof	WT7x34 braces	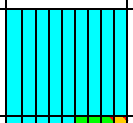	0.00138	Impact lateral in Y-dir & Structures+Pipe load inclined in the YZ plane	0
2	-1	Braces	None	W12x26 Column	W18x46 Beams 1st floor	W12x35 Beams 2nd floor	W10x15 Beams on roof	W14x34 Beams on roof	W10x22 Beams on roof	W21x44 perimeter beams on roof	W14x43 Perimeter beams on roof	W24x62 Perimeter beams on roof	REMOVED	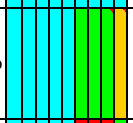	0.00186	Impact lateral in Y-dir & Structures+Pipe load inclined in the YZ plane	18723
3	-2	Braces	None	W12x22 Column	W18x40 Beams 1st floor	W12x26 Beams 2nd floor	W10x12 Beams on roof	W14x30 Beams on roof	W10x15 Beams on roof	W18x106 perimeter beams on roof	W14x34 Perimeter beams on roof	W24x55 Perimeter beams on roof	REMOVED		0.00535	Impact lateral in Y-dir & Structures+Pipe load inclined in the YZ plane	21821
4	-3	Braces	None	W12x26 Column	W18x40 Beams 1st floor	W12x26 Beams 2nd floor	W10x12 Beams on roof	W14x30 Beams on roof	W10x15 Beams on roof	W18x106 perimeter beams on roof	W14x34 Perimeter beams on roof	W24x55 Perimeter beams on roof	REMOVED	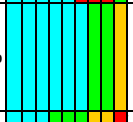	0.00229	Impact lateral in Y-dir & Structures+Pipe load inclined in the YZ plane	20890
5	-4	Braces	None	W12x26 Column	W18x35 Beams 1st floor	W12x22 Beams 2nd floor	W8x48 Beams on roof	W14x26 Beams on roof	W10x12 Beams on roof	W18x86 perimeter beams on roof	W14x30 Perimeter beams on roof	W21x122 Perimeter beams on roof	REMOVED	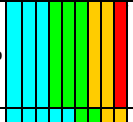	0.00229	Impact lateral in Y-dir & Structures+Pipe load inclined in the YZ plane	18904
6	-5	Braces	None	W12x26 Column	W18x35 Beams 1st floor	W12x26 Beams 2nd floor	W8x48 Beams on roof	W14x26 Beams on roof	W10x12 Beams on roof	W18x86 perimeter beams on roof	W14x30 Perimeter beams on roof	W21x122 Perimeter beams on roof	REMOVED		0.00218	Impact lateral in Y-dir & Structures+Pipe load inclined in the YZ plane	17686
7	-6	Braces	None	W12x26 Column	W16x67 Beams 1st floor	W12x26 Beams 2nd floor	W8x35 Beams on roof	W12x87 Beams on roof	W8x48 Beams on roof	W18x76 perimeter beams on roof	W14x26 Perimeter beams on roof	W21x101 Perimeter beams on roof	REMOVED	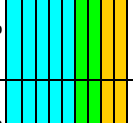	0.00183	Impact lateral in Y-dir & Structures+Pipe load inclined in the YZ plane	3538
8	-7	Braces	None	W12x26 Column	W16x50 Beams 1st floor	W12x26 Beams 2nd floor	W8x31 Beams on roof	W12x72 Beams on roof	W8x35 Beams on roof	W18X65 perimeter beams on roof	W12x87 Perimeter beams on roof	W21x93 Perimeter beams on roof	REMOVED	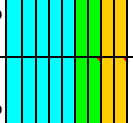	0.00193	Impact lateral in Y-dir & Structures+Pipe load inclined in the YZ plane	10079
9	-8	Braces	None	W12x26 Column	W16x40 Beams 1st floor	W12x26 Beams 2nd floor	W8x28 Beams on roof	W12x58 Beams on roof	W8x31 Beams on roof	W18x55 perimeter beams on roof	W12x72 Perimeter beams on roof	W21x83 Perimeter beams on roof	REMOVED	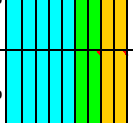	0.00201	Impact lateral in Y-dir & Structures+Pipe load inclined in the YZ plane	14528
10	-9	Braces	None	W12x26 Column	W16x31 Beams 1st floor	W12x26 Beams 2nd floor	W8x24 Beams on roof	W12x50 Beams on roof	W8x28 Beams on roof	W18x50 perimeter beams on roof	W12x58 Perimeter beams on roof	W21x68 Perimeter beams on roof	REMOVED	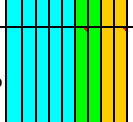	0.00214	Impact lateral in Y-dir & Structures+Pipe load inclined in the YZ plane	19061
11	-10	Braces	None	W12x26 Column	W16x26 Beams 1st floor	W12x26 Beams 2nd floor	W8x21 Beams on roof	W12x35 Beams on roof	W8x24 Beams on roof	W18x46 perimeter beams on roof	W12x50 Perimeter beams on roof	W21x62 Perimeter beams on roof	REMOVED	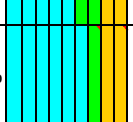	0.00224	Impact lateral in Y-dir & Structures+Pipe load inclined in the YZ plane	25702
12	-11	Braces	None	W12x26 Column	W14x120 Beams 1st floor	W12x26 Beams 2nd floor	W8x15 Beams on roof	W12x26 Beams on roof	W8x21 Beams on roof	W18x40 perimeter beams on roof	W12x35 Perimeter beams on roof	W21x50 Perimeter beams on roof	REMOVED		0.00224	Impact lateral in Y-dir & Structures+Pipe load inclined in the YZ plane	5995
13	-12	Braces	None	W12x26 Column	W14x90 Beams 1st floor	W12x26 Beams 2nd floor	W8x10 Beams on roof	W12x22 Beams on roof	W8x15 Beams on roof	W18x35 perimeter beams on roof	W12x26 Perimeter beams on roof	W21x44 Perimeter beams on roof	REMOVED	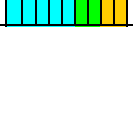	0.00228	Impact lateral in Y-dir & Structures+Pipe load inclined in the YZ plane	15257

Trial	Member Size Reduction Step	Sections Removed	Connections Weakened	Sections										Section Colors/Strength Check	Lateral Displacement(ft)/ Height(ft)	Most critical Joint displacement case	Reduced Cost $
14	-13	Braces	None	W12x26 Column	W14x74 Beams 1st floor	W12x26 Beams 2nd floor	W6x20 Beams on roof	W12x16 Beams on roof	W8x10 Beams on roof	W16x67 perimeter beams on roof	W12x22 Perimeter beams on roof	W18x106 Perimeter beams on roof	REMOVED		0.00226	Impact lateral in Y-dir & Structures+Pipe load inclined in the YZ plane	14212
15	-14	Braces	None	W12x26 Column	W14x53 Beams 1st floor	W12x26 Beams 2nd floor	W6x15 Beams on roof	W10x49 Beams on roof	W6x20 Beams on roof	W16x50 perimeter beams on roof	W12x16 Perimeter beams on roof	W18x86 Perimeter beams on roof	REMOVED		0.00214	Impact lateral in Y-dir & Structures+Pipe load inclined in the YZ plane	17339
16	-15	Braces	None	W12x26 Column	W14x43 Beams 1st floor	W12x26 Beams 2nd floor	W6x9 Beams on roof	W10x33 Beams on roof	W6x15 Beams on roof	W16x40 perimeter beams on roof	W10x49 Perimeter beams on roof	W18x76 Perimeter beams on roof	REMOVED		0.00221	Impact lateral in Y-dir & Structures+Pipe load inclined in the YZ plane	22747
17	-16	Braces	None	W12x26 Column	W14x34 Beams 1st floor	W12x26 Beams 2nd floor	W6x9 Beams on roof	W10x26 Beams on roof	W6x9 Beams on roof	W16x31 perimeter beams on roof	W10x33 Perimeter beams on roof	W18x65 Perimeter beams on roof	REMOVED		0.00236	Impact lateral in Y-dir & Structures+Pipe load inclined in the YZ plane	27713
18	-17	Braces	None	W12x26 Column	W14x30 Beams 1st floor	W12x26 Beams 2nd floor	W6x9 Beams on roof	W10x22 Beams on roof	W6x9 Beams on roof	W16x26 perimeter beams on roof	W10x26 Perimeter beams on roof	W18x55 Perimeter beams on roof	REMOVED		0.00239	Impact lateral in Y-dir & Structures+Pipe load inclined in the YZ plane	30224
19	-18	Braces	None	W12x26 Column	W14x26 Beams 1st floor	W12x26 Beams 2nd floor	W6x9 Beams on roof	W10x15 Beams on roof	W6x9 Beams on roof	W14x120 perimeter beams on roof	W10x22 Perimeter beams on roof	W18x50 Perimeter beams on roof	REMOVED		0.00226	Structures+Pipe load inclined in the XZ plane	24703
20	-19	Braces	None	W12x26 Column	W12x87 Beams 1st floor	W12x26 Beams 2nd floor	W6x9 Beams on roof	W10x12 Beams on roof	W6x9 Beams on roof	W14x90 perimeter beams on roof	W10x15 Perimeter beams on roof	W18x46 Perimeter beams on roof	REMOVED		0.00217	Impact lateral in Y-dir & Structures+Pipe load inclined in the YZ plane	12811
21	-20	Braces	None	W12x26 Column	W12x72 Beams 1st floor	W12x26 Beams 2nd floor	W6x9 Beams on roof	W8x48 Beams on roof	W6x9 Beams on roof	W14x74 perimeter beams on roof	W10x12 Perimeter beams on roof	W18x40 Perimeter beams on roof	REMOVED		0.00215	Impact lateral in Y-dir & Structures+Pipe load inclined in the YZ plane	13637
22	-21	Braces	None	W12x26 Column	W12x58 Beams 1st floor	W12x26 Beams 2nd floor	W6x9 Beams on roof	W8x35 Beams on roof	W6x9 Beams on roof	W14x53 perimeter beams on roof	W8x48 Perimeter beams on roof	W18x35 Perimeter beams on roof	REMOVED		0.00224	Impact lateral in Y-dir & Structures+Pipe load inclined in the YZ plane	19818
23	-22	Braces	None	W12x26 Column	W12x50 Beams 1st floor	W12x26 Beams 2nd floor	W6x9 Beams on roof	W8x31 Beams on roof	W6x9 Beams on roof	W14x43 perimeter beams on roof	W8x35 Perimeter beams on roof	W16x67 Perimeter beams on roof	REMOVED		0.00225	Impact lateral in Y-dir & Structures+Pipe load inclined in the YZ plane	21966
24	-23	Braces	None	W12x26 Column	W12x35 Beams 1st floor	W12x26 Beams 2nd floor	W6x9 Beams on roof	W8x28 Beams on roof	W6x9 Beams on roof	W14x34 perimeter beams on roof	W8x31 Perimeter beams on roof	W16x50 Perimeter beams on roof	REMOVED		0.00235	Impact lateral in Y-dir & Structures+Pipe load inclined in the YZ plane	27565
25	-24	Braces	None	W12x26 Column	W12x26 Beams 1st floor	W12x26 Beams 2nd floor	W6x9 Beams on roof	W8x24 Beams on roof	W6x9 Beams on roof	W14x30 perimeter beams on roof	W8x28 Perimeter beams on roof	W16x40 Perimeter beams on roof	REMOVED		0.00251	Structures+Pipe load inclined in the XZ plane	31124
26	-25	Braces	None	W12x26 Column	W12x22 Beams 1st floor	W12x26 Beams 2nd floor	W6x9 Beams on roof	W8x21 Beams on roof	W6x9 Beams on roof	W14x26 perimeter beams on roof	W8x24 Perimeter beams on roof	W16x31 Perimeter beams on roof	REMOVED		0.00273	Structures+Pipe load inclined in the XZ plane	33326
27	-26	Braces	None	W12x26 Column	W12x26 Beams 1st floor	W12x26 Beams 2nd floor	W6x9 Beams on roof	W8x21 Beams on roof	W6x9 Beams on roof	W14x26 perimeter beams on roof	W8x24 Perimeter beams on roof	W16x31 Perimeter beams on roof	REMOVED		0.00258	Structures+Pipe load inclined in the XZ plane	32402

Trial	Member Size Reduction Step	Sections Removed	Connections Weakened	Sections										Section Colors/Strength Check	Lateral Displacement(ft)/ Height(ft)	Most critical Joint displacement case	Reduced Cost $
28	-27	Braces	None	W12x26 Column	W12x26 Beams 1st floor	W12x26 Beams 2nd floor	W6x9 Beams on roof	W8x15 Beams on roof	W6x9 Beams on roof	W12x87 perimeter beams on roof	W8x21 Perimeter beams on roof	W16x26 Perimeter beams on roof	REMOVED		0.00243	Structures+Pipe load inclined in the XZ plane	28311
29	-28	Braces	None	W12x26 Column	W12x26 Beams 1st floor	W12x26 Beams 2nd floor	W6x9 Beams on roof	W8x10 Beams on roof	W6x9 Beams on roof	W12x72 perimeter beams on roof	W8x15 Perimeter beams on roof	W14x120 Perimeter beams on roof	REMOVED		0.00246	Structures+Pipe load inclined in the XZ plane	26334
30	-29	Braces	None	W12x26 Column	W12x26 Beams 1st floor	W12x26 Beams 2nd floor	W6x9 Beams on roof	W6x20 Beams on roof	W6x9 Beams on roof	W12x58 perimeter beams on roof	W8x10 Perimeter beams on roof	W14x90 Perimeter beams on roof	REMOVED		0.00245	Structures+Pipe load inclined in the XZ plane	27732
31	-30	Braces	None	W12x26 Column	W12x26 Beams 1st floor	W12x26 Beams 2nd floor	W6x9 Beams on roof	W6x15 Beams on roof	W6x9 Beams on roof	W12x50 perimeter beams on roof	W6x20 Perimeter beams on roof	W14x74 Perimeter beams on roof	REMOVED		0.00249	Structures+Pipe load inclined in the XZ plane	29389
32	-31	Braces	None	W12x26 Column	W12x26 Beams 1st floor	W12x26 Beams 2nd floor	W6x9 Beams on roof	W6x9 Beams on roof	W6x9 Beams on roof	W12x35 perimeter beams on roof	W6x15 Perimeter beams on roof	W14x53 Perimeter beams on roof	REMOVED		0.00260	Structures+Pipe load inclined in the XZ plane	32314
33	-32	Braces	None	W12x26 Column	W12x26 Beams 1st floor	W12x26 Beams 2nd floor	W6x9 Beams on roof	W6x9 Beams on roof	W6x9 Beams on roof	W12x26 perimeter beams on roof	W6x9 Perimeter beams on roof	W14x43 Perimeter beams on roof	REMOVED		0.00268	Structures+Pipe load inclined in the XZ plane	33637
34	-33	Braces	None	W12x26 Column	W12x26 Beams 1st floor	W12x26 Beams 2nd floor	W6x9 Beams on roof	W6x9 Beams on roof	W6x9 Beams on roof	W12x22 perimeter beams on roof	W6x9 Perimeter beams on roof	W14x34 Perimeter beams on roof	REMOVED		0.00274	Structures+Pipe load inclined in the XZ plane	34324
35	-34	Braces	None	W12x26 Column	W12x26 Beams 1st floor	W12x26 Beams 2nd floor	W6x9 Beams on roof	W6x9 Beams on roof	W6x9 Beams on roof	W12x16 perimeter beams on roof	W6x9 Perimeter beams on roof	W14x30 Perimeter beams on roof	REMOVED		0.00284	Structures+Pipe load inclined in the XZ plane	34987
36	-35	Braces	None	W12x26 Column	W12x26 Beams 1st floor	W12x26 Beams 2nd floor	W6x9 Beams on roof	W6x9 Beams on roof	W6x9 Beams on roof	W10x49 perimeter beams on roof	W6x9 Perimeter beams on roof	W14x26 Perimeter beams on roof	REMOVED		0.00263	Structures+Pipe load inclined in the XZ plane	32299
37	-36	Braces	None	W12x26 Column	W12x26 Beams 1st floor	W12x26 Beams 2nd floor	W6x9 Beams on roof	W6x9 Beams on roof	W6x9 Beams on roof	W10x33 perimeter beams on roof	W6x9 Perimeter beams on roof	W12x87 Perimeter beams on roof	REMOVED		0.00271	Structures+Pipe load inclined in the XZ plane	31039
38	-37	Braces	None	W12x26 Column	W12x26 Beams 1st floor	W12x26 Beams 2nd floor	W6x9 Beams on roof	W6x9 Beams on roof	W6x9 Beams on roof	W10x26 perimeter beams on roof	W6x9 Perimeter beams on roof	W12x72 Perimeter beams on roof	REMOVED		0.00275	Structures+Pipe load inclined in the XZ plane	32276
39	-38	Braces	None	W12x26 Column	W12x26 Beams 1st floor	W12x26 Beams 2nd floor	W6x9 Beams on roof	W6x9 Beams on roof	W6x9 Beams on roof	W10x22 perimeter beams on roof	W6x9 Perimeter beams on roof	W12x58 Perimeter beams on roof	REMOVED		0.00280	Structures+Pipe load inclined in the XZ plane	33199
40	-39	Braces	None	W12x26 Column	W12x26 Beams 1st floor	W12x26 Beams 2nd floor	W6x9 Beams on roof	W6x9 Beams on roof	W6x9 Beams on roof	W10x15 perimeter beams on roof	W6x9 Perimeter beams on roof	W12x50 Perimeter beams on roof	REMOVED		0.00292	Structures+Pipe load inclined in the XZ plane	34099
41	-40	Braces	None	W12x26 Column	W12x26 Beams 1st floor	W12x26 Beams 2nd floor	W6x9 Beams on roof	W6x9 Beams on roof	W6x9 Beams on roof	W10x12 perimeter beams on roof	W6x9 Perimeter beams on roof	W12x35 Perimeter beams on roof	REMOVED		0.00299	Structures+Pipe load inclined in the XZ plane	34954
42	-41	Braces	None	W12x26 Column	W12x26 Beams 1st floor	W12x26 Beams 2nd floor	W6x9 Beams on roof	W6x9 Beams on roof	W6x9 Beams on roof	W8x48 perimeter beams on roof	W6x9 Perimeter beams on roof	W12x26 Perimeter beams on roof	REMOVED		0.00271	Structures+Pipe load inclined in the XZ plane	32366
43	-42	Braces	None	W12x26 Column	W12x26 Beams 1st floor	W12x26 Beams 2nd floor	W6x9 Beams on roof	W6x9 Beams on roof	W6x9 Beams on roof	W8x35 perimeter beams on roof	W6x9 Perimeter beams on roof	W12x22 Perimeter beams on roof	REMOVED		0.00281	Structures+Pipe load inclined in the XZ plane	33581
44	-43	Braces	None	W12x26 Column	W12x26 Beams 1st floor	W12x26 Beams 2nd floor	W6x9 Beams on roof	W6x9 Beams on roof	W6x9 Beams on roof	W8x31 perimeter beams on roof	W6x9 Perimeter beams on roof	W12x16 Perimeter beams on roof	REMOVED		0.00285	Structures+Pipe load inclined in the XZ plane	34144
45	-44	Braces	None	W12x26 Column	W12x26 Beams 1st floor	W12x26 Beams 2nd floor	W6x9 Beams on roof	W6x9 Beams on roof	W6x9 Beams on roof	W8x28 perimeter beams on roof	W6x9 Perimeter beams on roof	W10x49 Perimeter beams on roof	REMOVED		0.00285	Structures+Pipe load inclined in the XZ plane	32951
46	-45	Braces	None	W12x26 Column	W12x26 Beams 1st floor	W12x26 Beams 2nd floor	W6x9 Beams on roof	W6x9 Beams on roof	W6x9 Beams on roof	W8x24 perimeter beams on roof	W6x9 Perimeter beams on roof	W10x33 Perimeter beams on roof	REMOVED		0.00290	Structures+Pipe load inclined in the XZ plane	33941

Trial	Member Size Reduction Step	Sections Removed	Connections Weakened	Sections										Section Colors/Strength Check	Lateral Displacement(ft)/ Height(ft)	Most critical Joint displacement case	Reduced Cost $
47	-46	Braces	None	W12x26 Column	W12x26 Beams 1st floor	W12x26 Beams 2nd floor	W6x9 Beams on roof	W6x9 Beams on roof	W6x9 Beams on roof	W8x21 perimeter beams on roof	W6x9 Perimeter beams on roof	W10x26 Perimeter beams on roof	REMOVED	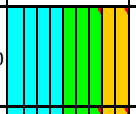	0.00292	Structures+Pipe load inclined in the XZ plane	34549
48	-47	Braces	None	W12x26 Column	W12x26 Beams 1st floor	W12x26 Beams 2nd floor	W6x9 Beams on roof	W6x9 Beams on roof	W6x9 Beams on roof	W8x15 perimeter beams on roof	W6x9 Perimeter beams on roof	W10x22 Perimeter beams on roof	REMOVED		0.00304	Structures+Pipe load inclined in the XZ plane	35201
49	-48	Braces	None	W12x26 Column	W12x26 Beams 1st floor	W12x26 Beams 2nd floor	W6x9 Beams on roof	W6x9 Beams on roof	W6x9 Beams on roof	W8x10 perimeter beams on roof	W6x9 Perimeter beams on roof	W10x15 Perimeter beams on roof	REMOVED		0.00316	Structures+Pipe load inclined in the XZ plane	35876
50	-49	Braces	None	W12x26 Column	W12x26 Beams 1st floor	W12x26 Beams 2nd floor	W6x9 Beams on roof	W6x9 Beams on roof	W6x9 Beams on roof	W6x20 perimeter beams on roof	W6x9 Perimeter beams on roof	W10x12 Perimeter beams on roof	REMOVED		0.00310	Structures+Pipe load inclined in the XZ plane	35179
51	-50	Braces	None	W12x26 Column	W12x26 Beams 1st floor	W12x26 Beams 2nd floor	W6x9 Beams on roof	W6x9 Beams on roof	W6x9 Beams on roof	W6x15 perimeter beams on roof	W6x9 Perimeter beams on roof	W8x48 Perimeter beams on roof	REMOVED		0.00314	Structures+Pipe load inclined in the XZ plane	34121
52	-51	Braces	None	W12x26 Column	W12x26 Beams 1st floor	W12x26 Beams 2nd floor	W6x9 Beams on roof	W6x9 Beams on roof	W6x9 Beams on roof	W6x9 perimeter beams on roof	W6x9 Perimeter beams on roof	W8x35 Perimeter beams on roof	REMOVED		0.00329	Structures+Pipe load inclined in the XZ plane	35122
53	-52	Braces	None	W12x26 Column	W12x26 Beams 1st floor	W12x26 Beams 2nd floor	W6x9 Beams on roof	W6x9 Beams on roof	W6x9 Beams on roof	W6x9 perimeter beams on roof	W6x9 Perimeter beams on roof	W8x31 Perimeter beams on roof	REMOVED		0.00329	Structures+Pipe load inclined in the XZ plane	35280
54	-53	Braces	None	W12x26 Column	W12x26 Beams 1st floor	W12x26 Beams 2nd floor	W6x9 Beams on roof	W6x9 Beams on roof	W6x9 Beams on roof	W6x9 perimeter beams on roof	W6x9 Perimeter beams on roof	W8x28 Perimeter beams on roof	REMOVED		0.00330	Structures+Pipe load inclined in the XZ plane	35404
55	-54	Braces	None	W12x26 Column	W12x26 Beams 1st floor	W12x26 Beams 2nd floor	W6x9 Beams on roof	W6x9 Beams on roof	W6x9 Beams on roof	W6x9 perimeter beams on roof	W6x9 Perimeter beams on roof	W8x24 Perimeter beams on roof	REMOVED		0.00330	Structures+Pipe load inclined in the XZ plane	35572
56	-55	Braces	None	W12x26 Column	W12x26 Beams 1st floor	W12x26 Beams 2nd floor	W6x9 Beams on roof	W6x9 Beams on roof	W6x9 Beams on roof	W6x9 perimeter beams on roof	W6x9 Perimeter beams on roof	W8x21 Perimeter beams on roof	REMOVED		0.00331	Structures+Pipe load inclined in the XZ plane	35719
57	-56	Braces	None	W12x26 Column	W12x26 Beams 1st floor	W12x26 Beams 2nd floor	W6x9 Beams on roof	W6x9 Beams on roof	W6x9 Beams on roof	W6x9 perimeter beams on roof	W6x9 Perimeter beams on roof	W8x15 Perimeter beams on roof	REMOVED		0.00333	Structures+Pipe load inclined in the XZ plane	35966
58	-57	Braces	None	W12x26 Column	W12x26 Beams 1st floor	W12x26 Beams 2nd floor	W6x9 Beams on roof	W6x9 Beams on roof	W6x9 Beams on roof	W6x9 perimeter beams on roof	W6x9 Perimeter beams on roof	W8x10 Perimeter beams on roof	REMOVED		0.00334	Structures+Pipe load inclined in the XZ plane	36157
59	-58	Braces	None	W12x26 Column	W12x26 Beams 1st floor	W12x26 Beams 2nd floor	W6x9 Beams on roof	W6x9 Beams on roof	W6x9 Beams on roof	W6x9 perimeter beams on roof	W6x9 Perimeter beams on roof	W6x20 Perimeter beams on roof	REMOVED		0.00332	Structures+Pipe load inclined in the XZ plane	35752
60	-59	Braces	None	W12x26 Column	W12x26 Beams 1st floor	W12x26 Beams 2nd floor	W6x9 Beams on roof	W6x9 Beams on roof	W6x9 Beams on roof	W6x9 perimeter beams on roof	W6x9 Perimeter beams on roof	W6x15 Perimeter beams on roof	REMOVED		0.00334	Structures+Pipe load inclined in the XZ plane	35966
61	-60	Braces	None	W12x26 Column	W12x26 Beams 1st floor	W12x26 Beams 2nd floor	W6x9 Beams on roof	W6x9 Beams on roof	W6x9 Beams on roof	W6x9 perimeter beams on roof	W6x9 Perimeter beams on roof	W6x9 Perimeter beams on roof	REMOVED		0.00335	Structures+Pipe load inclined in the XZ plane	36202

Total fabrication cost calculation steps for reduction step 0

Section size	W12x35 Column	W18x50 Beams 1st floor	W12x40 Beams 2nd floor	W10x22 Beams on roof	W14x43 Beams on roof	W10x26 Beams on roof	W21x50 perimeter beams on roof	W14x48 Perimeter beams on roof	W24x68 Perimeter beams on roof	WT7x34 braces
Length(ft)	133	132	174	42.0	65.0	28.0	45.0	13.5	22.5	104
Total design hour (hr)	9.18	11.7	13.1	3.91	4.49	2.61	3.38	0.946	1.63	10.7
Total fabrication cost per unit length(ft)	71.0	100	99.0	50.0	85.5	57.0	98.5	104	130	74.5
Cost per section ($)	9443.0	13200	17226	2100.0	5558.0	1596.0	4433.0	1404.0	2925.0	7748.0
Total Cost ($)	65633									

Total fabrication cost calculation steps for reduction step -1

Section size	W12x26 Column	W18x46 Beams 1st floor	W12x35 Beams 2nd floor	W10x15 Beams on roof	W14x34 Beams on roof	W10x22 Beams on roof	W21x44 perimeter beams on roof	W14x43 Perimeter beams on roof	W24x62 Perimeter beams on roof	WT7x34 braces
Length(ft)	133	132	174	42.0	65.0	28.0	45.0	13.5	22.5	104
Total design hour (hr)	8.52	11.0	12.1	3.91	4.49	2.61	3.38	0.932	1.63	REMOVED
Total fabrication cost per unit length(ft)	54.0	92.0	71.0	37.0	69.0	50.0	87.5	85.5	120	REMOVED
Cost per section ($)	7182.0	12144	12354	1554.0	4485.0	1400.0	3938.0	1155.0	2700.0	REMOVED
Total Cost ($)	46911									

Total fabrication cost calculation steps for reduction step -2

Section size	W12x22 Column	W18x40 Beams 1st floor	W12x26 Beams 2nd floor	W10x12 Beams on roof	W14x30 Beams on roof	W10x15 Beams on roof	W18x106 perimeter beams on roof	W14x34 Perimeter beams on roof	W24x55 Perimeter beams on roof	WT7x34 braces
Length(ft)	133	132	174	42.0	65.0	28.0	45.0	13.5	22.5	104.0000
Total design hour (hr)	8.52	11.1	11.2	3.91	4.04	2.61	4.01	0.838	1.63	REMOVED
Total fabrication cost per unit length(ft)	47.0	72.0	54.0	32.0	61.5	37.0	201	61.5	107	REMOVED
Cost per section ($)	6251.0	9504.0	9396.0	1344.0	3998.0	1036.0	9045.0	83026	2408.0	REMOVED
Total Cost ($)	43812									

Total fabrication cost calculation steps for reduction step -3

Section size	W12x26 Column	W18x40 Beams 1st floor	W12x26 Beams 2nd floor	W10x12 Beams on roof	W14x30 Beams on roof	W10x15 Beams on roof	W18x106 perimeter beams on roof	W14x34 Perimeter beams on roof	W24x55 Perimeter beams on roof	WT7x34 braces
Length(ft)	133	132	174	42.0	65.0	28.0	45.0	13.5	22.5	104
Total design hour (hr)	8.52	11.0	11.2	3.91	4.04	2.61	4.01	0.838	1.63	REMOVED
Total fabrication cost per unit length(ft)	54.0	72.0	54.0	32.0	61.5	37.0	201	61.5	107	REMOVED
Cost per section ($)	7182	9504	9396	1344	3998	1036	9045	831.0	2408	REMOVED
Total Cost ($)	44743									

Appendix F:

Risk and Fabrication Cost Function Data

Configuration Step	Lateral Displacement(ft) /Height(ft)	Total Fabrication Cost ($)	Probability of rework	Rework Risk ($)	shipping Cost ($)	Transportation Risk ($)	Total Design Hours (hr)	Alignment Risk ($)	Safety Risk ($)	TOTAL ($)
1	0.00138	65634	0.01	50.00	1044	4982.0	61.4	3089	3888	77643
2	0.00186	46913	0.02	120.0	1005	4475.0	48.4	3237	3146	57891
3	0.00229	44744	0.04	190.0	966	4903.0	47.6	3374	3166	56377
4	0.00218	47949	0.05	260.0	930	5820.0	47.8	3338	3251	60618
5	0.00183	62096	0.07	330.0	894	8097.0	48.9	3229	3384	77136
6	0.00193	55555	0.08	400.0	860	8082.0	39.6	3260	2874	70171
7	0.00201	51107	0.09	470.0	828	8186.0	47.9	3287	3462	66511
8	0.00214	46573	0.11	540.0	796	8154.0	47.6	3325	3517	62108
9	0.00224	39932	0.12	610.0	766	7634.0	44.8	3358	3409	54943
10	0.00224	59640	0.14	680.0	737	11830	47.0	3358	3617	79124
11	0.00228	50378	0.15	750.0	709	10784	44.1	3369	3509	68790
12	0.00226	51422	0.16	820.0	682	11686	46.3	3363	3714	71004
13	0.00214	48295	0.18	890.0	656	11667	48.0	3327	3894	68073
14	0.00221	42888	0.19	960.0	631	11010	48.4	3349	3988	62194
15	0.00236	37922	0.21	1030	607	10315	65.5	3394	5125	57785
16	0.00239	35410	0.22	1100	584	10145	46.1	3403	3985	54042
17	0.00226	40931	0.23	1170	562	12186	46.5	3365	4076	61727
18	0.00217	52824	0.25	1240	541	16282	50.4	3336	4389	78070
19	0.00215	51997	0.26	1310	520	16743	50.9	3329	4490	77869
20	0.00224	45817	0.28	1380	501	15436	49.1	3358	4449	70439
21	0.00225	43669	0.29	1450	482	15328	48.8	3360	4503	68311
22	0.00235	38070	0.30	1520	463	13939	48.0	3392	4518	61438
23	0.00251	34510	0.32	1590	446	13145	47.0	3441	4527	57213
24	0.00258	33233	0.33	1660	429	13123	46.0	3463	4535	56014
25	0.00243	37324	0.35	1730	413	15192	47.1	3416	4676	62338
26	0.00246	39300	0.36	1800	397	16509	47.6	3427	4777	65814
27	0.00245	37903	0.37	1870	382	16452	47.0	3423	4808	64455
28	0.00249	36246	0.39	1940	367	16242	46.9	3436	4875	62739
29	0.00260	33320	0.40	2010	354	15413	46.6	3470	4923	59136
30	0.00268	31997	0.42	2080	340	15250	46.3	3494	4977	57798

Configuration Step	Lateral Displacement (ft) /Height(ft)	Total Fabrication Cost ($)	Probability of rework	Rework Risk ($)	shipping Cost ($)	Transportation Risk ($)	Total Design Hours (hr)	Alignment Risk ($)	Safety Risk ($)	TOTAL ($)
31	0.00274	31311	0.43	2150	327	15355	46.3	3512	5047	57376
32	0.00284	30647	0.44	2220	315	15454	46.2	3543	5107	56971
33	0.00263	33336	0.46	2290	303	17237	47.8	3479	5277	61618
34	0.00271	34596	0.47	2360	291	18349	48.5	3505	5391	64201
35	0.00275	33358	0.49	2430	280	18159	48.1	3517	5435	62900
36	0.00280	32436	0.50	2500	270	18108	47.8	3532	5487	62064
37	0.00292	31536	0.51	2570	260	18045	47.8	3570	5557	61278
38	0.00299	30681	0.53	2640	250	17982	47.6	3590	5619	60512
39	0.00271	33268	0.54	2710	240	19934	47.9	3505	5707	65125
40	0.00281	32053	0.56	2780	231	19654	47.9	3534	5777	63799
41	0.00285	31491	0.57	2850	222	19746	47.9	3548	5847	63481
42	0.00285	32683	0.58	2920	214	20934	48.8	3548	5970	66056
43	0.00290	31693	0.60	2990	206	20742	48.8	3564	6040	65029
44	0.00292	31086	0.61	3060	198	20776	48.2	3570	6073	64564
45	0.00304	30433	0.63	3130	191	20762	48.2	3606	6143	64074
46	0.00316	29758	0.64	3200	183	20715	48.2	3646	6213	63532
47	0.00310	30456	0.65	3270	177	21616	48.2	3626	6283	65250
48	0.00314	31513	0.67	3340	170	22795	48.4	3639	6365	67653
49	0.00329	30512	0.68	3410	163	22497	48.4	3684	6435	66538
50	0.00329	30355	0.70	3480	157	22800	48.4	3686	6505	66826
51	0.00330	30231	0.71	3550	151	23125	48.4	3689	6575	67170
52	0.00330	30062	0.72	3620	146	23412	48.4	3689	6645	67428
53	0.00331	29916	0.74	3690	140	23712	48.2	3691	6703	67711
54	0.00333	29668	0.75	3760	135	23927	48.2	3697	6773	67825
55	0.00332	29882	0.77	3830	130	24512	48.2	3695	6843	68762
56	0.00334	29668	0.78	3900	125	24748	48.2	3700	6913	68928
57	0.00575	29668	1.0	5000	125	31274	48.2	4454	8013	78409

Reference

Accelerated Bridge Construction Manual . (2011). *Federal Highway Administration*, 242-244.

Albert, C. (2010). *Handbook of Steel Construction.* Ontario: Canadian Institute of Steel Construction.

Bar-Zohar, D. (2007). Using induced earthquakes to prevent large magnitude natural earthquakes.

Berk, J. (1951). *Cost Reduction and Optimization for Manufacturing and Industrial Companies.* Wiley - Scrivener.

Bosche, F., & Haas, C. (2008). Automated retrieval of 3D CAD model objects in construction range images. *Automation in Construction*, 499-512.

Brilakis, I., Dai, F., Radopoulou, S. (2012). "Achievements and Challenges in Recognizing and Reconstructing Civil Infrastructure." Lecture Notes in Computer Science, Springer, pp 151-176.

Bruneau, M., Chang, S. E., Eguchi, R. T., Lee, G.C., O'Rourke, T. D., Reinhorn A. M., Shinozuka, M., Tierney, K., Wallace, W. A., and vonWinterfeldti, D., (2003). "A Framework to Quantitatively
Assess and Enhance the Seismic Resilience of Communities," *Earthquake Spectra*, V.19, No.4, pp 733–752

Bureau of Indian Standards (BIS), (1990). "Recommendations for Modular Co-ordination in Building Industry: Tolerance." *Indian Standard*, IS 6408 (Part 1), First revision, New Delhi.

Burke, G. P., & Miller, R. C. (1998). Modularization Speeds Construction. *Power Engineering*, 20-22.

Chanmeka, A., Thomas, S. R., Caldas, C. H., & Mulva, S. P. (2012). Assesing Key Factors Impacting the Performance and Productivity of Oil and Gas Projects in Alberta. *NRC Research Press*, 259-270.

Chen, Y., Okudan, G. E., & Riley, D. R. (2010). Sustainable Performance Criteria for Construction Method Selection in Concrete Buildings. *Automation in Construction* , 235-244.

Court, P. F., Pasquire, C. L., Gibb, A. G., & Bower, D. (2009). Modular Assembly With Postponement to Improve Health, Safety and Productivity in Construction. *Structural Design and Construction* , 81-89.

Ericsson, A., & Erixon, G. (1999). *Controlling design variants.* Houston : Modular management AB and society of manufacturing engineers.

Friedman, A., Sprecher, A., & Mohamed, B. (2013). A computer-based system for mass customization of prefabricated housing. *Open House International*, 20-30.

Freight Insurance Coverage Terms & Conditions. (2003). Retrieved 1 9, 2014, from panfins: http://www.pafins.com/freightinsurancecoverage.htm

Friedman, A., Sprecher, A., & Mohamed, B. (2013). A computer-based system for mass customization of prefabricated housing. *Open House International*, 20-30.

Gadzala, J. L. (1959). *Dimensional control in precision manufacturing* . Toronto: McGraw-Hill book company Inc.

Gibb, A. (1999). *Off-site Fabrication: Prefabrication, Pre-assembly and Modularization.* NY: Wiley & Sons.

Goulding, J., Nadim, W., Petridis, P., & Alshawi, M. (2011). Construction industry offsite production: A virtual reality interactive training. *Advanced Engineering Informatics*, 103-116.

Haas, C. T., O'Connor, J. T., Tucker, R. L., Eickmann, J. A., & Fagerlund, W. R. (2000). *Prefabrication and Preassembly Trends and Effects on the Construction Workforce.* Texas: The University of Texas at Austin.

Hallowell, M. R., & Gambatese, J. A. (2009). Activity-Based Safety Risk Quantification for Concrete. *Journal of Construction Engineering and Management*, 990-998.

Han, S. H., Al-Hussein, M., Al-Jibouri, S., & Yu, H. (2012). Automated post-simulation visualization of modular building production assembly line. *Automation in Construction*, 229-236.

Hinze, J. (1997). *Construction Safety.* Englewood: Prentice-Hall.

Hwang, B.-G., Thomas, S. R., Haas, C. T., & Caldas, C. H. (2009). Measuring the Impact of Rework on Construction Cost Performance . *Journal of Construction Engineering and Management* , 187-198.

Construction Industry Institute (CII) Research Team 252 (2011). Innovations in Mechanical Construction Productivity. Implementation Resource 252-2, Austin, TX, 2011 *Construction Industry Institute*, 36-42.

Integrated Finite Element Analysis and Design of Structures . (1995). California : Computers and Structures, Inc.

Jaillon, L., & Poon, C. (2008). The evolution of prefabricated residential building systems in Hong Kong: A review of. *Automation in Construction*, 239-248.

Jaillon, L., Poon, C., & Chiang, Y. (2008). Quantifying the waste reduction potential of using prefabrication in building. *Waste Management*, 309-320.

Jannadi, O. A., & Almishari, S. (2003). Risk Assessment in Construction. *Journal of Contsruction Engineering and Management*, 492-500.

Kahneman, D., Tversky, A., "Prospect Theory: An Analysis of Decision Under Risk." Econometrica, Volume 47, Number 2, pp 263-292, Mar. 1979.

Kang, L.S., Kim, S., Moon, H.S., Kim, H.S., "Development of a 4D object-based system for visualizing the risk information of construction projects." *Journal of Automation in Construction*, Elsevier, pp 186-203, Jan 2013.

Jergeas, G., & Put, V. d. (2001). Benefits of Constructability in Construction Projects . *Journal of Construction Engineering and Management*, 281-290.

Lawson, M., Ogden, R., & Bergin, R. (2012). Application of Modular Construction. *American Society of Civil Engineers*, 18148-18154.

Lawson, R. M., & Richards, J. (2010). Modular design for high-rise buildings. *Proceedings of the ICE - Structures and Buildings*, 151-164.

Love, P. D. (2002). Influence of Project Type and Procurement Method on Rework. *Journal of contruction management and engineering* , 12818-12829.

Love, P. E., & Smith, J. (2003). Benchmarking, Benchaction, and Benchlearning: Rework Mitigation in Projects. *Journal of Management in Engineering*, 147-159.

Love, P. E., Irani, Z., & Edwards, D. J. (2004). A Rework Reduction Model for Construction Projects. *Transactions on engineering management*, 426-440.

Milberg, C., & Tommelein, I. (2003). Role of Tolerances and Process Capability Data. *Construction Reseach Congress* , 1 to 8.

Moghadam, M., Alwisy, A., & Al-Hussein, M. (2012). Integrated BIM/Lean Base Production Line Schedule Model for Modular. *ASCE Construction Research Congress*, 1271-1280.

Nadim, W., & Goudling, J. S. (2009). Offsite Production in the UK: The Construction Industry and Academia. *Journal of Architectural Engineering and Design Management*, 136-152.

Nadim, W., & Goudling, J. S. (2010). Offsite Production in the UK: The Way Forward? A UK Construction Industry Prespective. *Construction Innovation*, 181-202.

Pan, W., & Goodier, C. (2012). House-Building Business Models. *Journal of Architectural Engineering*, 84-93.

Pan, W., Gibb, A. G., & Dainty, A. R. (2008). Leading UK housebuilders' utilisation of offsite modern methods for construction. *Building Research and Information*, 56-67.

Pan, W., Gibb, A., & Dainty, A. (2007). Perspectives of UK housebuilders on the use of offsite. *Construction Management and Economics*, 183-194.

Pan, W., Gibb, A., & Sellars, A. (2008). Maintenance Cost Implications of Utilising Bathroom Modules Manufactured Offsite. *Construction Management and Economics* , 1067-1077.

Post, N. M. (2013). High-Rise Modular Construction Forces Major Adjustments. *ENR*, 24-25.

Rodrigue, J.-P., & Notteboom, T. (1998). *The Geography of Transport System.* New York: Department of Global Studies and Geography.

Sacks, R., Koskela, L., Dave, A. B., & Owen, R. (2010). Interaction of Lean and Building Information Modeling. *ASCE Journal of Construction Engineering and Manegement* , 968-980.

Skidmore, Owings, & Merrill. (2009, 8 11). *Pin-Fuse Joint.* Retrieved 2 27, 2014, from Architect Magazine: http://www.architectmagazine.com/technology/pin-fuse-joint.aspx

Song, J., Fagerlund, W., Haas, C., Tatum, C., & Vanegas, J. (2005). Considering Prework on Industrial Projects. *JOURNAL OF CONSTRUCTION ENGINEERING AND MANAGEMENT*, 723-733.

Song, J., W., F., Haas, C., Tatum, C., & Vanegas, J. (2005). Considering prework on industrial projects. *Journal of constructin engineering and management* , 131723-131733.

Taylor, T. R., & Ford, D. N. (2008). Managing Tipping Point Dynamics in Complex Contruction Projects. *Journal of Construction Engineering and Management*, 421-431.

Toole, M. T., & Gambatese, J. (2008). The Trajectories of Prevention through Design in Construction. *Journal of Safety Research*, 225-230.

Waier, P. R. (2009). *RSMeans building construction cost data.* Kingston, MA: R.S. Means Company.

Wilson, E. L., & Emeritus. (2013). *CSI Analysis Reference Manual.* California: Computers and Structures Inc.

Yu, H., Al-Hussein, M., Al-Jibouri, S., & Telyas, A. (2013). Lean Transformation in a Modular Building Company. *ASCE Journal of Management in Engineering*, 103-111.

Zhang, D., Haas, C. T., Goodrum, P. M., Caldas, C. H., & Granger, R. (2012). Construction Small-Projects Rework Reduction for Capital Facilities . *Journal of Construction Engineering and Management* , 1377-1385.